Neuron Guiding *in Vitro*

-

Construction of Defined Low Density Networks

Von der Fakultät für Mathematik, Informatik und Naturwissenschaften der RWTH Aachen University zur Erlangung des akademischen Grades einer Doktorin der Naturwissenschaften genehmigte Dissertation

vorgelegt von

Diplom-Biologin

Katharina Walczuch

aus Lingen (Ems)

Berichter:
Univ.-Prof. Dr. rer. nat. Peter Bräunig
Univ.-Prof. Dr. rer. nat. Hermann Wagner

Tag der mündlichen Prüfung: 13. April 2016

Diese Dissertation ist auf den Seiten der Universitätsbibliothek online verfügbar.

Contents

1 General Introduction 9

2 Aims of the Project 17

3 A Microfluidic Device for a Defined Neuron Position *in Vitro* 21

3.1 Statement of Shared Workload and Publications 21

3.2 Introduction 23

3.3 Methods 26

3.3.1 General Conceptual Design 26

3.3.2 Design of First Generation Cell Traps 26

3.3.3 Design of Second Generation Cell Traps 29

3.3.4 Simulation 32

3.3.5 Template Production 32

3.3.6 Device Production 32

3.3.7 Experimental Setup 33

3.3.8 Animals 34

3.3.9 Cell/Bead Preparation 35

3.4 Results 36

3.4.1 Flow Rate Simulation 36

3.4.2 Trapping Experiments with Beads and Neurons 39

3.5 Discussion 49
3.5.1 Channel Dimensions 49
3.5.2 Flow Ratio and Trapping Success 51
3.5.3 Flow Velocity and Cell Strain 54
3.5.4 Cell Trap Arrangement 56
3.6 Conclusion 58

4 Agarose-Based Substrate Modification Technique for Chemical and Physical Guiding of Neurons *in Vitro* 59

4.1 Statement of Shared Workload and Publications 59
4.2 Introduction 61
4.3 Methods 63
4.3.1 Template Design 63
4.3.2 Photolithography 65
4.3.3 Agarose Slice Fabrication 66
4.3.4 Culture Substrate Preparation 68
4.3.5 Long-Term Attachment Test 68
4.3.6 Determination of Agarose Slice Thickness 68
4.3.7 Animals 69
4.3.8 Cell Culture 69
4.3.9 Influence of Agarose Slice Thickness on Cell Survival 70
4.3.10 Immunohistochemistry 71
4.3.11 Electrophysiology 71
4.4 Results 72
4.4.1 Agarose Molding 72
4.4.2 Slice Stability, Handling and Attachment 72
4.4.3 Slice Thickness 73

4.4.4 Guiding of Cell Growth & Electrophysiology....74
4.5 Discussion....81
4.5.1 Methodology....81
4.5.2 Guiding by Physical Cues....82
4.5.3 Cell Culture in Wells....83
4.5.4 Agarose as Patterning Material....83
4.6 Conclusion....86

5 Improvements of Culture Conditions and Neuronal Cell Growth on Iridium Oxide....87

5.1 Statement of Shared Workload....87
5.2 Introduction....88
5.3 Methods....91
5.3.1 Animals....91
5.3.2 Cell Culture....91
5.3.3 Cell Culture Supplements....91
5.3.4 Iridium Oxide (IrO) Substrates....92
5.3.5 Analysis....92
5.4 Results....94
5.4.1 B27....94
5.4.2 Retinoic Acid....95
5.4.3 Biocompatibility Test with Iridium Oxide....96
5.5 Discussion....98
5.5.1 Supplement Tests for Improved Culture Conditions....98
5.5.2 Biocompatibility Test with Iridium Oxide:....101
5.6 Conclusion....103

6 General Discussion....105

Summary 111

Zusammenfassung 115

References 119

Supplementary Information on CD-ROM 135

Danksagung 137

Lebenslauf 139

1 General Introduction

By the current state of knowledge a vertebrate brain contains up to about 10^{10} neurons, far more glial cells and over 10^{12} synaptic connections (Herculano-Houzel 2005). It is obvious that the ambitions of decoding basic mechanisms underlying such a huge network will never be realized by trying to look at the intact system. One will surely loose the overview at some point. The investigation of neuronal networks *in vitro* helps to overcome the highly complex situation *in vivo* (Bulloch & Syed 1992; Schmold & Syed 2012; Massobrio et al. 2015). With cell culture technologies, it is possible to isolate single neuron populations from brains and seed them on special culture substrates. Here, they can develop neurites and synaptic connections to neighboring cells, which results in small networks. Depending on the cell type, cultured neuron populations are able to survive for long periods of time or even permanently in terms of cell lines with neuronal properties derived from distinct embryonic stem cells (Lang et al. 2004) for example. These properties offer innumerable application opportunities in medical or developmental research, amongst various other fields of interest. Neurons *in vitro* can be investigated from different viewpoints and with various methods. In the context of neuronal cell cultures, beside morphological aspects, primarily physiological questions become processed. In this context, network or single cell activity *in vitro* can be investigated with different methods, intracellularly or extracellularly. Intracellular techniques only allow a snapshot of the given activity situation because in general the penetrated neuron does not survive the electrode intrusion. In contrast, extracellular measuring, as it occurs non-invasively, allows for long-term analysis.

This fact provides tremendous advantages to current intracellular applications because it opens a far wider research field, for example concerning questions about developmental processes building up neuronal networks, like plasticity within small cell assemblies. Anyway, high quality recordings with extracellular electrodes still can be challenging as the distance between signal and detecting site is much larger and the signal amplitudes to detect therefore much smaller. This causes the need of adequate technical equipment. In addition to other extracellular recording techniques (Moriguchi et al. 2007; Kwiat et al. 2012; Edwards et al. 2013) as well as optical methods like Ca^{2+}-imaging (Sugio et al. 2004; Li et al. 2014), multi-electrode-arrays (MEAs) are routinely used tools (Thomas et al. 1972; Novak & Wheeler 1988; Gross et al. 1995). With MEAs, it is possible to record, non-invasively, simultaneously at different positions and this over a long period of time in terms of a so called biohybrid system (Thomas et al. 1972; Novak & Wheeler 1988; Gross et al. 1995; Massobrio et al. 2015). The possibilities offered by this highly developed technical standard, let these biohybrid systems to become important tools used in basic dynamic network research (Mazzoni et al. 2007). Common MEAs consist of an electronic chip, made of either glass or silicone with integrated planar electrodes. They commonly can be used for stimulation as well as for recording of cells directly cultured on the electrode surface. The electrodes are integrated in glass or a printed passivation layer (e.g. silicon nitride/oxide, polyamide or parylene), most commonly arranged in a square array of 8 x 8 pads, and their size generally varies between 10 µm and 100 µm (Fig. 1). Typically, the electrode material is gold-plated indium tin oxide (ITO) (Gross et al. 1993), titanium nitride (TiN) (Wagenaar & Potter 2004) or platinum (Heuschkel et al. 2002). Recently used electrodes are additionally coated with polymers such as Poly-3,4-ethylendioxythiophen (PEDOT) (Richardson-Burns et al. 2007) or carbon nanotubes (Lovat et al. 2005) because of their electrochemical properties. Further, iridium oxide (IrO) as electrode coating attracted attention. It showed promising properties concerning charge delivery per area (Tanghe et al. 1990; Wessling et al. 2006; Gawad et al. 2009), and was already successfully tested for compatibility with rat (Eick et al. 2009) as well as locust and chicken neurons (Göbbels et al. 2010b). Electrode number, size, inter-electrode distance and material can vary between

different commercially available types, adapting particular experimental requirements.

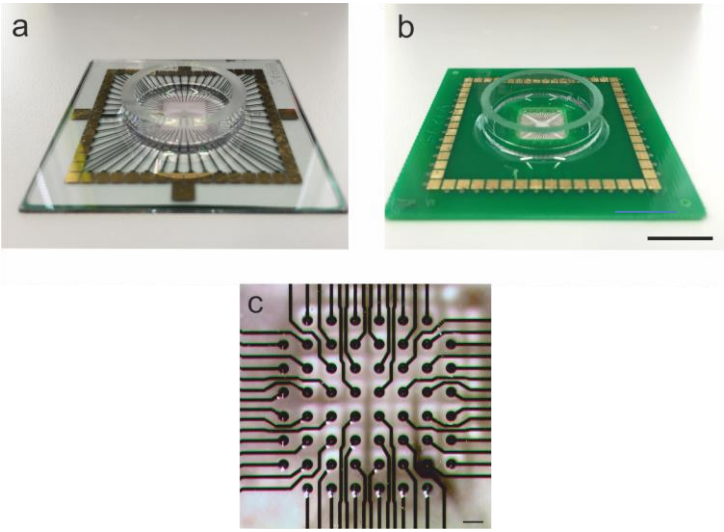


Figure 1: Multielectrode Arrays (MEAs) with 8 x 8-electrode configuration. a) Contact pads integrated in glass chip (Multichannel Systems GmbH); b) Contact pads integrated in a plastic chip (Qwane Bioscience). c) Planar electrode array in detail. Scale bar a) & b) 1 cm, c) 200 µm

However, it has to be emphasized that the quality of extracellular investigations on cells *in vitro* strongly depends on the electrode-neuron-connection (Buitenweg et al. 1998; Blau 2013) as well as on the electrode material. As signal-recording device-distance is extended at extracellular applications and therefore the signals are much weaker, neurons in culture have to grow in very close proximity to or better directly on the electrode with a tight connection to achieve the recording of strong signals (Sorribas et al. 2001). Most *in vitro* studies with vertebrates use cell cultures with extremely high cell densities with thousands of cells that randomly distribute over the whole MEA-surface. In these studies high complex networks develop, where only multi-neuron stimulation and recording can be achieved, as the number of electrodes is always much smaller than the number cells. To overcome this problem, spatial resolution of recorded signals of such net-

works can be increased with the newest complementary metal oxide semiconductor (CMOS) technology (Eversmann et al. 2003; Ballini et al. 2014). It enables the use of high density MEAs with up to thousands of electrodes per chip. Here, complex spike sorting analysis helps to get an overview of the mass of recorded signals but the identification of individual neurons is not possible with these devices. Thus, success rate in this context still strongly depends on the cell density (Jäckel et al. 2012). For this reason, compared to *in vivo* investigations, further simplification of complex networks seems to be necessary also in *in vitro* approaches to achieve a detailed understanding of function and formation of individual synaptic contacts. For network analysis on MEAs, a one-to-one neuron-electrode-interface would achieve most promising conditions. Thus, highest temporal-spatial resolution of a probed network would be achieved where recorded signals can be assigned to individual neurons and individual synaptic connections were able to be studied in detail (for review see: Schmold & Syed 2012). For a 60 electrode array this would represent an at most 60 neuron network, where, in the best case, every neuron is only connected to its four direct neighbors. For this to be achieved, somata, as singles or in small clusters, have to become positioned to electrode locations, and neuritic connections between somata have to be directed. However, this directed positioning of individual cells on the electrodes of a MEA is still a problem. Literature already revealed different approaches trying to achieve similar conditions by actively reducing the number of network participants, therefore reducing its complexity and direct their position in the network (Claverol-Tinturé et al. 2007; Suzuki et al. 2007; Massobrio et al. 2015). Two of the most common tools in this context are the guidance of cell growth on substrates by either patterning the growth substrates with different methods (Tsai et al. 2007) or by the use of microfluidic devices (Tehranirokh et al. 2013). With the primarily used 2D patterning method, special chemical coatings in a defined pattern (Kleinfeld et al. 1988; Corey et al. 1991; Prinz & Fromherz 2000; Jun et al. 2007) become deposited on the growth substrate. Consequently, applied cells, only able to adhere to the locations with the chemical anchor, grow in the desired pattern. With microfluidic devices, cells can be transported to defined locations by a laminar flow within channels in micrometer scale (Andersson & Berg 2004). Some other studies even used magnetic cues or dielectrophoresis in addition to traditional pattern

technology to achieve neuron positioning (Jaber et al. 2013; Delacour et al. 2014). However, many of these and other techniques show disadvantages because they are still complicated, time consuming, expensive, expose fragile cells to mechanical forces affecting their viability or simply do not offer a reliable and gentle trapping efficiency. Every approach has its advantages and drawbacks and it is challenging to achieve satisfying results with a given system that provides the aspired properties like functionality, universal and easy application, reproducibility and low cost at the same time.

In this project, we are working on new technical solutions for developing small and defined neuronal networks cultured on MEAs. The challenge here is not only the right position of the soma on the electrode surface, but the fixation to its initial position and the defined outgrowth of the neurites to neighboring cells to achieve a controlled network pattern as well. In addition, the need of a strong cell adherence to the substrate and the viability over long periods is obvious, but at the same time challenging, especially in case of aspiring a universal application possibility with different cell models. Depending on the species, cells may have completely different demands on their microenvironment in culture (for review see: Théry 2010), like for example certain substrate properties to adhere to. Thus, different factors have to be considered, ranging from optimal culture conditions in general to the choice of the right guiding technique to achieve the objective.
Our cell models are invertebrate neurons of locusts (*Locust migratoria*) and pond snails (*Lymnaea stagnalis*) (Fig. 2) for several reasons. First of all, the central nervous systems of invertebrates are far less complex than these of vertebrates concerning neuron number and therefore synaptic connections (Schmold & Syed 2012). For example, according to cautious calculations, the cerebral ganglion of a locust contains only some 360000 neurons, the thoracic and abdominal ganglia even far less (Burrows 1996). Furthermore, invertebrate cell cultures allow for translating the idea of understanding fundamental network processes best by reducing its complexity to a minimum. Their neurons are able to grow in extremely low density (Fromherz et al. 1991; Bulloch & Syed 1992; Göbbels et al. 2010a; Weigel et al. 2012; Massobrio et al. 2013). Like this, in contrast to vertebrate cell cultures, which in general need a high cell density (Wagenaar et al. 2005; Minerbi et al. 2009), invertebrate cells, like mollusk or insect neurons, became of high

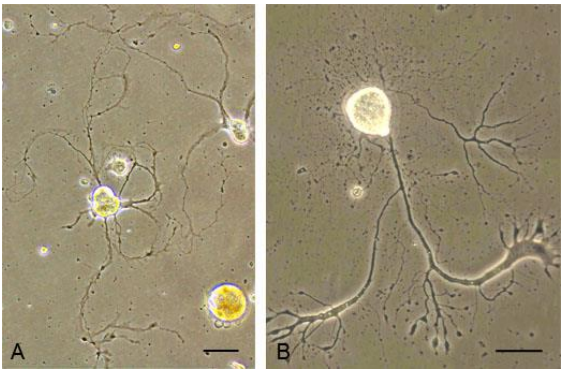


Figure 2. Cultured neurons at low density, sprouting numerous neurites. a) *Lymnaea* neurons. Scale bar: 50 µm b) *Locusta* neuron. Scale bars: 30 µm

interest for the investigation of really small networks, where it is possible to study individual synaptic connections in detail (Weigel et al. 2012; Massobrio et al. 2015). In particular, this opportunity lead to several fascinating experiments in the past decades, where defined neuronal circuits that are directly associated with defined behavior patterns of the animal could be reconstructed *in vitro* (Review: Schmold & Syed 2012). Not least, cell culture in general is easier with invertebrate neurons than with vertebrate neurons as the somata are more robust, undemanding and generally have larger diameters (up to 120 µm) than most vertebrate neurons (10-20 µm). Like this, they are easier to manipulate and achieve a complete electrode covering, as electrodes of current MEAs generally have diameters between 30 and a few hundred micrometers. Large-scaled electrodes in general show a better signal-to-noise ratio and a fully covered electrode with tight contact to the cell leads to stronger signals (Sorribas et al. 2001; Blau 2013). Therefore, the application of invertebrate neurons is advantageous and they are already proven to be promising candidates for the application with semiconductor technologies (Zeck & Fromherz 2001; Jenkner et al. 2001; Kaul et al. 2004; Schoen & Fromherz 2007; Massobrio et al. 2009; Göbbels et al. 2010). Progress in fundamental research of network physiology in invertebrate nervous systems offers different practical applications. Beside the development of species specific compositions of pesticides (Smagghe et al. 2009), new findings in basic cell-cell-interactions derived

from invertebrates are most probably relevant to biomedical research, as well (Sattelle & Buckingham, 2006). Indeed, many concepts of circuitry are different in the vertebrate nervous system. However, the invertebrate nervous system shares many features with that of vertebrates, as basic functionality is conserved throughout evolution.

2 Aims of the Project

Long-term objective of this interdisciplinary project is the development towards an automated system for the bi-directed coupling of neuronal cells and electrodes of MEAs *in vitro*. Within this miniaturized biohybrid system those neurons are supposed to develop small and defined networks that enable physiological long-term examinations of cell-cell interactions.

The doctoral thesis of Göbbels (2011) describes essential spadework in this project for the development and characterization of a biohybrid system in general terms. There, in terms of biocompatibility- and electrophysiological tests, the suitability of insect neurons for coupling with electronic devices, using the example of neurons from the locust *Locusta migratoria*, could be confirmed. Further, first results to solve the problem of the construction of defined networks by specialized substrate patterning and microfluidic manipulation was performed.

Within this study, we raised to the challenge of concrete technical solutions to achieve the directed positioning of individual neurons on distinct electrode locations and the control of their neuritic development towards a defined network. Progress in this context constitutes a valuable stage achievement, essential to achieve the long-term objective.

We decided to complement the already used biological test system by a further species, the pond snail *Lymnaea stagnalis*, to confirm a wider application opportunity. Both, locust and pond snail neurons, were already successfully used in the context of a biohybrid system. Pond snail brains contain even larger neurons than locusts, which can be beneficial. In addition, it is easier to manipulate the neurons of the pond snail as single neurons can be visually differentiated within the ganglia.

This study now comprises two main approaches, first the processing of the positioning problem of individual neurons on defined locations and second the improvement of culture conditions that allows network building and long-term viability of *in vitro* networks on MEA electrodes. The problem of positioning was approached by a microfluidic tool on the one hand and substrate patterning on the other. Both were going to be realized in cooperation with the Institute of Materials in Electrical Engineering 1 (IWE 1). In context of the microfluidic approach, we worked towards a new gentle channel trap application (chapter 3). Different channel geometries were tested and their flow properties and cell- and bead positioning-efficiency characterized. Concrete conditions the device had to meet were the following:

- Particle filling and transport within laminar flow should be as gentle as possible to maintain viability of sensitive neurons.
- The elected channel geometry should be suitable to deflect particles reliably to the favored pathway and to hold trapped particles in place.
- The channel geometry should reduce the risk of blockages leading to irrevocable flow disturbances.

In terms of the patterning approach, findings of Göbbels (2011) concerning chemical and topographical guiding properties of agarose on locust neurons shall be used and modified to apply to the two biological test systems. Further, the development of a concrete substrate modification technique for patterning the cell growth substrate was aimed for (chapter 4). This technique should fulfill the following conditions:

- The method should be of reproducible quality, as simple as possible and cost effective at the same time.
- The raised pattern should be easy to apply to any culture substrates like MEA chips, but easy to remove at the same time for a possible reuse of MEA chips.
- Applied neurons should be impressed by the topography as well as by the chemical conditions of the material in order to adhere only to the patterned locations and to be detained to adhere to the other locations.

- Pattern geometry should hold applied neurons in place and direct their neuritic branching.
- Neurons should maintain viability over longer periods.

For a long lasting viability of neurons and a reliable outgrowth of their extensions and the successful building of connections to neighboring cells, it seems to be necessary to improve culture conditions. Here, different supplements for culture media were tested regarding their positive influence on cell survival and neuritic branching of neuronal cultures from pond snails.
Further, as the benefit of iridium oxide (IrO) for electrode material was pointed out by Göbbels (2011), a biocompatibility test of this electrode material with pond snail neurons was envisaged (chapter 5). Here, as well as in the medium supplement study, cell survival over time and the portion of cells developing neuritic branching were determined and compared with control groups.

3 A Microfluidic Device for a Defined Neuron Position *in Vitro*

3.1 Statement of Shared Workload and Publications

The study was carried out under the supervision of Univ.-Prof. Dr. Peter Bräunig and Dr. Katrin Bui-Göbbels. The geometrical design and a preliminary experimental setup of the first generation devices has already been published in parts in a conference proceeding: Krumpholz et al. (2014): **A microfluidic device for selective positioning of invertebrate neurons,** Conference proceeding, 9th International Meeting on Substrate-Integrated Microelectrode Arrays (MEA Meeting), Reutlingen, Germany.

The content of this chapter dealing with the second generation of devices has not yet been published.

Dr. Katrin Bui-Göbbels, Univ.-Prof. Dr. Peter Bräunig, Dr. Andreas Buchenauer and Dr. Uwe Schnakenberg developed the initial concept, the geometrical design of the first generation devices and initial experimental procedures. Martin Rüßler and Rudolf Degen performed first tests and characterized the devices in the course of their master and bachelor thesis, respectively. The following modifications of the first generation of devices and modifications of the experimental procedures were developed by the contributions from Katharina Walczuch, Dr. Katrin Bui-Göbbels, Univ.-Prof. Dr. Peter Bräunig, Akram El Hasni, Dr. Uwe Schnakenberg and the assistance of Rudolf Degen. Katharina Walczuch performed the data collection for the

characterization of the functionality of the latest devices from the first generation.

The conceptual design of the second generation traps was developed by Dr. Phong Bui and Dr. Katrin Bui-Göbbels. Rudolf Degen and Katharina Walczuch realized them. Rudolf Degen and Katharina Walczuch performed the simulation analysis under guidance of Dr. Phong Bui. Katharina Walczuch performed data collection for the characterization of the functionality of the devices from the second generation. Katharina Walczuch analyzed and interpreted the results with the support from Dr. Katrin Bui-Göbbels and Univ.-Prof. Dr. Peter Bräunig. During the whole study, technical support and advice was provided by Dr. Uwe Schnakenberg and Akram El Hasni from the Institute of Materials in Electrical Engineering 1 (IWE 1), RWTH Aachen University. The IWE 1 provided the production of the silicon wafer as well. Softlithography was done by Katharina Walczuch and Rudolf Degen at the IWE 1. Katharina Walczuch wrote the manuscript

3.2 Introduction

The investigation of basic developmental processes within neuronal networks, like plasticity, requires observation over a longer period of time (Wagenaar et al. 2005; Minerbi et al. 2009). The use of non-invasive recording techniques measuring the activity extracellularly is state of the art in contrast to common intracellular recording methods. In this context, the use of MEAs are effective tools (Thomas et al. 1972; Novak & Wheeler 1988; Gross et al. 1995). To get an insight into individually activity patterns the use of *in vitro* approaches with much less neurons are advantageous over the use of those *in vivo*, in which activity patterns are additionally modulated by a series of further unknown sources. Generally, MEA chips are equipped with corresponding culture chambers. Neurons in a culture suspension can be applied directly onto the chip. However, as a matter of principle, applied cells are randomly distributed over the MEA surface and it is necessary to increase the cell density strongly, otherwise the electrodes probably do not become covered. Unfortunately, this results in networks with a participant number that strongly exceeds the number of electrodes, which is undesirable. To gain detailed insight in network activity, it seems to be necessary to have an overview of individual network participants and their particular influence on the overall network dynamics (Massobrio et al. 2015). To implement these conditions the number of network participants has to be lowered extremely, especially in cell culture systems with vertebrates (Wagenaar et al. 2005; Minerbi et al. 2009; Ballini et al. 2014), otherwise an unambiguous allocation of certain signals to individual cells is a problem. To achieve a maximum of spatial resolution, it is desirable to culture always precisely one neuron per electrode, and at best case, the neuron should cover the electrode completely to improve the signal-to-noise ratio. As electrodes of standard MEAs are rarely smaller than about 30 µm, cells should be of adequate size as well. A good signal-to-noise ratio, low-density culture and the directed positioning of cells in culture are still the prominent problems in this field of interest. In this context, the use of invertebrate neurons provides the advantage over vertebrate cells because they can be cultured at extremely low cell density (Göbbels et al. 2010a; Massobrio et al. 2013). Furthermore, many neurons of invertebrates are very large. That way, they can cover individual electrodes completely. We chose locust and pond snails for our biological test systems as their neurons

comply best with the desired properties. Cell size in combination with their frugality in culture, makes these neuron types an excellent test object for the study. In particular, pond snail neurons can be visually differentiated as they are colored, which is beneficial during the dissection procedure (Schmold & Syed 2012).

The defined positioning and maintenance of vitality of cells *in vitro* is a critical point. One approach of great importance in this and similar context is the use of microfluidic devices consisting of closed channels and chambers in cell scale with controlled fluid movements (Beebe et al. 2002; Andersson & Berg 2004; Whitesides 2006; Nilsson et al. 2009; Tehranirokh et al. 2013). Nowadays, microfluidic devices represent important tools for cell culture systems in different fields of interest (El-Ali et al. 2006; Zervantonakis et al. 2011), including medical research, like stem cell differentiation approaches (Kobel et al. 2012) or long-term hepatocyte cultures applied in liver malfunction therapies (Park et al. 2007). But also for neuronal studies, microfluidic applications became more and more important (Gross et al. 2007; Taylor & Jeon 2010). The advantages are simply striking:

- The conditions in microscale environments resemble more the conditions *in vivo.*
- Closed chambers and channels can maintain sterility and allow maximum controlled environments.
- A defined geometry provides the opportunity to create spatial separations from cell bodies, which allow the investigation of defined cell-cell-interactions.
- The fluidic flow produced in such channels can be used to guide the cells in a suspension to defined locations by the laws of physics of a laminar flow (Tehranirokh et al. 2013).
- Continuous perfusion provides the opportunity to exchange the medium conveniently, which is assumed to improve nutrient supply as well as waste product disposal (Millet et al. 2007).

Already Göbbels et al. (2010a) showed the successful low density cultivation of locust thoracic neurons in microfluidic channels based on the model of Walker et al. (2002) under static-bath conditions over a period of more than 15 days. A similar system with dynamic-bath conditions in terms of continuous medium perfusion might even prolong vitality. In the literature numer-

ous different geometric designs with a wide range of different trapping concepts can be found (Braschler et al. 2005; Di Carlo et al. 2006; Skelley et al. 2009; Wheeler et al. 2010; Frimat et al. 2011; Dinh et al. 2013). Many approaches thereby use the concept of differential fluidic resistances in different channel types in a fluidic system with laminar flow to achieve functionality (Tan & Takeuchi 2007; Frimat et al. 2011; Kobel et al. 2010; Dinh et al. 2013). By the concept of different fluidic resistances, cells and particles in general tend to follow the path of least resistance. The easiest way to create differential fluidic resistances within a channel system is to use different channel lengths. One channel type is much longer, therefore representing the path of higher fluidic resistance R_1. In contrast, the second channel type represents the path of less resistance R_2 (R_1>R_2). This yield to a higher linear flow rate Q_2 in the second channel type compared to the first channel path Q_1 resulting in a flow rate ratio larger 1:

$$\frac{Q2}{Q1} > 1$$

The path of higher resistance is often realized by one main long path, forming a serpentine geometry for space-saving and short transverse channels of less resistance with far smaller dimensions so that cells can be trapped. As this concept showed promising results in the literature (Tan & Takeuchi 2007; Kobel et al. 2010; Frimat et al. 2011; Kobel et al. 2012), the general geometrical design of the mentioned studies was adopted in this study and modified fitting to our conditions. Further, the effectiveness was tested with our cell types, which have not been used in combination with microfluidics so far. Experiments with the common geometric design resulted in the realization that the current requirements of the applied biological test objects do not suit the properties of these systems. Nevertheless, the focus in this study should lie on a completely new geometrical design, not shown before. Basic geometrical modifications were managed yielding better results with pond snail neurons as the improvements are essential for large and sensitive cells. The devices work with lowest flow rates and are therefore gentler for the applied cells. Additionally, due to geometrical conditions, they are less prone to disturbances evoked by particles blocking peripheral channel parts.

3.3 Methods

3.3.1 General Conceptual Design

The microfluidic devices for cell positioning by differential fluidic resistances are always composed of a main channel, connecting an inlet and an outlet and a transverse channel system. The transverse channels contain a "trap gap" area where the channel narrows under the dimensions of the particles to be captured. The area directly upstream from the trap gap represents the cell trap. Generally, the amount of transverse channels always corresponds to the number of cell traps. Cell trapping is predicted to function as follows: Until none of the traps is occupied, the path of less resistance should lead through the first transverse channel. Once a cell is trapped in the first trap, it should act as a plug leading to an immediate increase of the flow resistance in the particular transverse channel. The main flow is redirected to the main channel and to the downstream transverse channels, respectively. Following this rule, the applied particles and cells are predicted to be guided in a way that the first entered particle occupies the first trap in the row along the main path, resulting in a redirection of the flow to the main path again and then towards the second trap and so forth.

3.3.2 Design of First Generation Cell Traps

In cooperation with the IWE 1 at the RWTH first generation cell traps of the mentioned serpentine type was developed (Tab. 1; Fig. 3). Here, different subtypes with different geometrical parameters and varying cell trapping arrangements were designed in order to find optimal fluidic proportions between main and transverse channels and therefore optimal capturing efficiency. Table 1 provides an overview of the most important varying parameters. The first subtype describes a four-looped serpentine of persistent length, height, and width. Transverse channels in terms of narrow trap gaps with upstream cell trapping areas are arranged along the main path, four in every loop that the potentially 16 trapped cells would be arranged in a 4 x 4 square. This arrangement was chosen, as it would fit to a common electrode arrangement on a MEA used in our lab (Fig 3 a)). Further design types then followed serving improvements by the means of flow proportions (Fig. 3 b) & c)). Thereby different loop lengths of the serpentine type as well as

different trap arrangements were tested to raise trapping efficiency, to create equal trapping probabilities for every cell trap, and to achieve a gentler cell handling. Here, only a single cell trap was either arranged in every loop (Fig. 3b)) or in every second (Fig. 3 c)). This either resulted in a six-looped serpentine with eight cell traps (Fig. 3 b)) or in a seven-looped serpentine with four cell traps (Fig. 3 c)).

Table 1: Varying parameters of microfluidic channel system of the first generation cell trapping devices.

Type	Loop length [µm]	Channel width [µm]	Trap number	Trap arrangement
1	1000	50	16	4x4
2a	4000	70	6	1 per loop
2b	8000	70	6	1 per loop
3a	4000	70	4	1 per every 2nd loop
3b	8000	70	4	1 per every 2nd loop

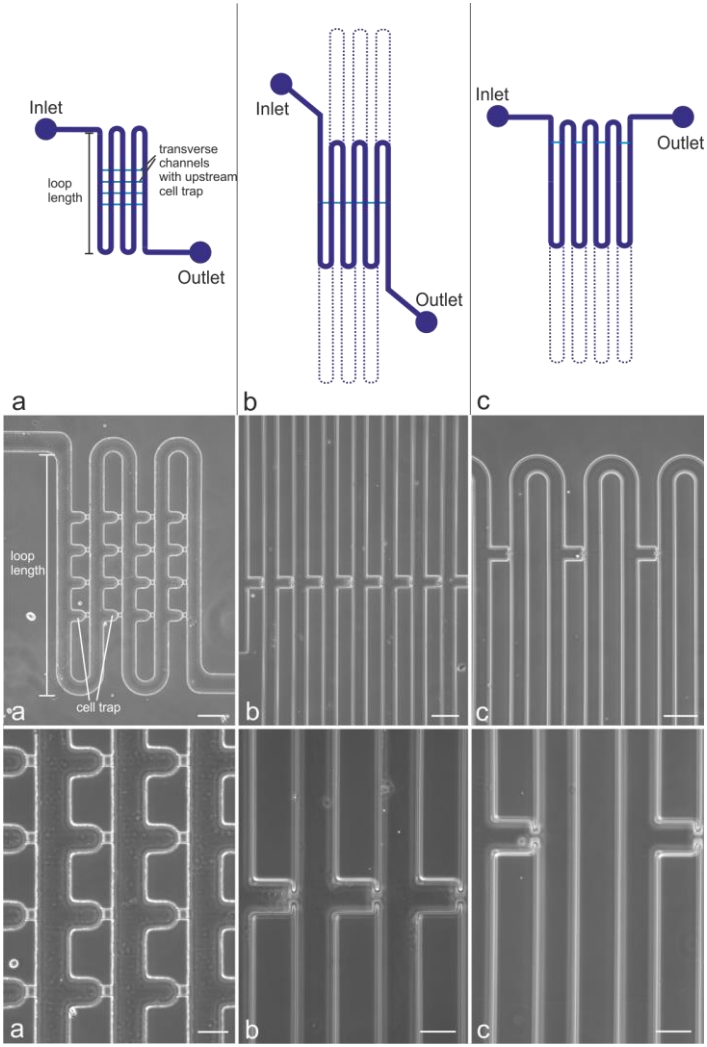

Inlet
transverse channels with upstream cell trap
loop length
Outlet
Inlet
Outlet
Inlet
Outlet
a
b
c
loop length
cell trap
a
b
c
a
b
c

Figure 3: First generation cell traps of the serpentine type. a) four-looped main channel with 4 x 4 trapping areas; b) six-looped main channel type with one cell trap in the center of every loop, corresponding to channel subtype 2 a and 2 b (dashed lines indicate different channel loop lengths for different flow proportions); c) seven-looped main channel with one cell trap in the first and then every second loop following, corresponding to subtype 3 a and 3 b. Upper row: schematics (not true to scale): middle row: overview of particular channel system cast in polydimethylsiloxane (PDMS). Lower row: magnifications of trapping areas in detail. Scale bars (middle row): 100 µm, scale bars (lower row): 50 µm

3.3.3 Design of Second Generation Cell Traps

The second generation of cell traps follows a completely different geometrical concept (Fig. 4). This system consists of two channel flanks arranged in a right angle connecting an inlet and an outlet. A transverse channel in turn interconnects these two flanks forming the hypotenuse of this isosceles triangle. The transverse channels describe the short cut between the main channel flanks, which represent the catheti of the triangle. Like this, the transverse channel represents the path of less resistance in comparison to the way through the main channel flanks. The channel systems are equipped with either five or nine of these short cut transverse channels, each containing a single cell trapping area in terms of a trap gap where the channel width narrows for a short distance. Here, channel widths fall below the average soma diameters of the neurons applied to the system so that they can be trapped in this area (Fig. 4). The transverse channels originate at different locations of the main channel, each forming a triangle with different side lengths. There exist different types, either with five or nine transverse channels. When the first transverse channel is closed, the path of least resistance is redirected through the second transverse channel, and so forth. Inlet and outlet are equipped with a funnel shaped area for a facilitated inward and outward transfer of the cells. The enhanced area of connection to the inlet round shall improve the suction effect on the particles at low rates.

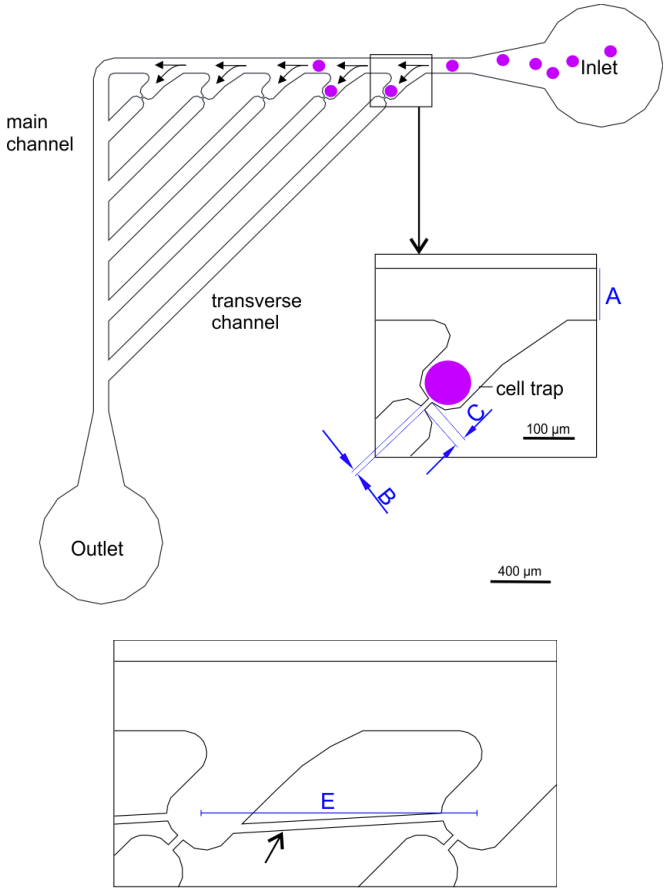


Figure 4: Design of a microfluidic channel system of the second generation for cell capturing. Arrows indicate direction of fluid flow. Trapping area shown in detail (inset) to illustrate the geometrical parameters: A: 100 µm; B: 10 µm; C: 20 µm; D (channel height; not shown in schematic): 100 µm; Lower picture: Variation of trapping areas with interconnecting channels for neurite outgrowth. E: distance between trapping areas (corresponds to possible inter-electrode distances of MEA)

The main parameters describing the channel geometry of the second generation cell traps are the main and transverse channel width (A) the gap forming narrow part of the transverse channel part downstream the trap-

ping area (B), the length of the gap (C) and the channel height (D). Parameters for channel width (A) and height (D) are persistent throughout the different subtypes with 100 µm each. The length of the narrow channel (B) is persistent as well at 20 µm. There exist two different distances between single trapping areas (E), either 200 µm or 400 µm (measured from center to center) (Fig. 4, lower part). A further varying parameter is the number of traps in a row along the main path. Selected prototypes of these designs include additional small channels between the single cell traps to enable neuritic branching towards neighboring traps and the possibility to form synapses, a first step towards network formation of single trapped cells. The height of the neurite channels was always set to five µm, the width to 10 µm. Final prototypes with respective parameter combinations are summarized in table 2.

Table 2. Dimensions of microfluidic channel systems of the second generation. A: channel width; B: trap gap width; C: trap gap length; D: channel height; E: inter-trap distance; F: number of trapping areas (transverse channels); G: neurite channel height; H: neurite channel width. Persistent parameters are the main channel height (A), the length of the trap gap (C) and the height G) and width (H) of the neurite channels. Varying Parameters compared to the previous type are marked in color.

Type	A [µm]	B [µm]	C [µm]	D [µm]	E [µm]	F	G [µm]	H [µm]
1	100	10	20	100	200	5	/	/
2	100	20	20	100	200	5	/	/
3	100	10	20	100	200	9	/	/
4	100	20	20	100	200	9	/	/
5	100	10	20	100	400	5	/	/
6	100	20	20	100	400	5	/	/
7	100	10	20	100	400	9	/	/
8	100	20	20	100	400	9	/	/
9	100	10	20	100	400	5	5	10
10	100	10	20	100	200	9	5	10

3.3.4 Simulation

To validate the estimated flow behavior, Computational Fluid Dynamics (CFD) Simulations using Ansys Workbench (ANSYS Inc., Canonsburg, Pennsylvania) were performed to predict the flow rate proportions in the different channel paths of the microfluidic devices.

3.3.5 Template Production

After construction of template patterns with appropriate software for technical drawing (AutoCAD, Autodesk Inc., San Rafael, California), the templates, described above, were fabricated on a silicon wafer with titanium undercoating by photolithographic techniques (Xia & Whitesides 1998; McDonald & Whitesides 2002) at the IWE 1. Pre-treatment with oxygen plasma (3 min; 300 W; 200 sccm of O2) and 10 min at 120 °C on a hotplate was done before the wafer was spin-coated with an UV-curable epoxy based photoresist (SU-8 5 and SU-8 100, Microchem Corp, Newton, Massachusetts). The desired structure heights were achieved in a two-step coating process. After each spin-coating process a relaxation time at room temperature followed. Then, soft baking of the deposited layer was performed with appropriate temperature profiles including temperature ramps to avoid film stress and cracks. Subsequently, exposure of the layer was achieved using UV light and the corresponding copper mask. Afterwards, a post exposure bake to increase cross-linking and to stabilize the irradiated areas of the resist was performed. Finally, the wafer was developed in mr-DEV 600 (micro resist technology, Berlin, Germany) followed by a parylene coating and final rinsing steps with isopropanol and water.

3.3.6 Device Production

Final channel structures were prepared from Polydimethylsiloxane (PDMS) (Sylgard 184, Dow Corning Co., Midland, Michigan) molds from corresponding silicon micro templates. To obtain channel structures, liquid PDMS was mixed with a curing agent in a 9:1 proportion and pored over the wafer. PDMS cured within 45 min at 60 °C. The hardened replica were peeled off the wafer and single channel structures were cut from the silicone layer. Afterwards, channel inlets and outlets of 0.8 mm width were punched out

under microscopic control. The devices were bonded on glass slides via oxygen plasma.

3.3.7 Experimental Setup

Silicon tubes (Microtube PTFE 0.3 x 0.76 mm) of 0.8 mm inner diameter and approximately 30 cm in length were inserted to the inlet and outlet of the channel system, which was positioned on the sample plate of an inverse microscope (Olympus CKX41, Olympus Europe GmbH, Hamburg, Germany). The other end of the inlet tube was connected via Luer lock (Globaco GmbH, Rödermark, Germany) to a 5 ml plastic syringe filled with 70 % ethanol. Handling of the syringe was managed by a syringe pump (LA-100, Landgraf Laborsysteme HLL GmbH, Langenhagen, Germany). The other end of the outlet tube was placed into a waste vessel. The channel system was filled with ethanol at a velocity of 100 µl min^{-1} until all channel compartments were completely filled with fluid and no air bubbles were present anymore. Subsequently, the syringe was replaced by a syringe of the same type filled with culture medium and the system was perfused a couple of minutes to remove the ethanol. Introduction of cells was tested with two different methods. With method 1, the cell suspension was sucked into the inlet tube. The tube end was inserted to the Channel inlet again and the pump pumped the fluid into the channel. Method 2 represents the final cell loading procedure, used with second generation channel types, and is schematically presented in figure 5: A 100 µl low binding pipette tip was filled with culture medium. While the perfusion flow with ethanol was still running, the inlet tube end, stucking in the inlet of the channel system, was replaced by the pipette tip filled with the medium. The waste vessel was positioned on a small lifting platform oriented at table height, whereby the channel system was arranged approximately 15 cm above this level. This difference in height (Δh) resulted in continuous medium flow by gravity feed at about 30 µl min^{-1} where the flow velocity could be adjusted by lifting or lowering the lifting platform. During cell loading, velocity of medium flow was strongly reduced by lifting the platform only a few centimeters below the fluid surface in the inlet tip. Flow behavior of cells was observed through an inverse microscope and trapping success was documented via microscope camera (Moticam 3.0 MP, Motic GmbH, Wetzlar, Germany).

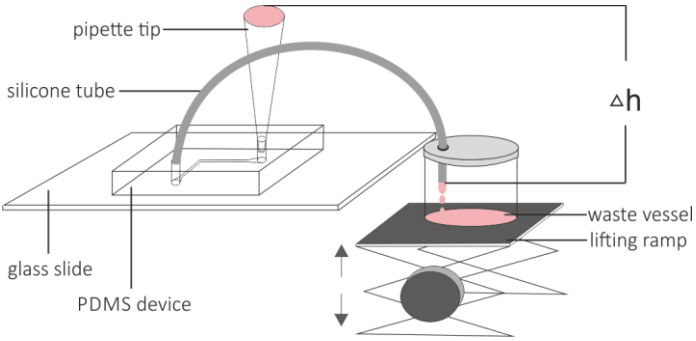


Figure 5: Schematic drawing of the experimental setup (not true to scale). After achieving continuous flow by a syringe pump within the channel system, the tube in the inlet was replaced by a pipette tip filled with medium and the lifting ramp was lowered to keep the flow running. A tube in the outlet directed the fluid to a waste vessel positioned on a lifting ramp. The cell suspension was applied to the pipette tip followed by an immediate lifting of the ramp until flow velocity reaches a minimum ($\Delta h \approx 3$ cm)

3.3.8 Animals

Locusts were kept in the department`s own crowded breeding colonies under a constant light/dark cycle of 12/12 h and were fed with wheat seedlings and wheat bran. Meso- and metathoracic ganglia of male and female *Locusta migratoria* within one week after their final molt were used.

As more homogenous cell suspensions are easier to achieve with pond snail neurons than with locust neurons, most experiments were done with the pond snail (*Lymnaea stagnalis*). The snails originated from the department`s own breeding colony. They were kept in 5 l tanks filled with pond water at room temperature and under a natural light/dark cycle. In the winter months, the light cycle was supported by artificial light with a light/dark cycle of 12/12 h. The animals were fed with lettuce and cucumber slices. For preparation, neurons from the ganglionic ring of young adults with shell lengths of 2 to 3 cm were used.

3.3.9 Cell/Bead Preparation

The preparation of a suspension of neurons of *Locusta migratoria* for cell culture was performed as described previously (Göbbels et al. 2010a & b). The preparation of snail neurons up to the step after enzymatic treatment essentially corresponds to techniques described previously (Ridgway et al. 1991; Kaul 2007) with the following exceptions: instead of using ampicillin for the defined medium (DM) solution a mixture of penicillin (10.000 units/ml) and streptomycin (10 mg/ml), (Sigma-Aldrich Co., Steinheim, Germany) was used. Preparation of ganglia was carried out in sterile normal saline (NS) instead of antibiotic normal saline (ABS). For the last preparation step, realized in DM, further non-neuronal tissue as well as the inner ganglionic sheets were removed from the two pedal, the right parietal, and the left visceral ganglia. These ganglia possess a great number of entities on the one hand and they contain the most cells with large soma diameters above 50 µm on the other. The neurons were mechanically dissociated using fine forceps. Close attention was paid to remove as much non-cellular tissue as possible. Thereby, selection of neurons was not limited to specific types. In order to get the cleanest cell suspension as possible, the neurons were transferred from the first preparation dish with a low binding pipette to another clean preparation dish. Here, they became manually sorted and separated from non-cellular tissue a second time. These neurons, in general between approximately 50 and 100 in number, became introduced by a low binding pipette in a small volume of 20 – 30 µl to the inlet of the channel system. For experiments with particles for preliminary tests, polystyrene beads (Microparticles GmbH, Berlin, Germany) of different diameters (20, 40, and 60 µm) were available in high-density suspensions with phosphate buffered saline (PBS, Sigma-Aldrich Co., Steinheim, Germany). Beads were applied by transferring a defined amount of the suspension to the channel inlet by a micropipette. Trapped cells became incubated at either room temperature or in a Peltier cooling incubator (IPP 55, Memmert GmbH + Co.KG, Schwabach) at 20°C, depending on weather conditions. Observation of cell growth within the following days of culture was managed using an inverse microscope (AxioVert.A1, Carl Zeiss AG, Oberkochen, Germany) and documented via microscope camera (AxioCam ICm1, Carl Zeiss AG, Oberkochen, Germany).

3.4 Results

3.4.1 Flow Rate Simulation

The velocity profiles derived from simulation analyses with CFD, directly correlates with the flow rates in the different channel paths (Fig. 6 & 7). The comparison of the flow velocity profiles in the serpentine geometry (Fig. 6) with the triangle geometry (Fig. 7) shows crucial differences. In the case of free traps, flow in the serpentine trap device is mainly very slow, decreases almost towards zero in the peripheral loops of the main channel area. The preferred path seems to be almost exclusively directed through the short transverse path, where the fluid velocity strongly increases in the narrow trap gaps. The velocity of the fluid in the second generation devices generally is highest in the main channel area of the inlet (Fig. 7). Arriving at the transverse channels towards the cell traps, flow velocity strongly decreases as the fluid divides to the single transverse channels and further along the main path. Fluid flow in the transverse channel areas is highest in the first, followed by the second, third and so forth. While the flow in the actual trapping areas strongly decreased, velocity increases again in the narrow gaps. The flow proportions and velocities are strongly influenced by the trap gap width (Fig. 7, Tab. 3). Narrowing the gap width increases the resistance in the respective channels. While in devices with wider trap gaps (20 µm) almost 70 % of the main fluid volume splits up on the transverse channels, this value decreases to less than the half by reducing the trap gap width to 10 µm.

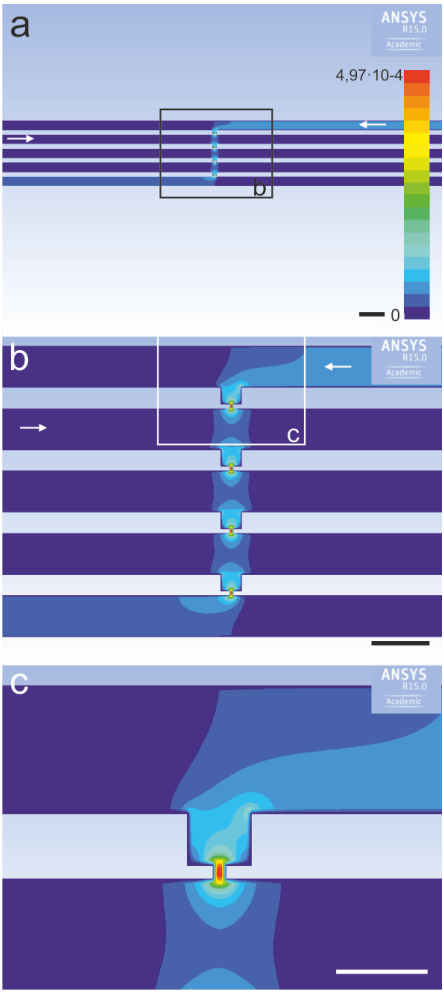


Figure 6. Ansys simulation output showing the velocity profile in a first generation cell trap device, which corresponds to the properties of subtype 3 b (Tab. 1). Flow portion through the transverse path is 70 %. a) Overview. b), c) Magnifications of a) and b) indicated by the rectangles. Arrows indicate flow direction. Scale bars: a), b) 100 µm, c) 50 µm. The color scale varies between dark blue (slow) and red (fast). Exact velocity values can be taken from the color map legend in a), unit: $m \cdot s^{-1}$

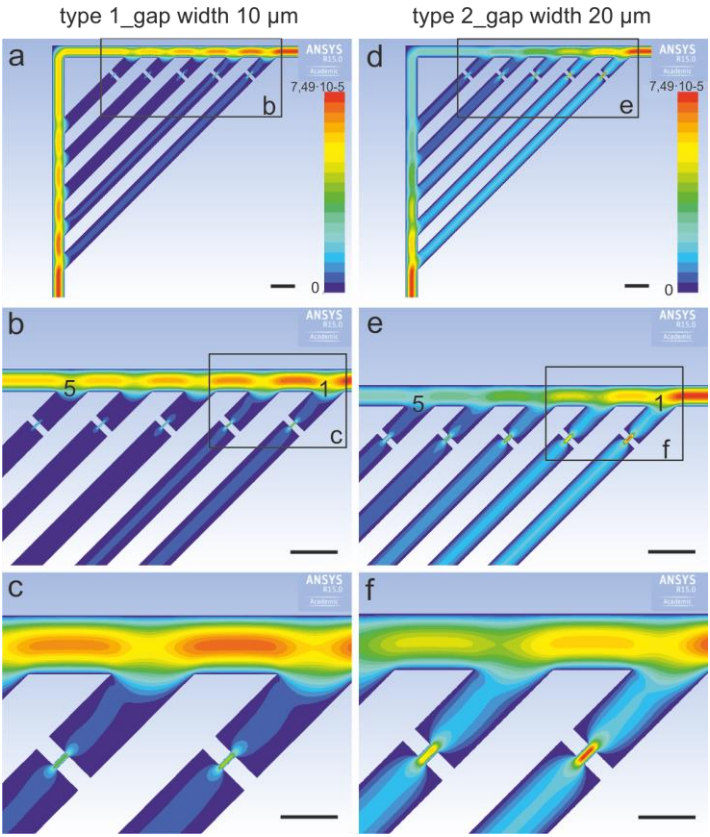


Figure 7. Ansys simulation output showing the velocity profiles of two triangle cell trap devices with varying gap widths. a) - c) Trap device of type 1 with a gap width of 10 µm; b) and c) are magnifications of a) indicated by the rectangles. d) - f) Trap device of type 2 with a gap width of 20 µm, e) and f) are magnifications of d) indicated by the rectangles. Trap 1 and 5 are inscribed in d) and e).Scale bars: a), b), d), and e): 200 µm, c) and f): 100 µm. The color scales vary between dark blue (slow) and red (fast). Exact velocity values can be taken from the color map legend in a) and d), unit: $m \cdot s^{-1}$

Table 3. Mass flow rate proportion in the different channel pathways of the second generation of trap devices (main channel; trap 1-5) as a function of the trap gap width exemplified by device type 1 and 2 (table 2) with 5 transverse channels each.

Gap width	Main [%]	Trap 5 [%]	Trap 4 [%]	Trap 3 [%]	Trap 2 [%]	Trap 1 [%]
10 µm	77,1	2,5	3,5	4,6	5,6	6,7
20 µm	32,7	7,1	9,9	13,0	16,7	20,7

3.4.2 Trapping Experiments with Beads and Neurons

All presented types of cell trap devices were able to capture reliably beads of different diameters (20/40 µm) by using a large number of beads and flow velocities above $1\mu l \cdot min^{-1}$ (Fig.8). On the other hand, functionality with applied neurons was strongly restricted with the initial variant of the first generation devices as well as with the modified devices of the same generation. The observations lead to the assumption that mainly the following distinct parameters are crucial for a successful outcome with invertebrate neurons:

- **Channel dimensions** should fit the applied test objects to prevent channel blocks. The overall geometry should be chosen to achieve a minimized inherent fluidic resistance. Trap gap dimensions should be adequate small to capture trapped cells reliably.
- **Flow ratio** between main and transverse channels should fit the present conditions to achieve maintained trapping success.
- **Flow velocity** should be as low as possible to protect fragile cells from fluid derived strains, like shear stress and fluidic pressure.

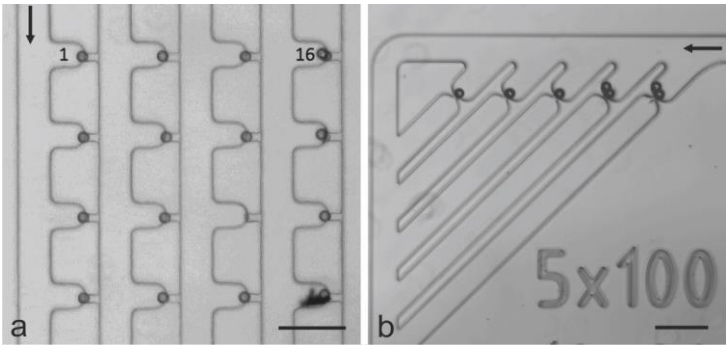


Figure 8. Bead trapping in microfluidic devices. a) First generation microfluidic cell trap device of the serpentine type with a 4 x 4 cell trap arrangement. Trap 1 and 16 are inscribed. With exception of trap 11, all traps are occupied by one or two beads of 20 µm. b) Second generation device of the triangle variant (type 1). All traps are occupied by one or two beads of 40 µm. Flow direction is indicated by arrows. Scale bars: a) 100 µm, b) 200 µm

Channel Dimensions:

Many particles and neurons of the applied cell suspensions turned out to be too large for the 50 µm wide channels of the initial cell trap variant. Consistently, bigger cells or cell clusters blocked the channels irreparably. Non-cellular tissues like neuropil and glial waste leftover from enzymatic treatment, which accumulated especially in locust neuron preparations, turned out to be especially disturbing. Less particles became stuck in the larger main channels of 70 µm of the modified first generation devices but the problem could not eliminated. Still, neurons congested the channel due to their size (SI, Figure 4).

Channel width of 100 µm and general channel geometry and arrangement of the main and transverse channels of the second generation devices resulted in an extremely decreased amount of channel blocks by larger neurons, cell clusters, or non-neuronal debris. However, as the general velocity and therefore pressure in the single traps was higher in the devices with less resistance in the transverse channels, wider gaps of 20 µm could not maintain to capture cells reliably. Most of the particles became squeezed through the larger gaps. In contrast, trap gaps of 10 µm width were more

efficient in capturing neurons and maintained their viability at the same time.

Flow Ratio and Trapping Success:
In case of the initial variant of the first generation devices with 16 traps, it was observed that only a small amount of cells was deflected towards the cell traps. A large part passed the system without being deflected by taking the main channel path towards the outlet. The issue was attempted to be improved by modified loop lengths (tab. 1, subtypes 2 and 3). The extension of the loop lengths lead to an enhanced resistance in the main path and therefore to a modification of the flux ratio between main and transverse channels. Under consideration of the formula presented in the introduction sections, which give evidence about the flow ratios Q1 (main channel) and Q2 (transverse channel), the value for Q1 decreased while the value for Q2 increased. This resulted in an increased proportion value. Consequently, the cells indeed became guided more efficiently to the traps but they could not be captured. The enhanced flow portion through the traps yielded to an enhanced pressure on the trapped particles, as well. Accordingly, they became pressed through the narrow trap gaps (supplementary Information (SI), Figure 1). At the same time, the flow portion through the main channel loops was as much reduced as the particles and cells settled there in several cases (SI, Figure 2). In these cases the main channel became congested, which lead to even more pressure through the transverse channels. Within long loop variants, the problem of an impeded particle transport within the main path could not even be compensated with higher velocities. Only, if a particle occupied a trap completely, flow portion switched sufficiently to the main path yielding to a functioned particle transport in the main channel. However, as the fixation of neurons could not be maintained, neurons that already entered the main path regularly adhered.

In contrast, with microfluidic devices of the second generation, trapping success of different neuron sizes was achieved (Fig. 9). Thereby, with the exception of the trap gap width, results were similar between different device types. Generally, deflection towards the transverse channels was observed to be more efficient in devices with gap widths of 20 µm than of 10 µm, which corresponds to the simulation results. Anyway, despite the low

flow ratios present in the transverse channels with narrow gap widths of 10 µm (Fig. 7) in comparison to wider gaps, trapping success was greater in these trapping devices.

Impureness of applied cell suspensions resulted in occupied traps by non-neuronal tissue occasionally (vertical arrows, Fig. 9 e). Bigger neurons seemed to arrive later at the channels system than smaller ones. These late arriving big neurons of adequate size, then eventually did not find a free trap where the deflection force was strong enough (asterisks, Fig. 9 e). Furthermore, the viability of trapped cells generally was maintained in second generation devices (Fig. 10).

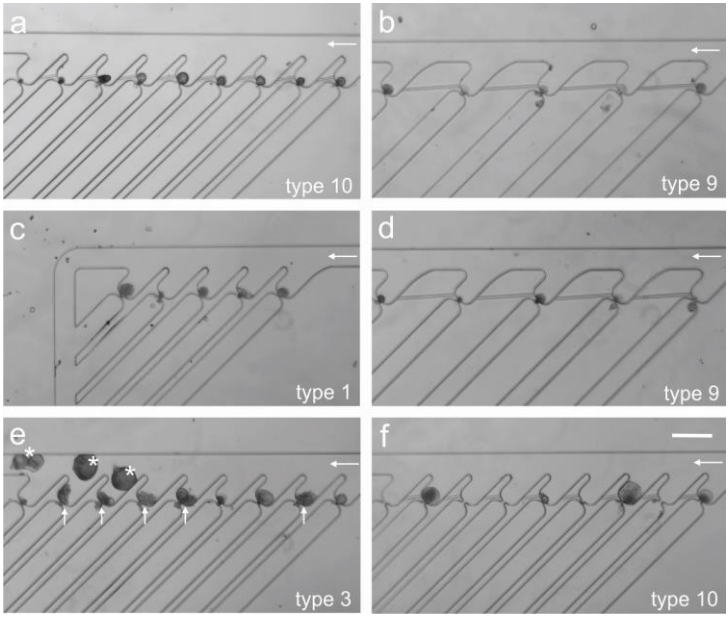


Figure 9. Captured pond snail neurons and particles in different second generation cell trap devices. a-f) Neurons of different diameters occupying the cell traps. e) Vertical arrows at trap 2, 5, 6, 7, and 8 show filling of traps additionally by non-neuronal tissue. Horizontal arrows indicate flow direction. Asterisks mark late arrived large neurons not deflected as already captured particles reduced the deflection force. Scale bar: 200 µm

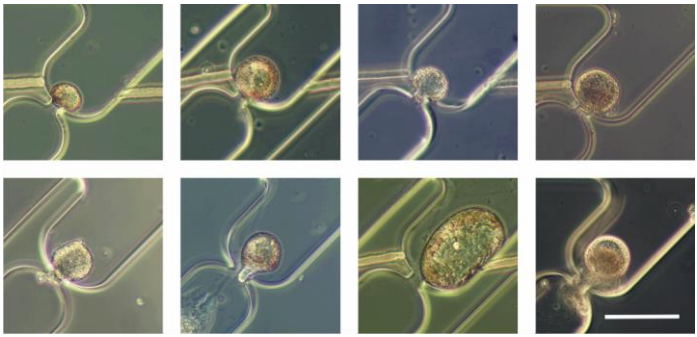


Figure 10. Captured pond snail neurons of different size in detail appearing in a vital shape and color. Scale bar: 100 µm

As the results from the velocity profiles already indicated, in contrast to modified first generation devices, the flow ratio between main and transverse channel was more balanced or even redirected towards the main path again. This resulted in a relatively large amount of cells and particles getting lost as a principle of fact. Thus, it was necessary to introduce a high number of particles (~ 30 to 50) to the pipette tip that strongly exceeded the trap number. Otherwise, it was highly probable that traps stayed empty. Further, order of occupancy, which directly correlates with the flow splitting up on the different transverse channels, did not enforcedly follow the order of traps. In most cases, a more or less random occupancy of the traps occurred (Fig. 11) (SI, Video 1 & 2) whereby this deviation assumed to be smaller in channel types with a larger inter-trap distance. A further observation was the occurrence of multitrapping, which means that several particles were occupied per trap (Fig. 11, Fig. 12) (SI, Video 1 & 2), which was already observed with preliminary device types of the first generation as well.

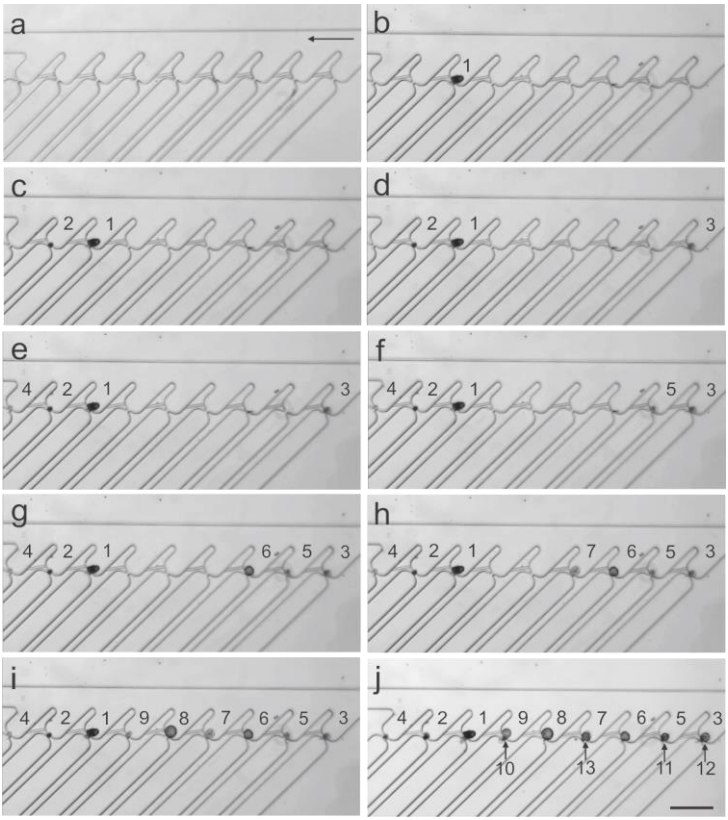


Figure 11. Order of occupancy of pond snail neurons within a microfluidic cell trap of type 10. The arrow in a) indicates the flow direction. The order of figures a) – j) is chronological, showing the apparently random filling of cell traps by arriving neurons. Note filling order of neurons 5-9, which performs the predicted sequential filling order. j) Trap 1, 2, 4 and 6 are occupied by two neurons each. Neurons 10 to 13 occupied the cell traps after the previous cell settled there. Scale bar: 200 µm

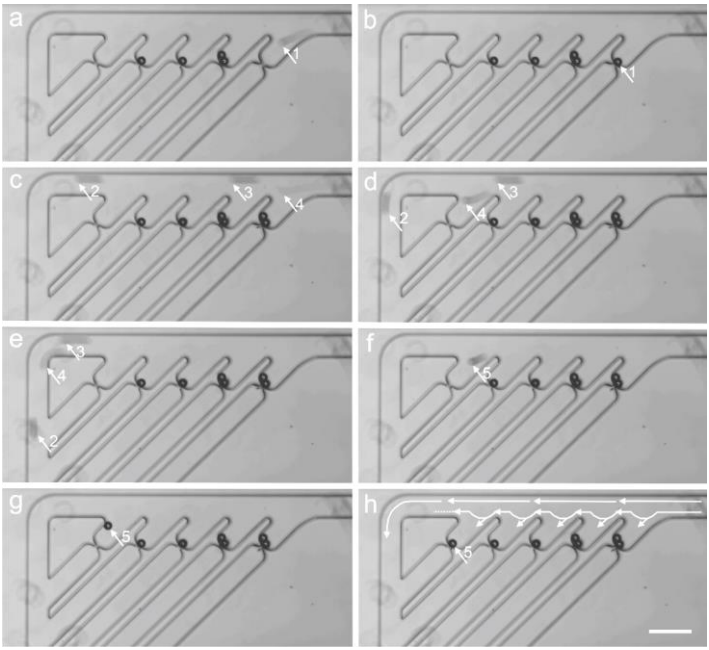


Figure 12. Captured beads in a second generation trap device of type 1. Pictures a) – h) show the experimental course presenting the order of occupancy and flow behavior of individual beads. Observed beads are marked by arrows and numbered in order of appearance to follow their way along the channels. Moving particles appear indistinct as their velocity exceeds technical possibilities to record the movement distinctly. a) Trap 2, 3 and 4 are occupied. Bead 1 appears to become sucked by the flow through trap 1. b) Bead 1 occupies trap 1. c), d), e) Bead 2 and 3 flowing along the outermost path without being deflected. Bead 4 follows the path in the center of the channel becoming slightly deflected by the traps but not captured. f), g), h) Bead 5 is being deflected to trap 5 (f) and captured (g), h)). h) White arrows in line along the main channel represent the alternative flow paths of beads. Scale bar: 200 µm.

Analysis of particle flow revealed at least two different flow paths along the first flank of the main channel (Fig. 12 h). Either, particles were orientated at the outermost border of the main channel across from the entrances to the transverse channels or along the channel center or even nearer to the traps, respectively. In the first case, particles did not seemed to be influenced by the suction towards the transverse channels at all. In contrast,

particles flowed along the main channel in a straight line without being deflected and captured (Fig. 12, c), d): bead 2 and 3). Alternatively, if particles flowed along a second flow path, the suction towards the transverse channels influenced them. That way, they were either captured (Fig. 12 a, b: bead 1; Fig 12 f, g, h: bead 5) or removed to the main path flow again (Fig. 12 d, e: bead 4) resulting in a wavelike flow behavior (Fig. 12 h).

Flow Velocity and Cell Strain:
In general, neurons seemed to be much more sensitive to fluidic pressure and shear stress within the microchannels at higher velocities in comparison to polystyrene beads. The neurons, the bigger they were, became easily ruptured at applied fluid velocities of >1µl · min^{-1} and showed an extreme likelihood to deform when they were subjected to the fluidic pressure in the cell traps. This resulted either in an immediate membrane rupture, or, when a cell was deflected into a trap, in a squeezing of the neuron through the gap. This incident was observed with all first generation variants. To try to compensate this, by lowering the flow velocity, did not succeed, as cells could not be introduced into the system at all any more. They either settled in the inlet (SI, Figure 3) or adhered at the inlet tube walls. Indeed, a changed cell loading procedure with a pipette tip by gravity (see Fig. 5) lead to an improved velocity control and facilitated cell loading slightly. Nevertheless still, only extremely few cells could be introduced into the channels. This problem even increased with longer main channel loops.
With devices of the second generation, the problem could be solved. Save for a few exceptions, neurons were guided by the slowest flow (< 1µl · min^{-1}) into the main channel by gravity feed. In a few cases, they sank down to the bottom of the inlet. This incident could be prevented by slightly raising up flow velocity. After entering the main channel, beads and neurons were observed to be transported by the laminar flow. Thereby, polystyrene beads could be fixed upstream the trap gaps reliably at different velocities. Trapping and gentle fixation of pond snail neurons of different diameters was observed to be more dependent on the velocity but possible as well. Indeed, squeezing of some neurons through the narrow trap gaps occurred occasionally, but this in much rarer cases than in previous device variants. It could be observed that squeezing through the gaps did not necessarily occurred with smaller soma diameters but especially often in the case of

neurons with larger diameters. Best trapping success could be achieved with soma diameters around 30-50 µm. Besides, a slight decrease of the flow velocity could decrease these incidents.

Trap Arrangements:
Observations with neurons in the initial variant of the first generation devices with 4x4 traps assumed an unbalanced deflection probability between the four individual transverse channels along a single loop row. The modified trap arrangement in the late devices of the same generation, where only one trap per loop was arranged, avoided this problem and created a balanced deflection probability to all traps. A difference concerning the alternating trap occurrence per loop in terms of trapping efficiency or cell strain could not be observed. Trapped cells seemed to underlie the same strain in both types. Concerning the serial trap arrangement of the second generation the tendency towards a rejected occupancy of the first and last trap appeared to occur. Indeed, complying with results from simulations, it appeared that the larger amount of cells was guided through the first transverse channel, but a fast and enduring cell trapping in the corresponding trap was observed to be declined in some cases. Several cells became directly squeezed through the gap or only temporarily trapped before they could not resist the pressure any more. The deflection force of the last trap seemed to be weaker than of the main path, when the remaining traps were already occupied.

Neurite Development:
It was possible to cultivate trapped cells for up to 14 days. They showed vitality and developed numerous neurites (Fig. 13). Until now, neuritic branching did not occur in an extent that neighboring cells were connected via neurite channels.

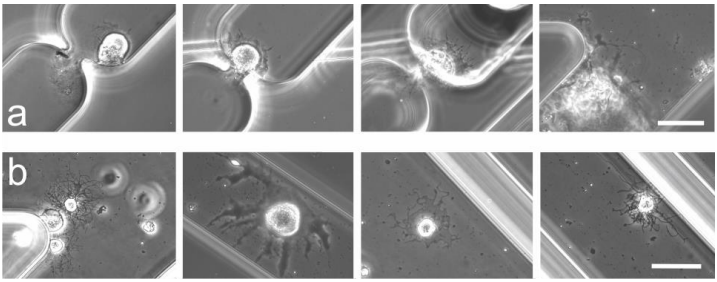


Figure 13: Cultured neurons in microfluidic traps and channels. a-row) Captured neurons at desired location in microfluidic cell trap devices at div 4 showing development of neurites. b-row) Neurons at other locations in microfluidic cell trap devices at div 4 showing development of neurites. Scale bars: 50 µm

3.5 Discussion

Two generally different geometrical concepts to guide mollusk and insect neurons to defined locations by differential fluidic resistances in a laminar flow were presented. First generation variants, which represented modifications of a conceptual design already seen in literature (Tan & Takeuchi 2007; Kobel et al. 2010; Frimat et al. 2011) did not lead to satisfying results with our cell models. Flux ratio, flow velocity and channel design were estimated to be the most important parameters for reliable trapping success. We assumed the necessity of an enhanced flow portion through the transverse channel and slowest velocities at the same time. However, these requirements could not be realized in combination with the present geometrical design of the serpentine type. Therefore, a second generation cell trap device with different geometrical parameters was configured. This type succeeded to compensate for the mentioned deficits observed in the first generation devices.

3.5.1 Channel Dimensions

Generally, channel dimensions of 30-40 % larger than the averaged cell sizes are recommended by similar studies (Kobel et al. 2010) to prevent channel congestions and maintain a reliable deflection towards the traps at the same time. However, this specification is not easy to apply by handling with cell sizes in such a huge range, as it is the case in the present approach. Most other cell suspensions used for similar single cell trapping approaches report much smaller size ranges. The epithelial and epithelial-like cancer cells at Frimat et al. (2010) comprise cell sizes from only nearly 12 µm to about 19 µm.

The widening of the main channel to 100 µm was decided based on the observations of frequent blockages, evoked by large neurons, large cell clusters, or some non-neuronal debris in smaller channels. At the latest since the biological test system *Locusta* was complemented by neurons from *Lymnaea*, channels of 50 and 70 µm width and height did not seem to be sufficient anymore for the great soma diameters that exist in the pond snail brain. Although a declined deflection towards the cell traps, especially with cells smaller than 50 µm, was suspected and later confirmed by simulation and observations of particle flow, this modulation turned out to be a

good choice, anyway. If our cell suspensions would be more homogenous in size, channel dimensions could become adjusted more easily, to fit to the averaged cell diameters.

The squeezing through the gaps, which could be observed mainly in first generation devices but in the second generation devices as well, resulted not only from too high flow rates but also from the fact that most of the cells were not able to block the gap behind the trap completely. Although cell loss might be increased, traps with even smaller gaps than the tested 10 and 20 µm might be even more effective and should be discussed for future cell trap generations. Frimat et al. (2010) used trap gaps of only s µm width. The height of the gaps of the transverse channels was the same as the main channel height, which was 50 or 70 µm in first generation devices and 100 µm in second generation devices. This "vertical gap" (Kobel et al. 2010) would be closed only by a neuron of corresponding size, acting as a plug to stop fluidic flow and therefore fluidic pressure. Kobel et al. (2010) confirmed the deficit of a vertical trap gap in the transverse channel to be a problem of an incomplete channel plug as well. This problem, was discussed in the context of the maintained shear stress on trapped cells and the resulting deformation (Lawrenz et al. 2012) and in terms of multitrapping of cells in one single trap (Di Carlo et al. 2006; Faley et al. 2008; Kobel et al. 2010), which is undesirable in these defined single cell trapping approaches. The "horizontal gaps" in Kobel et. al. (2010) were described to be only three µm in height. Unfortunately, until now, due to technical limitations concerning print resolution for creating the masks by photolithography used for this study, gaps smaller than 10 µm are not realizable. The general geometry of horizontal gaps can be realized by a two-layered SU-8 mold (Kobel et al. 2010), instead of a one-layered for vertical gaps. Although, the production of two layers demands two copper masks, which raises technical and financial expense strikingly, future investments in this direction have to be taken into consideration. However, the defined influence of those low trap gap heights should be checked in detail. Observations and the simulation results confirmed that smaller trap gap cross sections impede deflection of particles (data not shown) as a smaller passage increases the resistance, especially in combination with large main channel widths of 100 µm. Thus, it has to be figured out in detail, which gap height in comparison to the main channel height is suitable. The deflection force

should be strong enough, but the gap has to be small enough at the same time that a single cell can act as the mentioned plug.
Concerning problems of trapping of small cells, multitrapping of several cells or trapping of non-neuronal debris, a previous selection of the cell suspension by size, seems to make sense, which could be achieved by existing inertial microfluidic sorting technologies (Di Carlo et al. 2007; Martel & Toner 2014). Here, particles, suspended to defined forces in special channel geometries, can be focused in different streamlines according to their size. Tests to sort locust and pond snail neurons by size with a spiral microfluidic channel of a type presented in the study of El Hasni et al. (2011) was already done (Neuhof 2014; Ingensiep 2015), but did not lead to satisfying results. Here as well, adequate geometry seems to have to fit to the applied cell size for a successful result, but these conditions differ with varying cell size. Most size separation applications seen in literature show separation efficiency only in very narrow size ranges (Lee et al. 2011). Because of this, we suspect the difficulty to lie in creating a channel geometry that is able to separate such huge size differences. Furthermore, in general, the systems use relatively high flow rates (> 1 ml · min^{-1}) for achieving the desired focusing of the particles. However, such high flow rates were just shown to be very destructive to our cell models. Because of these and similar facts, the possibility of a successful application of such a system with our cell models is questionable to date and alternative solution strategies have to be taken in account.

3.5.2 Flow Ratio and Trapping Success

One of the main points that have to be discussed in terms of the first generation devices is the chosen geometry defining the flux ratios. Kobel (2010) and Tan & Takeuchi (2007) who used a cell trap device with serpentine geometry, as well, calculated the necessity of a flow ratio of 1:2 to 1:3 for a reliable trapping efficiency. These conditions were not complied with the 4 x 4-trap array device of the serpentine type.
The simple lengthening of the main channel, as a model of the predictions of (Kobel, 2010), indeed lead to the desired increase of flow through the transverse channel path and therefore to an enhanced deflection of cells into the traps. Thereby, no differences between the two longer loop length

variants could be confirmed. This is probably corresponding to the observations of Kobel et al. (2010) who proposed a direct correlation between flux ratio and trapping efficiency in general. Indeed, they could achieve an increased trapping efficiency with longer main channel loops, but this effect was only linear to a certain point, where a plateau was reached. From up there, trapping efficiency may not be able to be increased by an increased flux ratio. Therefore, we assume that different loop lengths in our study already ranged in the mentioned plateau region. Tests with beads and high velocities resulted in a trapping efficiency of nearly 100 %. However, as results show, an enhanced deflection force to the traps caused to much strain on trapped objects, while their transport along the main loops did not function with low velocities.

The second generation of cell traps represented drastically geometrical improvements to the common serpentine type. In contrast to the first generation devices, flow ratio between main and transverse path is more balanced again. The main flow rate is not directed exclusively through the only transverse path anymore, but splits up to the several transverse pathways and a large portion to the main path. These observations correspond to the velocity profiles processed by simulation calculations

In this context, observations of particle flow behavior within the second generation devices showed different flow paths within the main channel. Thereby, the deflection force towards the cell traps did not seem to influence the by outer path. Cells and beads generally could not be captured if they took this outermost path. The chosen geometry caused this issue. Lengths of the transverse channel are only slightly shorter than the path through the main channel flanks and the narrow trap gaps increases fluidic resistance, as well. Thus, flow ratio through the traps is comparatively low. However, results from experiments confirmed that the deflection force and therefore trapping success is still strong enough, even in devices with narrow trap gaps. We decided to accept a declined deflection force towards the traps, because the system was in need for a decreased strain on the cells, which could be achieved with the present geometry. In addition, the loss of a relatively large amount of cells during a cell trapping experiment is to be coped with, as it is easy to receive a great amount of cells from the brains. For other single cell trapping approaches, often a far larger amount

of cells per application is being used, probably not at least to enhance trapping success (Wlodokowic, 2009). Through further modifications in terms of a calculated lengthening of the first main channel flank, an influence on trapping efficiency could be proven. With this method, Kobel (2010) achieved a trapping efficiency of 97.2 % in a device with the serpentine design. However, it has to be kept in mind that an extension of the main channel probably might increase the overall fluidic resistance of the device again, which would impede cell loading.

In contrast to the predicted order of trap filling from the first to the last, the filling of the traps occurred more randomly. Even if one trap was already occupied but not completely blocked, yet, which should decrease deflection forces extremely, it was possible to observe multitrapping events here. It is assumed that these observations are mainly due to the observed splitting of the flow ratios on the different transverse channels and the related different flow streams within the main channel. It cannot be excluded that a particle possibly can change between the streamlines along the main channel resulting in a late deflection. A scenario like this is thinkable especially for bigger cell sizes that are probably influenced naturally by two adjoined narrow streamlines. However, the heterogeneous cell suspensions in terms of size, particle type (neuron or other tissue) and arrival time probably might be responsible as well. Here, different cells, flowing on different flow streams in the same channel, may influence each other. In case of impinging, suddenly flow stream might change due to the collision. In addition, short-term turbulences in the branching region towards the cell traps are thinkable. A third possibility is that they are deflected first but then again deflected back to the main channel due to the wavelike flow stream (Fig. 12 h). These conditions possibly could cause some short-term irregularities, which balance again, when the trap is passed. Probably this might explain preliminary differing observations with different trap distances concerning trapping order. The deviation from the predicted order seemed to occur less often in devices with larger trap distance. Here, short term turbulences in the area of a channel intersection might have more time to become balanced again as the distance to the next intersection is increased. However, until this point, we do not evaluate these incidents of an irregular capture order negatively. As long as trapping in all traps occurs, the order does not seem to be important.

3.5.3 Flow Velocity and Cell Strain

The combination of syringe pump, inlet tube, slowest flow rates, and first generation devices was not applicable. Needed flow rates of down to 0,1 µl · min^{-1}, produced by the syringe pump, lead to an intolerable loss of especially bigger cells, but beads as well, already in the inlet tube. Here, flow rate turned out to be too low to overcome the high inherent fluidic resistance of the system and thus to transport the neurons in the fluid stream. They simply settled and adhered to the tube walls, which could be proved by nucleus stainings with 4′,6-Diamidin-2-phenylindol (DAPI) after an experiment (data not shown). If they did not adhere to the tube wall, they probably settled at the bottom of the inlet round (SI, Figure 3). Generally, only cells with smaller diameters, similar to, or even smaller than the trap gaps, arrived at all, but of course they could pass the traps without being hindered. Short-term flow rate raises could compensate this incident to a certain degree. However, the used syringe pump was very inert, so flow rate adjustments lasted up to minutes, which caused cell loss as well, as they passed the cell trap within a far too high flow rate. Induced flow by driven by gravity (Fig. 5) in combination with the use of a pipette tip instead of a long inlet tube represented an improvement. Thus, height adjustments of the outlet tube could directly adjust, start and stop the flow and cells only had to overcome only a short distance until they reached the channel. However, the results still were not satisfying as most cells still adhered to the glass of the inlet round. In addition, flux velocity in the outermost parts of the loops was too slow to transport the particles reliably within the flow. The long distances along the single meandering path increased the inherent fluidic resistance of the system, which turned out to be difficult to overcome with low velocities. Difficulties with cell loss in the inlet or within the long paths of the main channel were not reported by other studies before, although equally low or even less flow rates are frequently used there as well (Kobel et al. 2010). For cell loading, Kobel (2010) even used flow rates of only 20 nl · min^{-1}. The spontaneous adherences at undesired locations, seems to be due to properties of our cell types, as this was not reported by other studies and with other cell types, yet. However, this is not surprising. It is known from most vertebrate cells that they do not adhere at all to artificial substrates without any ECM-protein coating. Further, frequently, the cell lines used for trapping approaches within microfluidic devices are from

a non-adherent type in the first place (Kobel, 2010). In contrast, insect and mollusk neurons are very undemanding concerning their growth substrate. They do not need any chemical coatings in terms of ECM-proteins, like laminin, for a good adherence on glass or polystyrene. Actually, these properties were assessed to be advantageous, as they allow for easy culture conditions, which is wanted as well in the context of *in vitro* networks. Besides, they allow the cultivation of neurons directly on the electrodes of a MEA, which is advantageous as well. In the context of failed adherences to undefined locations within a microfluidic channel, solutions have to be discussed. Future channel surfaces, outside the trapping and culture area, should be of non-adherent material or be coated with non-adhesive chemicals. Until now, the only materials that at least strongly restrict cell adherence are agarose and Polydimethylsiloxane (PDMS) for *Locusta* neurons (Göbbels et al. 2010a) and agarose for *Lymnaea* neurons.

To achieve efficient application with the corresponding devices of the first generation, high flow velocities were necessary to overcome the inherent fluidic resistance of the long channel and to impede cell adherences. While the necessity of high flow velocities (>10 µl·min^{-1}) is possible to implement with artificial beads, for invertebrate neurons those flow rates turned out to be far too high to achieve cell trapping and to maintain vitality of the neurons at the same time.

The differences between beads and neurons are main points in this context and therefore at least partly responsible for the success with beads on the one hand and the failure with neurons at high flow velocities on the other. Beads and cells seem to have completely different requirements on such a system and are therefore only comparable to a certain degree.

Artificial, inelastic beads are always homogenous in size and weight. In contrast, living, deformable neurons with most diverse cell sizes (10-120 µm) are deformable and their shape is often not distinctly defined. Due to attached axonal processes or non-neuronal tissue, an unrestricted prediction of their flow behavior is challenging. Shear stress and fluidic pressure due to high velocities lead to membrane ruptures. In addition, Neurons of larger size often seemed to be even more sensible to the strain. The greater cell surfaces of far larger neurons from invertebrates, although known to be very robust and undemanding under culture conditions, are influenced by increased pressure and therefore these cells underlie even more strains.

With smaller cell types used in other studies, like stem cells (Kobel et al. 2010, 2012), fibroblasts (Marimuthu & Kim 2013), epithelial cells (Frimat et a. 2010), yeast cells (Braschler et al. 2005), liver cells (Park et al. 2007) or blood cells (Wheeler et al. 2003), this seems to be not such a big issue. At least in the case of blood and lymph cell types, whose natural environment is the constant flow, it seems obvious that they have to be far more robust to strains present in laminar flow.
Dinh et al. (2013) described problems with deformation of cells and loss of cells because of squeezing through the gaps, as well. There, it was pointed out that cell-loading procedure, thus strain, should be as short as possible.
From our point of view, not only the fact of using living cells but the used cell types and the used cell sizes are further essential points, although the problem of shear stress induced apoptosis and cell lysis absolutely is being discussed elsewhere with other cell types and sizes (Faley et al. 2008; Kobel et al. 2010; Dinh et al. 2013).
We conclude that successful results with beads can only represent a proof of principle, but they cannot guarantee a universal application.

3.5.4 Cell Trap Arrangement

Cell traps of the second generation are arranged in a linear row along the first flank of the main channel within the transverse channels. First prototypes already tested small interconnecting channels, for neurite guidance towards neighboring network participants. Thus, trapped cell are allowed to connect to two neighboring cells. Location of trap gaps were chosen to be located about 150 µm below the transverse channel entrance in the present prototypes for two different reasons. First, we decided that a trapped cell should not be influenced by the maintained current flow within the main channel and run the risk to become adrift again. Complying with this condition, we chose a distance, which corresponds to one and half time to twice the diameter of the biggest cell expected to capture. In contrast to trap arrangements of the initial variant of the first generation devices, the actual serial arrangement is not conform to the aimed network of cells arranged in an array, yet. Due to the current problem of multi-neuron-trapping, deeper cell traps were avoided until now, although the possibility of different trap locations can be advantageous, especially concerning the desired arrangement of neurons in an array fitting to common MEA-electrode

arrangements. So, in future types of microfluidic cell traps that solved the problem of multitrapping, trap arrangement could be modified. Trap gaps at different locations along the long transverse channel could converge towards more array-like formation of neurons. Here, interconnecting neurite channels could be integrated like it was already shown in this study. If main channel paths should not be crossed by a neurite channel and a more defined interconnection between single cells should be achieved, a second possibility is thinkable. By a second PDMS level above the trapping level with a defined neurite channel network, a three dimensional network could be achieved. The corresponding community agrees on the advantages of 3D network construction of cells *in vitro* in contrast to 2D interconnections already for quite some time, as cell growth in three dimensions resemble more the *in vivo* conditions (for reviews see: Griffith & Swartz 2006; Tehranirokh et al. 2013). Geometrically modifications by creating devices with corresponding transverse channel number can easily adjust the number of traps and therefore the number of trapped cells on demand. It is assumed that flow conditions do not change with different device sizes or different transverse channel numbers.

3.6 Conclusion

Common microfluidic designs of the serpentine type are applicable with beads but only heavily with invertebrate neurons. We concluded that distinct differentiations between the inherent properties of artificial beads and living cells, responsible for the deviating results, have to be stated. The main points to mention are:

-The varying particle size and inhomogeneous neuronal suspensions vs. a constant particle size and homogenous suspensions concerning beads

-Inelastic plastic surface of beads vs. deformable, fluid filled somata of neurons

-Defined shape of beads vs. undefined shape of neurons due to axonal processes and attached non-neuronal tissue

Consequently, the geometrical conditions of the first generation devices, with high inherent fluidic resistance were not compatible with the demands of the invertebrate neurons.

We developed a new geometry for microfluidic cell trapping, which finally achieves gentle and maintained trapping success at low flow rates of large and sensitive pond snail neurons and reduces channel blocks and pressure fluctuations. Slow flow is able to guide particles gently towards the cell traps and reduces the fluidic pressure and shear stress on already trapped cells.

Future modifications concerning trap gap size and shape, and trap arrangements are proposed to further improve trapping efficiency and gentle handling of cells, and to facilitate the combination with electrode arrangements of common MEA chips.

4 Agarose-Based Substrate Modification Technique for Chemical and Physical Guiding of Neurons *in Vitro*

4.1 Statement of Shared Workload and Publications

This study was carried out under the supervision of Univ.-Prof. Dr. Peter Bräunig and Dr. Katrin Bui-Göbbels. Except for the results presented in figure 22, 24, and the appendant text parts in the methods- and results section, this chapter has been published previously: Krumpholz et al. (2015), Agarose-Based Substrate Modification Technique for Chemical and Physical Guiding of Neurons *in Vitro*, ACS Appl. Mater. Interfaces, 7, 18769-18777.
Dr. Katrin Bui-Göbbels, Univ.-Prof. Dr. Peter Bräunig, undergraduate student Julia Rogal and Katharina Walczuch were involved in the development of the conceptual design of the production technique and its application. The experimental part in terms of technical development, cell culture and their examination was done by Katharina Walczuch and Julia Rogal in the course of her bachelor thesis with support from Dr. Katrin Bui-Göbbels and Univ.-Prof. Dr. Peter Bräunig. Julia Rogal performed initial application tests with locust neurons and Katharina Walczuch completed the results and carried out the experiments with pond snail neurons. Univ.-Prof. Dr. Peter Bräunig, Dr. Uwe Schnakenberg and Akram El Hasni from the IWE 1, RWTH Aachen University, provided technical support and advice. The production of the silicon wafer for pattern molding was provided by the IWE 1 as well.

Results were analyzed and interpreted by Katharina Walczuch, Julia Rogal, and Dr. Katrin Bui-Göbbels with support from Univ.-Prof. Dr. Peter Bräunig. Katharina Walczuch wrote the manuscript.

4.2 Introduction

The understanding of the development and function of neuronal networks is of high interest but at the same time a big challenge. The investigation of neuronal networks *in vitro* helps to overcome the highly complex situation *in vivo*. However, also in *in vitro* approaches, simplification of complex networks seems to be necessary for a detailed understanding of network processing.

This simplification could be achieved by creating defined small networks *in vitro*. In really small networks, with less than 20 neurons, individual cells can be identified and a better overview of the activity of single units and their influence on the functionality of the network can be established (Massobrio et al. 2009; Massobrio et al. 2013). These conditions can easily be achieved by using invertebrate neurons. Network activity *in vitro* can be investigated with different methods. Meanwhile, non-invasive electrophysiological methods are state of the art as they allow for long-term observations of neuronal activity. A common method here is the use of multielectrode arrays (MEAs) (Thomas et al. 1972; Novak & Wheeler 1988; Gross et al. 1995), but other extracellular recording electrodes (Moriguchi et al. 2007; Kwiat et al. 2012; Edwards et al. 2013) as well as optical methods like Ca^{2+}-imaging (Sugio et al. 2004; Li et al. 2014) are also used.

The development of small and defined neuronal networks requires patterning of the growth substrate. Patterning means subdivision of the substrate with special chemical coatings and/or topographically raised barriers into cell attracting regions and regions where cell adhesion and neurite outgrowth is inhibited. Over the years, different technologies to achieve such network patterns were developed ranging from printing, adsorption, photo - and soft-lithography to laser writing or combinations of these (Kleinfeld et al. 1988; Corey et al. 1991; Branch et al. 2000; Prinz & Fromherz 2000; Moriguchi et al. 2002; Merz & Fromherz 2002; Sugio et al. 2004; Suzuki et al. 2004; Merz & Fromherz 2005; Suzuki & Yasuda 2007; Jun et al. 2007; Jungblut et al. 2009; Pirlo et al. 2011; Marconi et al. 2012; Kwiat et al. 2012; Odawara et al. 2013; Li et al. 2014). More recent studies even used magnetic (Delacour et al. 2014) cues as well as electrophoresis (Jaber et al.

2013) in addition to traditional pattern technology to improve neuron positioning. However, all these and related studies focus on the specific demands of the applied cell system to its microenvironment (Théry 2010).
A widely used patterning substance is agarose. Agarose is a natural, non-cytotoxic, and transparent hydrogel allowing easy conversion from gel to liquid. Agarose is non-adhesive for many cell types. Thereby, agarose substrates may provide a chemical as well as physical barrier for cells in culture (Moriguchi et al. 2002a; Suzuki et al. 2004b; Sugio et al. 2004; Tourniaire et al. 2006; Kang et al. 2009; Mercey et al. 2010). Agarose patterning can be used for the positioning of single cells but also for isolation of small cell clusters. Moreover, agarose patterned small networks on electronic devices or other substrates can be utilized for neuronal activity investigations (Sugio et al. 2004; Suzuki et al. 2004a; Suzuki & Yasuda 2007; Kang et al. 2009) with various methods.
In this study, a new and simple method for the fabrication of agarose substrates patterned by soft-lithographic techniques is presented. We used photolithographic microstructured templates for molding defined topologies in agarose. The final product consists of thin agarose slices of defined thickness cut by a vibratome and containing open wells and closed channels, which are positioned on a variety of substrates. The vibratome slices were tested for patterning of cultures of two different invertebrate biological test systems. Neurons of the locust *Locusta migratoria* and of the pond snail *Lymnaea stagnalis* were used. Insect and mollusk neurons provide the advantage over vertebrate cells of their suitability for the building of small networks *in vitro* as they can be cultured in low cell density (Fromherz et al. 1991; Claverol-Tinturé et al. 2007; Massobrio et al. 2009; Greenbaum et al. 2009; Massobrio et al. 2013; Massobrio et al. 2015). Furthermore, many neurons of invertebrates are very large (>100 µm). So they can cover individual electrodes of a MEA completely which leads to a better signal-to-noise ratio. In addition, a one-to-one coupling of neuron and electrode in such networks is attractive as like this, the unambiguous allocation of signals to certain cells can be done. Nevertheless, the presented slices for cell growth guiding produced by our technique provide the potential for the application of a far wider range of cell systems, which include cells from vertebrates.

4.3 Methods

4.3.1 Template Design

The template devices consisted of either four by four arrangements of 16 circular pins (Fig. 14a, c) or eight by eight arrangements of 60 circular pins (Fig. 14b). The pins were either completely isolated from each other or connected by low bars. Each pin molded a corresponding hole in an agarose hydrogel and each bar a low channel, respectively. Pin diameter, pin interspace and the length and number of bars varied between different arrangements either to suit different MEA layouts or to test different conditions for cultured neurons. Detailed parameters can be obtained from figure 1. Onto each 16-pin arrangement with bars, two triangular shapes were added. These triangles, after cutting slices, helped to choose the correct orientation of the agarose slice with the channels pointing towards the substrate as the channels were open only to one side of the subsequent slice. The orientation was correct when the acute angles pointed clockwise.

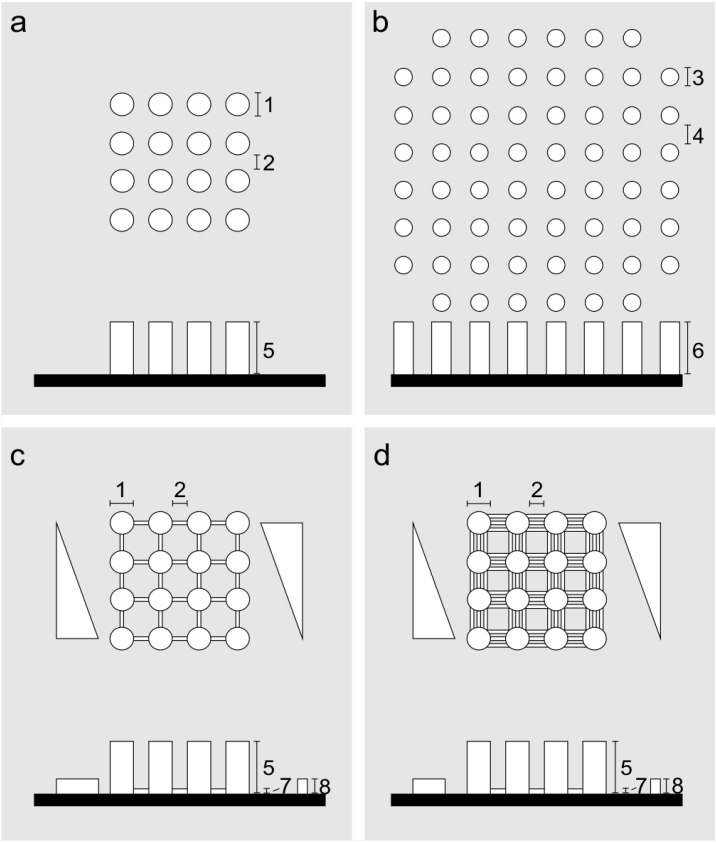


Figure 14: Schematic illustration of silicon template geometries and dimensions as top and side view. a) 16 pin arrangement without bars. b) 60 pin arrangement without bars. The arrangement was produced with interconnecting bars as well. c) 16 pin arrangement with pins interconnected by single bars and triangles for agarose slice orientation. d) 16 pin arrangement with pins interconnected by triple bars and triangles for agarose slice orientation. Dimensions (not true to scale): pin diameter (1): 110 µm, pin interspace (2): 90 µm, pin diameter (3): 90 µm, pin interspace (4): 110 µm, pin height (5): 250 µm, pin height (6): 180 µm, bar height (7): 5 µm, triangle height (8): 15 µm

4.3.2 Photolithography

The templates described above were fabricated on a silicon wafer with titanium undercoating by photolithographic techniques (Fig. 15) (Xia & Whitesides 1998; McDonald & Whitesides 2002). Pre-treatment with oxygen plasma (3 min; 300 W; 200 sccm of O2) and 10 min at 120 °C on a hotplate was done before the wafer was spin-coated with an UV-curable epoxy based photoresist (SU-8 5 and SU-8 100, Microchem Corp, Newton, USA). The desired structure heights were achieved in a two-step coating process, one for the bar height and one for the pin height using SU-8 5 and SU-8 100, respectively. After each spin-coating process a relaxation time at room temperature followed. Then, soft baking of the deposited layer was performed with appropriate temperature profiles including temperature ramps to avoid film stress and cracks. Subsequently, exposure of the layer was achieved using UV light and the corresponding foil mask. Afterwards, a post exposure bake to increase cross-linking and to stabilize the irradiated areas of the resist was performed. Finally, the wafer was developed in mr-DEV 600 (micro resist technology, Berlin, Germany) followed by rinsing steps with isopropanol and water. Several hundreds of arrangements with the described dimensions were arrayed on one silicon wafer (Fig. 15 a).

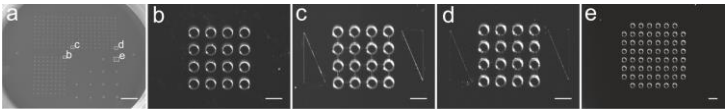


Figure 15: Silicon wafer with pin and bar templates for substrate patterning. a) The overview shows the arrangement on the wafer of four fields, each consisting of multiples of one of the 4 different pin arrangement designs. b)-e) Different pin designs as indicated by rectangles in a) at higher magnification. b) 16 pins without bar connections c) 16 pins with single interconnecting bars d) 16 pins with triple interconnecting bars e) 60 pins for MEA applications with larger interspace between single arrangements as only one arrangement per MEA and slice was needed. Scale bars: (a): 1 cm, (b)-(e): 200 µm

4.3.3 Agarose Slice Fabrication

In order to produce agarose gel slices with guiding structures, an agarose stock solution of either 3 % or 4 % agarose (NEEO ultra-quality, Carl Roth, Karlsruhe, Germany) in phosphate buffered saline (PBS, Sigma-Aldrich Co., Steinheim, Germany) was prepared and sterilized by autoclaving (121 °C, 20 min). Both concentrations were equally suitable for the application. Lower as well as higher agarose concentrations resulted in either instable or brittle gel layers. The cured agarose stock solution could be re-used several times by warming in a microwave oven. The following procedure is shown schematically in Fig. 16: First, the wafer with the templates was preheated on a hotplate (50 °C) to avoid fast hardening of the gel. Liquid agarose was cast over the silicon wafer until the pins were fully covered. The culture dish with the wafer was panned to get an equal distribution of the gel over the whole wafer and to prevent the inclusion of air bubbles between the agarose and the wafer surface. The wafer was transferred to a refrigerator where the agarose solidified in a couple of minutes. Afterwards, the hardened replica on the wafer surface, about 0.5 cm thick, was peeled off. Agarose gel cylinders for cultures on glass or culture dishes were punched out such that the bottom part of each cylinder contained several well arrangements. For cultures on MEAs, only one arrangement in the middle of the cylinder was taken. The diameters of the cylinders were chosen to suit the growth substrate used for cell culture. The agarose guiding structures were produced by cutting slices off the cylinders using a vibratome (VT1000 S, Leica Microsystems, Wetzlar, Germany). An agarose cylinder with the well arrangements pointing upwards was glued onto the mounting plate of the vibratome, which was located in a trough filled with distilled water. The vibration frequency of the vibratome was set to 50 Hz, the cutting velocity to 1.6 mm/s and the thickness of the slices to 30 µm, 50 µm, 80 µm or 120 µm, respectively, to test for slice stability and the influence of the well depth on neurons in culture. In case of well arrangements with channels, naturally, because of the low bar height, only the first slice contained wells and channels. Every further slice still contained isolated wells. According to the pin heights of the wafer, it was possible to produce three to five 50 µm thick agarose slices per cylinder. After cutting, slices were transferred from the trough to a dish filled with distilled water. Here, they could be stored over a period of at least eight weeks.

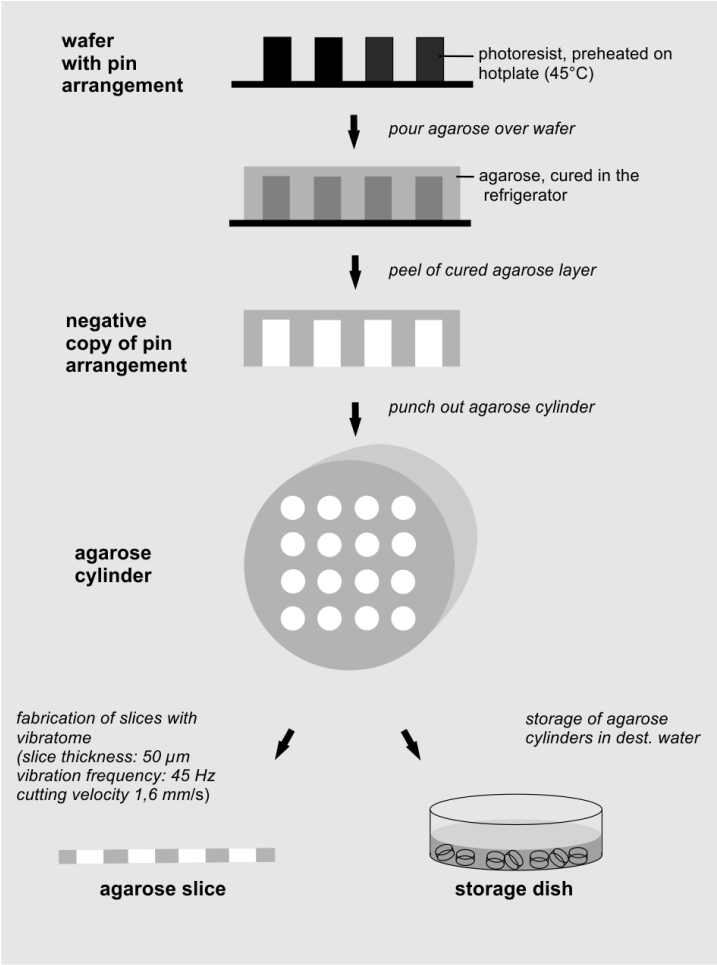


Figure 16: Schematic illustration of agarose slice production process (not true to scale). The silicon wafer was preheated on a hotplate before liquid agarose was poured on the wafer. Agarose curing occurred in the refrigerator within minutes. Subsequently it could be peeled off the template. Cylinders of favored diameter was punched out and either cut into vibratome slices or stored in distilled water for later use.

4.3.4 Culture Substrate Preparation

Agarose slices were positioned on different substrates. We used either glass coverslips (Ø 12mm, Marienfeld, Lauda-Königshofen, Germany) or polystyrene culture dish surfaces (Ø 35mm, ThermoScientific Nunc, Braunschweig, Germany) as these are used as standard substrates for locust and pond snail cell culture. In addition, the agarose slices were tested on MEA-surfaces, where the electrode material was gold, titanium nitride (Multichannel Systems (MCS), Reutlingen, Germany) or platinum (Qwane Bioscience, Lausanne, Switzerland) and the passivation layer was composed of SU-8 (Qwane Bioscience, Lausanne, Switzerland) or silicon nitride (MSC, Reutlingen, Germany). Agarose slices for cell culture were sterilized in 70 % ethanol for five minutes, subsequently rinsed two times in sterile PBS or distilled water and then positioned on the substrates. When culturing on glass, coverslips were sterilized by an ethanol flame and positioned in cell culture dishes. Afterwards, a droplet of 100 µl PBS or water was given to the glass coverslips and agarose slices were fixed on them. The correct position of the channels and wells was determined and adjusted under microscopic control. PBS/water had to evaporate before further steps followed.

4.3.5 Long-Term Attachment Test

For long-term attachment and stability tests, agarose slices were positioned and culture chambers were filled with cell culture medium and incubated at either 20 °C or 30 °C without cells. We tested four MEAs and four glass coverslips covered with agarose slices. Four culture dishes with agarose slice covered glass coverslips were placed on a shaking device at room temperature for three days, simulating immunohistochemically staining procedure. Attachment was controlled every day. These tests occurred independently from several cell culture experiments with agarose slices, where slice adhesion usually was maintained within the period of the cell culture experiments, which generally was aborted after about one week.

4.3.6 Determination of Agarose Slice Thickness

In order to investigate the precision of the vibratome, the thickness of different agarose slices was measured using a confocal laser scanning microscope (TCS SP2, Leica Microsystems, Wetzlar, Germany). For this purpose,

the agarose was stained with 1% fluorescent microspheres (FluoSpheres® sulfate microspheres, 0.2 µm, yellow-green fluorescent), (Molecular Probes, Life Technologies Invitrogen, Darmstadt, Germany) but otherwise treated as described above. The vibratome was set to cut 50 µm thick slices. Four slices of different agarose cylinders were produced and positioned on glass coverslips. For each of the four slices, three different 16 well arrangements per slice were chosen and three to four well depths per arrangement were measured. In this way, data of 40 wells were obtained. Confocal Z-stacks of stained agarose slices were collected using a 64 x oil immersion objective in combination with an argon/krypton laser (excitation wavelength 488 nm, detection range 500-535 nm). The maximum extension of the Z-stacks served as a measure for the thickness of the slices. The obtained data were averaged.

4.3.7 Animals

They were kept in department`s own crowded breeding colonies under a constant light/dark cycle of 12/12 h and were fed with wheat seedlings and wheat bran. Ganglionic rings of the pond snail *Lymnaea stagnalis* were used. Meso- and metathoracic ganglia of male and female *Locusta migratoria* within one week after their final molt were used. The snails originated from the department`s own breeding colony. They were kept in 5 l tanks filled with pond water at room temperature and under a natural light/dark cycle. In the winter months, the light cycle was supported by artificial light with a light/dark cycle of 12/12 h. The animals were fed with lettuce and cucumber slices. For preparation, young adults with shell lengths of 2 to 3 cm were used.

4.3.8 Cell Culture

Preparation of suspension of neurons of *Locusta migratoria* for cell culture was performed as described previously (Göbbels et al. 2010a & b). A droplet of 100 µl cell suspension was added to the agarose substrates to plate the cells. Cells dispersed randomly into the wells or outside the wells on the agarose surface. The number of cells within the wells could be increased by either raising the cell density of the suspension or by manually positioning of single neurons into the wells using an eyelash. After plating, the cells were allowed to adhere to the substrate for about one hour before 3 ml

medium was added to each culture dish. For cultivation, the dishes were maintained at 30 °C. The preparation of snail neurons up to the step after enzymatic treatment essentially correspond to techniques described previously (Ridgway et al. 1991; Kaul 2007) with the following exceptions: instead of using ampicillin for defined medium (DM) solution a mixture of penicillin (10.000 units/ml) and streptomycin (10 mg/ml), (Sigma-Aldrich Co., Steinheim, Germany) was used. Preparation of ganglia was carried out in sterile normal saline (NS) instead of antibiotic normal saline (ABS). For the last preparation step, realized in DM, further non-neuronal tissue as well as the inner ganglionic sheets was removed and the neurons were mechanically dissociated using fine forceps. The inner neuropil was also removed. Thereby, selection of neurons was not limited to specific types. Rather, every ganglion of the ring was dissociated and all cells were used for cell culture to enlarge cell crop and therefor to enlarge chance of well occupancy with cells. Cells were transferred into a low binding tube (2000 µl, Biozym, Hamburg, Germany) filled with DM by a low binding micropipette (200 µl, Biozym, Hamburg, Germany). Further steps correspond to the locust preparation procedure described at (Göbbels et al. 2010a & b) after enzymatic treatment. For cultivation, the culture dishes were maintained at 20 °C. Neurite outgrowth and viability of the cells were observed by phase-contrast microscopy (Olympus CKX41, Hamburg, Germany) and documented using a microscope camera (Moticam CMOS 3.0 MP, Motic, Wetzlar, Germany).

4.3.9 Influence of Agarose Slice Thickness on Cell Survival

For culture condition analysis of neurons in different well depths, locust cell culture was performed with three different agarose slice thicknesses. Therefore, agarose slices with corresponding 4x4 arrangements of three different heights, 50 µm, 80 µm and 120 µm were produced at the vibratome. For each height condition, four independent cell culture experiments were conducted. Thus, every experiment consisted of four culture dishes, one for every substrate height condition and one for control, which contained no agarose slice. The cultured neurons of one experiment derived from meso- and metathorax of two animals, which were pooled previously to ensure equal original conditions. The number of living cells within

the agarose impressions was counted on day *in vitro* (div) 1, 2, 3, and 7. The particular results of every condition were averaged.

4.3.10 Immunohistochemistry

Immunohistochemically staining was done using cell cultures between div 4 and 7, because previous observations showed the maximum of neurite outgrowth in this period. The cells were fixed with 4 % formaldehyde (FA, 37% Applichem, Darmstadt, Germany). Locust neurons were specifically marked by an antiserum against horseradish peroxidase (1:10.000), (rabbit-anti-HRP, Sigma-Aldrich Co., Steinheim, Germany) (Jan & Jan 1982) and visualized with a Cy3-conjugated secondary antibody (1:5000), (goat-anti-rabbit-Cy3, Jackson Immuno Research, Newmarket, Suffolk, UK). For mollusk neurons, no specific marker exist. Staining of cells was achieved by using an antiserum against α-tubulin (1:500), (mouse-anti-tubulin, Exbio Antibodies, Vestec, Czech Republic). The antibody was visualized with a Cy3-conjugated secondary antibody (1:5000), (goat-anti-mouse-Cy3, Jackson Immuno Research Europe Ltd., Newmarket, Suffolk, UK). After staining, substrates were mounted to glass slides with Mowiol® (poly(vinyl alcohol), Sigma-Aldrich Co., Steinheim, Germany) and analyzed with the confocal laser scanning microscope.

4.3.11 Electrophysiology

To test neuron activity in culture and compatibility with the electrode material, neurons were cultured in agarose wells on standard TiN electrodes of a MEA (MEA60-70-100-TiN, Qwane Bioscience SA, Lausanne, Switzerland) and spike activity was recorded extracellularly with a Multichannel System (MCS) 64 Channel data acquisition system with MEA 1060 amplifier and MC Rack software (Multichannel Systems GmbH, Reutlingen, Germany).

4.4 Results

4.4.1 Agarose Molding

The templates with the positive relief features produced perfectly patterned agarose hydrogels (Fig. 17). With the vibratome, thin agarose slices containing agarose-free circular wells and closed micro channels of defined dimensions were successfully produced. All different designs tested here produced equally satisfying results. Even the fine geometries of the three parallel micro bars only a few microns wide and in very close proximity to each other could be replicated perfectly (Fig. 17 b).

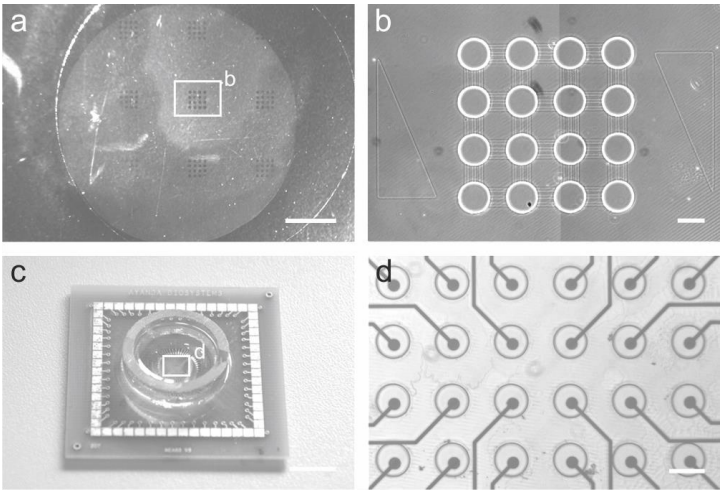


Figure 17: Agarose slice application on glass coverslips and MEA platform. a) Overview of agarose slice with eight arrangements of 16 well/triple channel connections design on a circular glass coverslip in culture medium. b) Single arrangement as marked by the rectangle in (a) at higher magnification. c) MEA device with agarose slice positioned in culture chamber under medium. d) MEA electrodes in detail with overlying agarose slice (area indicated by rectangle in c). Scale bars: (a), (c): 1cm, (b), (d): 100 µm

4.4.2 Slice Stability, Handling and Attachment

Agarose hydrogel slices were cut down to a thickness of 30 µm without tearing. Although the slices were thin, they were quite stable and could easily

be transferred to different dishes. Positioning of the slices on the substrates worked well and wrinkle formation did not occur. The slices adhered reliable to all tested substrates, glass, cell culture dish, and MEA, without the need of any adhesive substances or bonding pre-treatment. Despite this, detachment of agarose slices at the end of an experiment also proved to be simple, which greatly facilitated the repeated use of agarose slices on standard reusable MEAs. The time of attachment of the agarose slices to the particular substrates was tested at 20 °C, 30 °C and at room temperature. The results are shown in table 4. Incubation of agarose slices on glass or MEA substrates at 20 °C and 30 °C led to an attachment time of around three weeks. Experiments were aborted after five weeks at the latest. The tests on a shaking device at room temperature lasted for three days. For optimal attachment of agarose slices, the substrates had to be particularly clean and smooth and agarose slices should be thoroughly dried after positioning and before medium application, respectively. Furthermore, medium change had to be done very cautiously.

Table 4. Long-term attachment of agarose slices under corresponding experimental conditions. (IHC: immunohistochemistry)

Substrate	Temperature/Condition	Days of attachment
MEA1	20°C/incubator	36
MEA2	20°C/incubator	20
MEA3	30°C/incubator	21
MEA4	30°C/incubator	29
glass1	20°C/incubator	25
glass2	20°C/incubator	26
glass3	30°C/incubator	25
glass4	30°C/incubator	28
glass5-8	room temperature/shaking device	3 (time for IHC)

4.4.3 Slice Thickness

Cells of the locust nervous system were cultivated in patterned agarose slices of different thickness on glass substrate to evaluate the influence of

this parameter. Figure 18 shows that the number of cells within the wells in the agarose generally declined over time, whereby the results indicate that cell survival was influenced by the slice thickness, respectively well depth at least from div 7 on. When long-term survival is considered, wells of 120 µm depth showed significant negative effects in comparison to 50 µm deep wells. The best compromise for successful positioning of cells, but also maintaining cell viability, was achieved with a slice of 50 µm thickness. We also tested whether the vibratome produced such 50 µm sections in a reliable fashion. Measuring the depth of 40 different wells on 11 slices with the confocal revealed an averaged well depth of 58 µm (± 5.7 µm). These minor deviations were tolerable for our application.

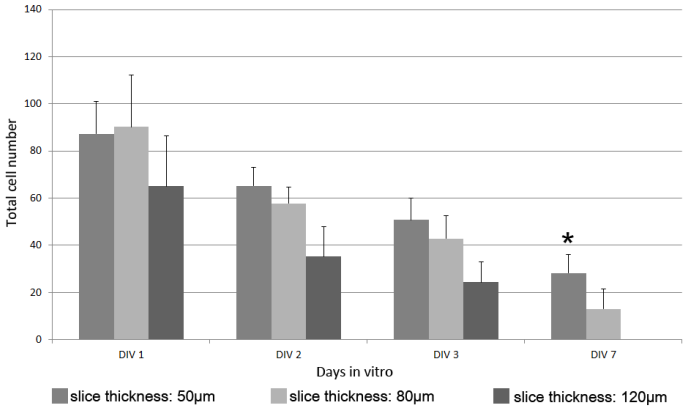


Figure 18: Influence of slice thickness on cell viability over time. Comparison of total cell numbers of *Locusta* in agarose wells of increasing depths within seven days. Variances on div 1, 2 and 3 could not be determined. The evaluation showed a variance among the three conditions only at div 7 (ANOVA, $P<0.05$). On div 7 cell viability was significantly higher on slices with 50 µm thickness in comparison to slices with 120 µm thickness (*post hoc Tukey test) (n = 4, independent cell cultures for each slice type).

4.4.4 Guiding of Cell Growth & Electrophysiology

Neurite growth was confined to the wells and channels where access to the cell adhesive substrate was provided. Figure 19 shows the development of

Lymnaea neurons in the wells connected by channels between div 1 and 4. They were cultured in a standard culture dish surface without surface coating. The neurons, which were manually placed into the wells, adhered to this substrate (Fig. 19 a) and developed neurites within the following days (Fig. 19 b).

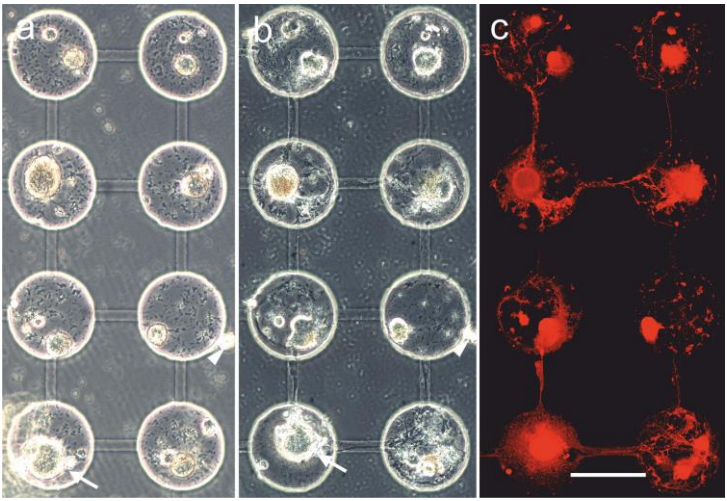


Figure 19: Neural growth within agarose wells (*Lymnaea*). a) *Lymnaea* neurons positioned in eight wells of a 16 well arrangement with single channel connections on div 1. A single cell adhered to the agarose next to one well (arrowhead). b) The same culture on div 4. Cells developed extensive neurite outgrowth. Numerous neurites follow the closed micro channels. The soma of the neuron in the lower left corner (arrow) moved during the culture period. The cell on the agarose surface (arrowhead) was still present but looked condensed and no longer viable. c) The same culture after fixation on div 4 and staining with α-tubulin antiserum. Immunostaining demonstrates the extent of neuritic branching and confirms growth restriction to the agarose free areas. Please note that several neurites have reached adjacent wells by growing through the microchannels. The cell located on the agarose layer (arrowhead in a) and b)) was lost during staining procedure indicating weak adhesion. Scale bar: 100 µm

Neurites followed the channels into adjacent wells without any need for other promoting guiding cues but the physical cue of the channel and the chemical non-adhesive property of the agarose itself. Thereby, the dimen-

sions of the micro channels seemed to play a critical role. Preliminary experiments with different channel dimensions showed that smaller channels of width and height of 5-10 µm yield better guidance than larger ones of 30 µm width and height. In general, the cells did not bridge the well edges of the agarose layer, thus branching was confined to the wells and channels. Staining showed this precise confinement of neurite branching even better (Fig. 19 c). Comparable results could be achieved with *Locusta* neurons in agarose well arrangements with single or triple channel connections (Fig. 20).

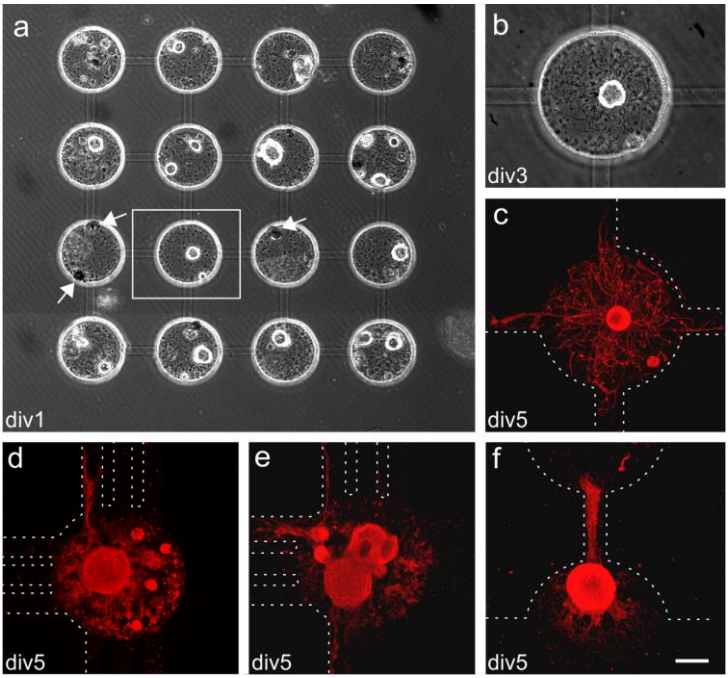


Figure 20: Neural growth within agarose wells (*Locusta*). a) *Locusta* neurons positioned in wells of a 16 well arrangement with one channel connection on div 1. Almost every well is occupied by one to three vital neurons. Arrows indicate dead neurons. b), c) One of the 16 wells (indicated by the rectangle in a)) at higher magnification on different days of culture. b) Neuron on div 3 shows viability as it began to develop multipolar neuritic branching. c) Neuron`s morphology on div 5 after Horseradish-peroxidase (HRP)-immunostaining which visualizes the whole neuritic extent.

d)-f) HRP-immunostained neurons on div 5 as further examples, which illustrate that neurite outgrowth, was confined to the wells and channels. Dashed lines indicate the borders of the agarose templates. Scale bars: a) 100 µm, b)-f) 40 µm

Directed Cell growth could also be achieved on MEA surfaces either by increasing the cell density per application and dispersing the cells randomly on the agarose slice, where generally several neurons occupied one well (Fig. 21), or by manual positioning of the cells where it is intended to occupy the wells at best case with only one or two neurons (Fig. 22). Cell adherence, neuritic growth confined to the wells (Fig. 23) as well as neuritic growth guidance by channels interconnecting the single wells (Fig. 22) was also observed within the later days of culture on these MEA surfaces. Pond snail neurons in some cases adhered to the surrounding agarose surface first, but the number of such cells generally rapidly declined until div 4 (Fig. 23). Neurons cultured within agarose wells on MEA chips sporadically show spontaneous activity. Spikes generated here are generally of low frequency and their amplitudes of up to 1 mV (Fig 24). Spike activity due to stimulation of silent neurons (100 µV – 1 mV) could not be detected.

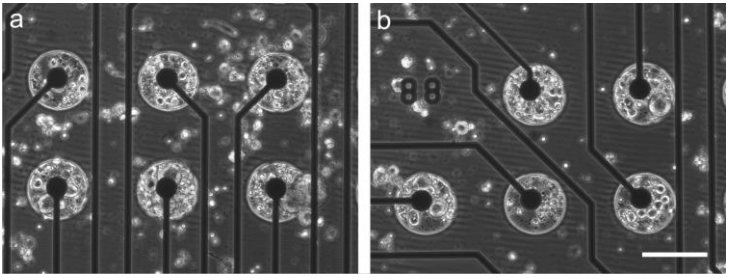


Figure 21: Neuron positioning in wells of an agarose slice on a MEA. Pictures a) and b) show two examples of *Lymnaea* neurons on div 1 applied by chance to the agarose slice. Neurons became positioned to the wells and adhered to the MEA surface. Most of the few neurons that ended up on the agarose layer did not manage to adhere to it, but swam in the medium. Scale bar: 100 µm

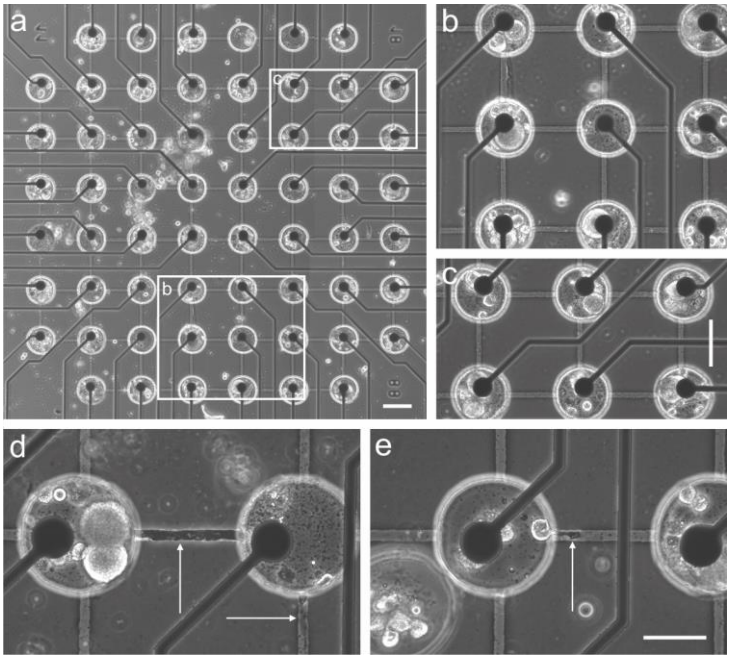


Figure 22: Neuron positioning in wells of an agarose slice on a MEA. The wells are interconnected with channels for a directed neurite guidance. a) Overview of MEA with positioned neurons on div 1. Detailed views on positioned neurons are shown in b) and c). The particular areas are indicated by the rectangles in a). d), e) Cutout of cell culture on div 4 showing examples of neurite guidance within agarose channels (arrows). Scale bar a) 100 µm. Scale bar b) - e) 50 µm.

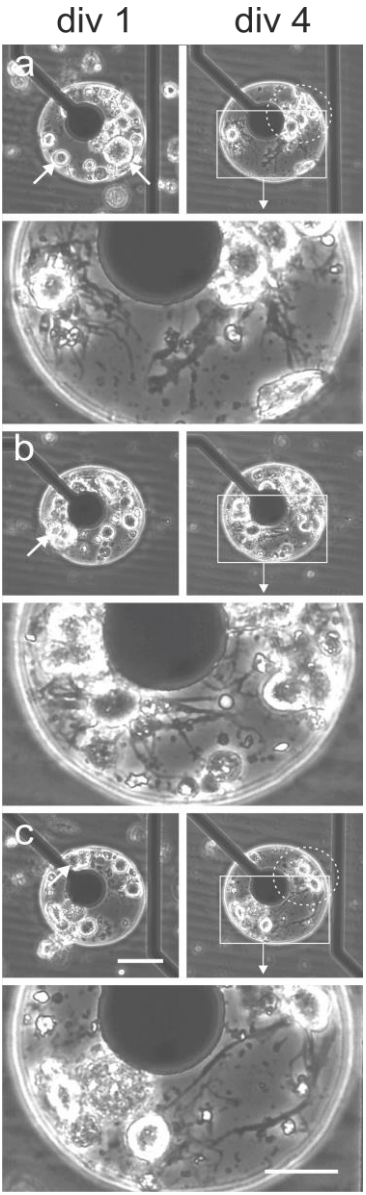


Figure 23: Network development within wells on MEA device. Pictures a)-c) show *Lymnaea* neurons within different wells of the same MEA on div 1 and div 4 for comparison of development. Within four days in culture neurons developed neurites that grew within the borders of the wells (for a detailed view on neurites see corresponding insets indicated by rectangles in the div 4 row of a), b) and c)). Cells that did not achieve proper adhesion on div 1 detached until div 4 and disappeared (white arrows). Several neurons showed mobility and indicated a tendency to assemble in clusters until div 4 (dashed line circles). The number of cells outside the wells on the agarose layer declined between div 1 and div 4. Scale bars: c) 20 µm, Inset: 40 µm

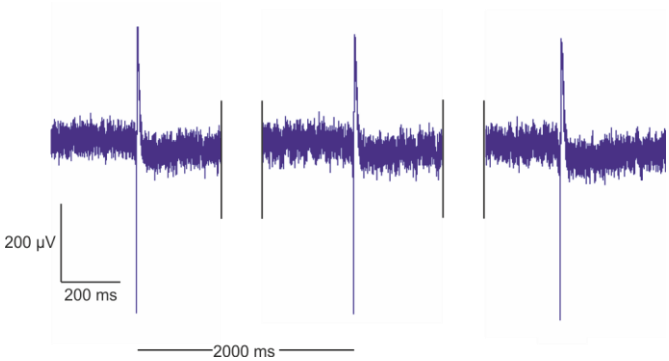


Figure 24: Extracellular recording with Multichannel System (MCS) 64 Channel data acquisition system with MEA 1060 amplifier from a pond snail neuron cultured in a well of an agarose slice. Spike frequency was 0.5 Hz, spike, amplitude 700 µV.

4.5 Discussion

An innovative technique for substrate patterning with agarose is presented. Exact molding from microstructured templates could be achieved reliably and production of thin slices with a vibratome provided stable agarose substrate modifications of consistent height and reproducible quality. Agarose slices showed long-term attachment to several different substrates without any additional treatment. The well and channel pattern succeeded to guide neuronal growth. Neurons adhered to the agarose free areas, whereby their somata were confined to the wells, while neurites were free to grow into the channels as well. Thereby, it is assumed that the physical impulse given by the narrow path impressed the neurites to grow aligned.

4.5.1 Methodology

In literature different but related methods of substrate production using agarose or other hydrogel or elastomer materials were described previously (Zeck & Fromherz 2001; Erickson et al. 2008; Kang et al. 2009; Mercey et al. 2010; Li et al. 2014). They allow for the production of several kinds of microwells, but not that of microchannels for a guided path finding of neurites. Some of the techniques show limitations in adjusting and achieving appropriate well depths (Kang et al. 2009; Mercey et al. 2010). The combination of microwells and channels in an agarose substrate for positioning and neurite guiding was shown by different studies (Moriguchi et al. 2002; Sugio et al. 2004; Hosokawa et al. 2010). These authors used photo-thermal etching processes or similar laser technology that demand relatively high technical effort for creating the channels. In contrast, our approach using in parallel processed templates with well-defined microstructures on a silicon wafer, is able to produce wells and closed microchannel within one molding step. Once the wafer is obtained, molds and slices can be prepared by simply casting and molding. Furthermore, the slice production technique by using a vibratome offers flexibility as the adjustment of any desired slice thickness can be achieved easily and fast on demand.

Deviations in slice thickness are most likely due to a swelling of the hydrogel during long-term incubation in medium. Until now, the production of accurate layer thicknesses are most likely only possible with spin coating tech-

nologies (Claverol-Tinturé et al. 2005). Otherwise, layer production of defined height may be challenging. The here presented method for the production of slices via vibratome shows a new approach to achieve reproducible and almost constant layer thickness.

In our experiments adherence of agarose slices on different substrates can be maintained for three weeks or longer if optimal experimental conditions are provided. This time span is sufficient for locust and snail neuron culture. Network development reaches its maximum within the first week. Furthermore, agarose slices although showing good attachment to MEAs or different reusable devices can be removed after completion of an experiment and replaced by new slices, which facilitates cleaning procedures. This point is not necessarily given if guiding modifications are irreversible fixed to the devices (Zeck & Fromherz 2001; Merz & Fromherz 2005; Erickson et al. 2008).

4.5.2 Guiding by Physical Cues

Finding optimal conditions for constructing networks of neurons is a critical point. Guiding by chemical cues alone, performed by microcontact printing or patterned laser ablation of adhesive coatings for example is often only applicable to a limited number of cell types. In addition, the mentioned techniques do not allow for a differentiation between soma position and neurite path in general (Suzuki et al. 2013). Then somata and neurite branching are randomly distributed over the printed grid. Furthermore, cells in culture often show extensive motility due to tension originating from growing neurites.48, 49 For these reasons, pattern quality of networks constructed by chemical cues alone can be limited (Corey et al. 1991; Fromherz et al. 1991; Ruardij et al. 2002; Suzuki et al. 2013), especially over longer periods of time (Marconi et al. 2012). Previous studies already revealed that chemicals might play a more minor role in cell extension guiding compared to raised topographical modifications (Merz & Fromherz 2002). Other studies showed that the direction of the outgrowth of cell extensions in culture is strongly influenced by the surface topography, as in dependence of the type cells tend to follow certain surface profiles (Rajnicek et al. 1997). Hence, cell pattern control studies focus more and more on the physical confinement of cells in culture. However, as many cell types, especially from vertebrates, need chemical substrate modifications to adhere at all, it has

to bear in mind that in dependence of the cell type a sole physical confinement probably does not suffice either (Sugio et al. 2004). If cell adherence to the substrate is warranted, the agarose slices presented here with open wells and closed channels provide a good guiding quality by physical impulses applicable for various cell types. The closed channels prevent somata from occupying the neurite path, the low height of the channels prevents somata from migrating into them, and the channel dimensions seem to provide a physical impulse to the neurites to grow aligned. The raised wells act as a physical barrier, which immobilize somata and prevent neurites from overcoming it.

4.5.3 Cell Culture in Wells

The observation of negative influences on long-term survival of cells in wells of 120 µm height in comparison to the 50 µm high wells might be due to an impediment of medium exchange and cell waste product accumulation in the deep cavities without medium flow. Insufficient nutrient supply and waste disposal, therefore, might result in a limited cell survival. As a result, dependent from cell type, the minimum required thickness of agarose hydrogel slices that ensure stable neuron positioning should be used. Reliable stable agarose slices down to a height of less than 30 µm are possible to produce, which should be sufficient for vertebrate neurons for example. However, as a reliable immobilization of locust and pond snail neurons could only be achieved with 50 µm high wells and up as their neurons have large diameters it was chosen to work with thicker slices.

For achieving isolated cell clusters with low cell number but less defined network structure in the wells without channels presented here, up to seven invertebrate neurons were collected per well, as the well diameter used here did not allow for a higher cell density. If requested, this limitation can be overcome by adjusting the pin diameter of the silicon templates, which would result in greater wells. Besides, as vertebrate neurons have lower diameters, here cell density could be raised even in smaller wells.

4.5.4 Agarose as Patterning Material

Invertebrate neurons, in comparison to vertebrate neurons, are comparatively unselective, concerning the substrate they grow on. This unpretentiousness impedes growth cone guiding by adhesive cues as often used with

vertebrate neurons. Indeed, growth guiding of *Lymnaea* neurons by chemical cues was managed previously by a substrate patterned with poly-L-lysine and brain derived conditioning factors (Prinz & Fromherz 2000). In our experience, however, *Lymnaea* neurons do not need any chemical coating to achieve strong adhesion to various culture substrates like polystyrene, glass or MEA surfaces. For this reason, chemical patterns here do not influence neurite growth as much as it is desired. The same is true for *Locusta* neurons. Therefore, we focused on a structured and non-adhesive material, to provide physical guiding in combination with repulsive chemical cues, rather than adhesive ones. Agarose is an established material, at least for vertebrate cell guiding strategies (Moriguchi et al. 2002; Nelson et al. 2003; Suzuki & Yasuda 2007; Kang et al. 2009), as it is non-adhesive for most of the cell types tested, but to our knowledge agarose was not used before to guide invertebrate neurons. For example, Polydimethylsiloxane (PDMS) and similar silicones, are prominent alternatives to agarose in substrate patterning technologies and are as well widely used for vertebrate cell guiding (Dworak & Wheeler 2009; Skelley et al. 2009; Hosokawa et al. 2010), especially in combination with microfluidics (Frimat et al. 2011; Kobel et al. 2012; Dinh et al. 2013; Lin et al. 2013). PDMS was already shown to be an almost non-adhesive material for locust neurons in microfluidic devices (Göbbels et al. 2010a). For *Helix* neurons in culture it was shown that adhesion is not impeded on PDMS (Claverol-Tinturé et al. 2005; Claverol-Tinturé et al. 2005). *Lymnaea* neurons did not show any restricted growth on PDMS, too, compared to control groups growing on glass or polystyrene (data not shown). And adherence of *Locusta* neurons is only strongly restricted as about 20 % of cells adhered to PDMS in comparison to the control group cultured on polystyrene (Göbbels et al. 2010a). Because of this, PDMS turned out to be unsuitable for our purposes. Other synthetic polymers that act as non-adhesive surfaces are PEG (polyethylene glycol) (Khademhosseini et al. 2004; Reska et al. 2008; Krsko et al. 2009), polyacrylamide (Nelson et al. 2003; Sasaki et al. 2009) or pluronics (Nelson et al. 2003; Gomez-Sjöberg et al. 2007) for example. Only PEG provides a non-adhesive surface modification for insect neurons (Reska et al. 2008). However, due to a difficult production process and poor reproducibility, this material appears unsuitable for routine applications. Agarose, in contrast, has

many practical advantages: It offers easy conversion from gel to liquid, making gel production and curing manageable within minutes. Sterility can easily be achieved by autoclaving. Agarose is a natural, non-cytotoxic, and relatively cheap material. Finally, it is transparent, which allows for the direct observation of cell behavior even in closed channels.

4.6 Conclusion

A new process based on photolithography and micromolding techniques is presented for the fabrication of structured agarose slices to create geometrically defined topologies for the controlled development of neuronal networks in culture. Further substrate modifications are not necessary. The slices were tested on conventional cell culture substrates (glass; polystyrene), but also on different types of multielectrode arrays (MEAs). The procedure provides high flexibility, as many parameters are easy to adapt to specific demands. Experiments with locust and pond snail neuron cultures demonstrated the great potential of the agarose slices for positioning and immobilizing cells. In addition, micro channels integrated into the slices are sufficient to guide directional growth of neurites. The combination of a chemically non-attractive material with a suitable topology most certainly allows the investigation of a large range of cell types and various analysis methods.

5 Improvements of Culture Conditions and Neuronal Cell Growth on Iridium Oxide

5.1 Statement of Shared Workload

This study was carried out under the supervision of Univ.-Prof. Dr. Peter Bräunig and Dr. Katrin Bui-Göbbels. The data have not yet been published. Katharina Walczuch and Dr. Katrin Bui-Göbbels designed the experiments. Katharina Walczuch supervised the experiments carried out by undergraduate students Fabio El Yassouri and Lennart Rüttger. Fabio El Yassouri collected and analyzed the data for the medium supplement study in the course of his bachelor thesis with support from Katharina Walczuch and Dr. Katrin Bui-Göbbels. Lennart Rüttger collected and analyzed the data for the biocompatibility test in the course of his bachelor thesis with support from Katharina Walczuch and Dr. Katrin Bui-Göbbels. Katharina Walczuch wrote the manuscript.

5.2 Introduction

In the intact brain, the modulating influence of thousands of possible interconnected sources is not able to become overviewed. Therefore, to answer questions about intrinsic properties of individual cells and basic mechanisms running the systems, a reduction of the complexity seems to be necessary. This can be achieved with *in vitro* approaches (for review see: Schmold & Syed 2012). Nowadays, it is possible to create small networks by isolating individual neurons from the brain and integrate them into a cell culture, to facilitate the complexity of the neuronal system. Here, one is able to control the environmental conditions precisely. With this approach, specific interactions between identified cells can be studied through observations and manipulations over long periods on the cellular level. In this context, the use of invertebrate cell cultures became more and more important in the last decades as they offer crucial advantages (Bulloch & Syed 1992; Schmold & Syed 2012). The more simple structure of invertebrate nervous systems, with much less network participants, allow the ambitious goal to completely analyze and decode mechanisms of defined neuronal circuits (Syed et al. 1990). Furthermore, cell culture in general is easier with invertebrate neurons. Their neurons are able to be cultured in extremely low density (Syed et al. 1990; Kirchhof & Bicker 1992; Merz & Fromherz 2005). This is hardly possible with vertebrate cells. Invertebrate neurons are more robust, undemanding and generally much larger. Like this, they are easier to manipulate and easier to be coupled with the planar electrodes of a MEA, which is nowadays a state-of-the-art technique for a non-invasive long-term observation of the electric activity of *in vitro* networks (Thomas et al. 1972; Novak & Wheeler 1988; Gross et al. 1995).

For these reasons, we are interested in the controlled development of defined and small neuronal networks of *pond snail* neurons on the surface of MEA-electrodes. The neurons from mollusks, like *Helisoma*, *Aplysia, Helix* or *Lymnaea* are established test systems, as they offer the properties for facilitating *in vitro* studies of defined neuron-neuron connections (Bulloch & Syed 1992; Lovell & Moroz 2006). Especially for these well-studied model organisms, well-established cell culture media have been developed. The main essential demands on a neuronal cell culture, thereby, are long-term survival, extensive neurite outgrowth, synapse formation, and tight substrate adherence. Over the years, researchers found different substances

influencing cell culture conditions of invertebrates in terms of neurite outgrowth, survival, or synaptic physiology. They may have the potential to be used as standards for the development of active and long lasting *in vitro* networks (Wong et al. 1983; Ridgway et al. 1991; Bulloch et al. 1994; Syed et al. 1996; Woodin et al. 1999; Hamakawa et al. 1999; Angevin et al. 2000; Dmetrichuk et al. 2006; Sukiban et al. 2014). To name some examples, already Wong et. al. (1983) found the importance of brain derived conditioning factors, produced by the central ganglia, for neuronal cell cultures of mollusks, which is being used as a standard in terms of a conditioned medium (CM) nowadays. Here, neurotrophic factors are known to play a key role (Bulloch et al. 1994; Woodin et al. 1999; Hamakawa et al. 1999), especially in the formation of excitatory synapses (Woodin et al. 1999; Hamakawa et al. 1999). Further, Ridgway et al. (1991) and Syed et al. (1996) tested the effect of murine nerve growth factor (NGF) and ciliary neurotrophic factor (CNTF) successfully on the neurite outgrowth (Ridgway et al. 1991; Syed et al. 1996) and synaptogenesis (Syed et al. 1996) of *Lymnaea* neurons. Both supplements are essential for vertebrate brain development and used as a standard in vertebrate neuronal cultures. Even an effect of 9-cis retinoic acid on neurite growth of *Lymnaea* neurons was reported (Dmetrichuk et al. 2006). Similar effects in terms of cell survival and neurite outgrowth could be shown by Sukiban et al. (2014) on defined stages of embryonic grasshoppers. Despite reported results like these, such supplements have not found their way to common use yet, with the exception of CM. Although standard culture substitutions lead to satisfactory results in general, improvements seem to be necessary to achieve reliably long-lasting and well-developed networks *in vitro*. For this reason, we started to test different culture supplements. As Ridgway et al. (1991) could show the successful application of the supplement nerve growth factor (NGF), generally used in vertebrate cultures, in invertebrate culture, we decided to test, two further supplements, B27 and 9-*cis*-retinoic acid (RA). The vitamin-containing cocktail B27, a commercially available serum-free supplement for neuronal cell cultures, is mainly used for vertebrate cell cultures. It was initially developed to maintain viability in rat hippocampal neurons (Brewer et al. 1993; Brewer 1995). Further, preliminary studies, testing the influence of B27 on embryonic neurons from the grasshopper *Locusta,* could show positive effects on cell survival (data not shown). Because of these findings, a

broader application field of B27 was assumed and therefore became tested on adult *Lymnaea* neurons in primary cell cultures. RA, the metabolite of retinol, is known to be present naturally in the vertebrate brain as well as in insect and mollusk brains and are known to play a key role in vertebrate brain development. The effect of retinoic acid (RA) was decided to be proven as well, as (Dmetrichuk et al. 2006) found an effect. Furthermore, first hints towards a nerve regeneration effect on insect neurons exist (Bui-Göbbels et al. 2015).

Beside neurite outgrowth and survival of neurons in culture, the ability of neurons to adhere to the substrate, is essential as well. Most vertebrate cells are generally not able to adhere to artificial growth substrates without certain protein coatings, like laminin. In addition to chemicals, surface texture and topography may have effects on cell adherence (Blau 2013). For cell cultures with insects and mollusks, lysine and concanavalin A are often used as a standard, although a protein coating, from our experience, is not necessary. In terms of the application of MEAs, for network activity research, the electrode material may be a critical point, because a tight cell adherence to the electrode enhances signal transduction between the cell and the recording or stimulation side (Blau 2013). Beside common electrode materials for MEAs, like gold and platinum (Thomas et al. 1972; Pine 1980; Maher et al. 1999), during the last years the interest focused on iridium oxide (IrO) (Lee et al. 2005). IrO was reported to be advantageous concerning its higher charge injection capacity (Wessling et al. 2007) in contrast to platinum. As Göbbels et. al. (2010b) already could confirm neurocompatibility of IrO and adult locust neurons, now its biocompatibility to *Lymnaea* neurons was proven as well.

For the cell culture supplement test as well as for the biocompatibility test with iridium oxide, cell survival over time and neurite outgrowth were determined. Neurite outgrowth, indispensable for network formation, is an indicator for good cell adhesion, which directly correlates with biocompatibility (Richards 1996; Göbbels et al. 2010b).

5.3 Methods

5.3.1 Animals

The pond snails originated from the department`s own breeding colony. They were kept in 5 l tanks filled with pond water at room temperature and under a natural light/dark cycle. In the winter months, the light cycle was supported by artificial light with a light/dark cycle of 12/12 h. The animals were fed with lettuce and cucumber slices. For preparation, ganglionic rings of young adults with shell lengths of 2 to 3 cm were used.

5.3.2 Cell Culture

The preparation of snail neurons up to the step after enzymatic treatment essentially corresponds to techniques described previously (Ridgway et al. 1991; Kaul 2007) with the following exceptions: instead of using ampicillin for defined medium (DM) solution a mixture of penicillin (10.000 units/ml) and streptomycin (10 mg/ml), (Sigma-Aldrich Co., Steinheim, Germany) was used. Preparation of ganglia was carried out in sterile normal saline (NS) instead of antibiotic normal saline (ABS). For the last preparation step, realized in DM, further non-neuronal tissue, as well as the inner ganglionic sheets was removed from the two pedal, the right parietal, and the left visceral ganglion. These ganglia possess a great number of entities on the one hand and they contain the most cells with large soma diameters above 50 µm on the other. The neurons were mechanically dissociated using fine forceps. The inner neuropil was also removed and close attention was paid to dissociate the single neurons from each other. Thereby, selection of neurons was not limited to specific types. The dissociated neurons became transferred to a 1.5 ml low binding micro tube by a 100 µl low binding micropipette. After gentle trituration with a low binding micropipette and concentration of the cell suspension to the volume of 600 µl for cell seeding, the cell suspension was plated to the culture substrates.

5.3.3 Cell Culture Supplements

100 µl of cell suspension was transferred to the 1 cm^2 area of the surface of a polystyrene culture dish (Ø 4cm) with counting array (cell density: ≈5000 cells/ml). Remaining cell suspension was discarded. Cells had time to

adhere to the polystyrene substrate for about 45 min before 3 ml DM was applied to the culture dishes. All culture dishes were incubated over night at 20 °C in a Peltier cooling incubator (Memmert, IPP 55, Schwabach, Germany) and counted on day *in vitro* 1 (div 1) before the supplements became applied to the corresponding culture dishes. For each of the two tested supplements, two independent experimental series were performed. One experimental series involved the preparation of one animal and the production of two cell culture dishes for every condition (control/supplement). In a last step, the corresponding supplement was applied to the test culture dishes. B27 (Life Technologies, Thermo Fisher Scientific, Darmstadt, Germany) was applied in a concentration of 2 % and a 10^{-7} M final concentration of 9-*cis*-RA (Sigma-Aldrich Co., Steinheim, Germany) in dimethyl sulfoxide (DMSO, Carl Roth GmbH + Co. KG, Karlsruhe, Germany) found application.

5.3.4 Iridium Oxide (IrO) Substrates

IrO templates in terms of 1 cm^2 platelets were provided by the IWE 1. IrO substrates were produced by chemical vapor deposition (CVD), where the corresponding metal is being sputtered in a very thin layer of 100 nm on average on a silicon wafer under defined temperature and pressure conditions (Göbbels et al. 2010b). Prior to cell culture, IrO platelets were cleaned in 50% ethanol in an ultrasonic bath (Bandelin, Sonorex TK52, Bandelin electronic GmbH + Co. KG, Berlin, Germany) for 5 min and sterilized subsequently 3 times in 70 % ethanol. Ethanol debris was removed by washing in sterilized distilled water. A single dry platelet was positioned in the center of a polystyrene culture dish. Preparation of cell suspension was performed as it was described in the previous section. 100 µl cell suspension was applied to the IrO platelet. For each test series two samples for each condition were prepared, meaning two culture dishes with cells cultured on IrO platelets and two culture dishes for control, with cells cultured on uncoated polystyrene. The experiment was repeated six times.

5.3.5 Analysis

For culture supplement tests, the number of living cells and cells with neurites was determined during the time span of 11-15 days by the help of inverse phase contrast microscopy (Zeiss Vert A1, Carl Zeiss AG, Oberkochen, Germany). Data acquisition of the B27/control test series occurred on day

in vitro (div) 1, 4, 7, 11, 13, and 15. Data acquisition of the RA/control test series occurred on div 1, 2, 3, 4, 7, 9, and 11. For biocompatibility test with IrO, the number of living cells and cells with neurites was determined during the time span of six days. Data acquisition occurred on div 1, 3 and 6. The evaluation of the observed cells in culture as to whether they are neurons and vital, thereby occurred qualitatively. A cell was counted to be a vital neuron if shape and color corresponded to that of vital neurons. Indicators for a vital invertebrate neuron are a bright yellow to orange color, the appearance of a halo and a more or less clear delineated membrane. Furthermore, soma diameters should exceed the approximate size of 10 µm as smaller cells were assumed to be probably glia cells (Wong et al. 1981). Cells with neurites were always counted as vital neurons. Darker cells, the occurrence of vacuoles or the degeneration of neurites were indicators for apoptotic cells, and therefore not counted. The particular results of every condition were averaged and plotted as a function of neuron number over time and as a function of neurite number over time. Cell number at div 1 was always scaled to 100 %. Statistical analysis was performed by a one-way analysis of variance (abbreviated one-way-ANOVA) and a post hoc Tukey´s-range test.

5.4 Results

5.4.1 B27

Survival of the neurons in the control group and in the group incubated with B27 supplement complementation was analyzed by the decrease in cell number over the time span of 15 days (Fig. 25 a).

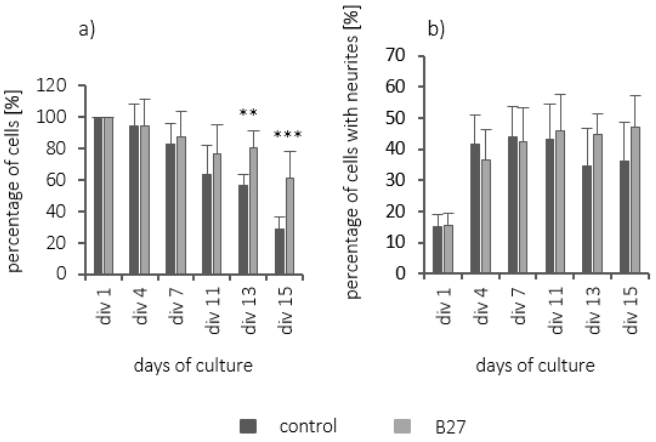


Figure 25. Influence of B27 on cell survival and neurite outgrowth of neurons from adult pond snails (*Lymnaea)*. a) Development of cell number over time; b) Development of cells with neurites over time. (Until div 11, n=6; until div 15, n=5). Post hoc tukeys´s range test ** = $p < 0.1$; *** = $p < 0.05$

Until day *in vitro* 11 (div 11) no difference in cell survival between the control groups and the B27 supplement groups could be confirmed. Results at div 13 and 15 showed a significant difference in cell survival between the control series and the cell cultures that were supplemented with B27. Cell number of the control groups decreased until div 13 to 60 % of the initial cell number. The cell number in the cultures influenced by B27 comprises still 80 % living cells at div 13 in comparison to the initial cell number at div 1. This difference in cell survival increased until div 15 from a 20 % higher cell survival at div 13 to an almost 30 % higher cell survival. At div 15, 30 %

of the control group cells are still alive, whereas the B27 cell group still consists of over 60 % of the initial cell number. Analysis of neurite development (Fig. 25 b)) could not show any differences between the two groups. 20 % of the cells in both groups developed neurites within the first day in culture. This portion increased until div 7 to about 40 % and then reached a plateau at the following days. Cell number with neurites decreased slightly from the div 11 on.

5.4.2 Retinoic Acid

Survival of the neurons in the control group and in the group incubated with 9-*cis* RA complementation was analyzed by the decrease in cell number over the time span of 11 days (Fig. 26 a). During the days of culture, no difference in cell survival between the control groups and the RA supplement groups could be confirmed.

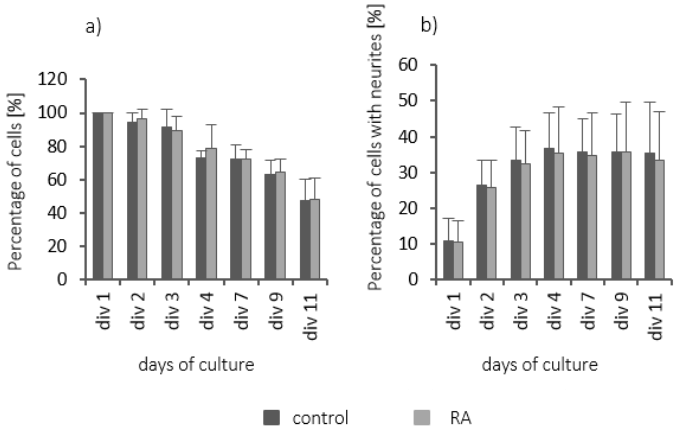


Figure 26: Influence of 9-*cis*-retinoic acid (RA) on cell survival and neurite outgrowth of neurons from adult pond snails (*Lymnaea*). *a)* Development of cell number over time; b) Development of cells with neurites over time. (n=5)

Both populations decreased over time. On div 11 about 50 % of the initial cell number was still present. Similar results were achieved by analyzing the development of neurites (Fig. 26 b). The portion of cells with neurites rose from initially 10 % on div 1 to a portion of almost 40 % at div 4. This plateau

is maintained throughout the following days. No differences between the control group and the group treated with RA could be observed.

5.4.3 Biocompatibility Test with Iridium Oxide

Survival of the neurons in the control group and in the group cultured on IrO was analyzed by the development of cell number over the time span of 6 days. Figure 27 a) shows the plotted results of cell numbers cultured on uncoated polystyrene dishes in comparison to cell numbers on IrO substrates.

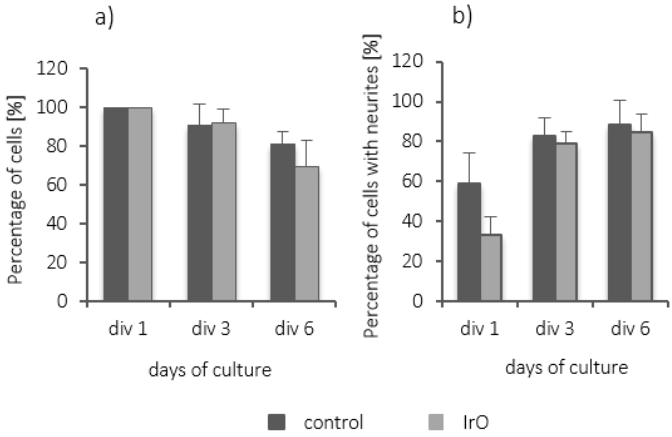


Figure 27: Cell survival and neurite outgrowth of neurons from the adult pond snail *Lymnaea* cultures on iridium oxide (IrO). a) Development of cell number on IrO substrate over time. (n=6)

During the days of incubation, the cell number decreased in equal measure. After 6 days, for both conditions, nearly 70 % of the initial cell number was still present. Thus, no difference in cell survival could be found. Figure 27 b) presents the results giving evidence about the cell adhesion and therefore cell culture quality. In the control group, on div 1 over 55 % of the cultured cells showed neuritic branching. The number slightly exceeded the portion of cells with neurites cultured on IrO, which was 42 %. This difference was observed to be almost balanced on div 3. Portion of cells with neurites continued to increase in both groups until div 6. On div 6, the control groups on polystyrene showed the presence of neurite branching at 90 % of the

cells. The portion of neuritic cells cultured on IrO is slightly lower, at 82 %. However, here as well, no statistically significant variances could be confirmed.

5.5 Discussion

The influence of B27 and RA on survival and neurite formation in neuronal cell cultures of adult pond snail neurons was tested. In summary, the application of B27 showed a significant increase in cell survival from the second week on in comparison to the control group. An increased neurite presence or an increased velocity of neurite development could not be shown under the influence of B27. Similar tests with RA did not show differences in cell survival and neurite outgrowth between RA-treated and RA-untreated neurons. In a second approach, the biocompatibility test of IrO with pond snail neurons resulted in a positive outcome. Cell number and neurite outgrowth over time of neurons cultured on plain polystyrene and those seeded on IrO lead to similar results.

5.5.1 Supplement Tests for Improved Culture Conditions

The investigation of the first part of this study focused on different aspects to evaluate the quality of our neuronal cultures with and without a defined supplement. Counting of the cells over time could give evidence of the length of the cell´s lives under defined culture conditions. An enlarged cell survival, due to a defined supplement, would be beneficial concerning long-term experiments. Network building generally takes time and the investigation of plasticity processes as well. By counting the number of cells that developed neuritic branching, predictions about the overall culture quality and about the ability for network formation could be made. The appearance of neurites give evidence of a good cell adherence and therefore of a good culture quality in general. Anyway, there are always cells that obviously adhered and showed a vital shape but did not develop neurites. Although it cannot be excluded that these cells are in optimal vital condition, they were not involved in network formation. Neurite formation and neurite shape may depend on the cell type, and it is possible that different cell types need different trophic factors for neurite formation. Our approach is the development of very small networks of less than 20 neurons on MEA chips. By using undefined neuron types that are probably not able to develop neurites under common culture conditions, we run the risk of putting these static cells into operation. If half of the cells in such small density cultures

does not participate with the network formation, the experimental outcome stays unsure. For these reasons, we believe that an increase of the portion of cells developing neurites seems to be necessary and the finding of an effect by the application of a defined supplement in this context would be beneficial.

B27:
Neuron cultures, influenced by the B27 supplement, showed an almost twice as high cell survival after 15 days. These data confirm the results from similar studies with embryonic locust neurons (data not published). Brewer (1995) could show a positive effect of B27 on cell survival of various different neuron types and brain regions of the rat as well, and even at human neuroepithelial cells positive influences could be confirmed (Shin et al. 2006). Because of these findings, the results obtained in the present study do not seem to be surprising. However, as the composition of the B27 supplement was developed for vertebrate cell cultures and even for these B27 showed different effectiveness at different neuron types (Brewer 1995), it is questionable whether the composition of B27 could not be modified to achieve optimal influences suiting the pond snail. It can be concluded that complementation with B27 seems to be helpful to achieve longevity of a cell population in culture and therefore can be recommended as standard medium supplement for the future.

Retinoic Acid:
The results neither showed significant differences in cell survival, nor in the portion of cells developing neurites. From our point of view, the deviating results from the studies of Dmetrichuk et al. (2008) can only be explained by the preparation procedure of the investigated neurons. While Dmetrichuk et al. (2008) isolated a defined population of neurons from the ganglion and applied them to the culture substrate we standardly dissociate great amounts of the whole ganglion and apply the suspension, consisting of neurons, glial cells and other non-neuronal tissue to the culture dish. Most probably, this suspension already includes undefined naturally neurotrophic factors, which are most probably most effective. As well, different isomers of retinoic acid have been shown to be generally present in the CNS of *Lymnaea* (Dmetrichuk et al. 2008). Therefore, it is possible, that the general effect of the natural RA and other neurotrophic factors, that already

existed in our control groups, lead to an effect that is not differentiable from the group additionally treated with RA. Actually, our expectation was that the RA-group should have an effect anyway, as the concentration of the natural trophic factors, present in the cultures, should be proportionally low. In general, the amount of CNS material per culture dish is only at most half of a ganglion per 3 ml medium volume. By comparison, the recommended amount of CNS material added to a cell culture to achieve a conditioned medium (CM) with a concentration of neurotrophic factors, sufficiently high to induce neuritic branching, is three ganglionic rings per milliliter (Ridgway et al. 1991). Concentration of natural RA in the CM fell below the detectable amount at Dmetrichuk et al. (2008). Thus, the effect that lead to neuritic branching in our control groups most certainly did not arise from natural RA, but probably other neurotrophins. As the applied concentration of 10^{-7} M of RA in the experimental group did not lead to further detectable effects, the development of the observed neurites most probably was not induced by RA as well, but most probably by other, natural neurotrophins, already present in the "CM-like"-culture medium we used. In the future, further approaches with higher RA-concentrations could investigate whether RA complementation makes sense for cultures that are already influenced by CM of even lower neurotrophin concentrations. A preliminary study with NGF-treated cultures was also done (dilution series: 10, 50, 100, 400 ng·ml^{-1} of nerve growth factor-2.5 from murine submaxillary gland (Sigma-Aldrich Co., Steinheim, Germany; data not shown). The results of (Ridgway et al. 1991) could not be reproduced in our cell culture experiments. Probably, the reasons that are responsible for the failure with RA are the same as in the tests with NGF.

What has not been considered in the present study was the extent of neurite outgrowth per individual neuron. Qualitatively, the extent of neurite outgrowth between the B27 group and the control group seemed to be equal, the same was true for the RA experimental series. However, this was not confirmed quantitatively, yet. A common method to analyze the extensiveness of the neuritic tree is the Sholl Analysis (Ristanović et al. 2006), an analysis form for neurite tracing and therefore able to quantitatively determine neurite branching and growth extent. It turned out that the requirements for a successful automated application of this method could not be served with pond snail neuron cultures. The neuritic trees of distinct neuron

types show no distinct arbors able to be differentiated from each other, but a more flattened homogenous surrounding of the soma (Lovell & Moroz 2006). Furthermore, cell clusters could not be recognized with the automated Sholl-method, thus several neurons would be recognized as being a single one. Furthermore, every cell in the culture would be taken in account, including glial cells, for example. Not least, the automated method, as it recognizes brightened pixel in order to determine an area belonging to a neuron, is in need for a homogenous brightness control, otherwise it is not able to recognize the whole neuron. This cannot be served with our neuron cultures as the soma always shows far more brightness than the neurites, even after fluorescent stainings. The method is manually applicable as well. Actually, the manual application on hundreds of cells would be too time consuming. Therefore, a different culture approach with defined and smaller neuron populations and neuron types with adequate neuritic tree shape would have to be used in the future to analyze questions about the individual properties of the neuritic trees.

5.5.2 Biocompatibility Test with Iridium Oxide:

The unselective behavior of pond snail neurons, concerning their growth substrate, applies to IrO as well. Neurons were able to achieve strong cell adhesion and survival on the electrode material without chemical coatings over longer periods in the same manner as it was observed on plain polystyrene. Thus, it could be shown that not only IrO does not have cytotoxic effects on the neurons, but also the surface obviously serves the right properties for a good cell attachment. The existence of pure biocompatibility with this metal is a crucial point. These results allow the approach of the development of neuronal biohybrid systems with these neurons and complements the positive biocompatibility tests of IrO and adult locust neurons done by (Göbbels et al. 2010b). Indeed, the use of chemical coatings are thinkable, as poly-D-lysine is necessary for embryonic chicken neurons as well, for example (Göbbels et al. 2010b), but the possibility to achieve a direct contact between the biological test system and the recording site is advantageous. Beside the direct electrode contact for an undisturbed strong signal record and stimulus transfer (Blau 2013), respectively, possible influences on the electrode properties by chemical films have to be considered. In addition, activity patterns of neurons may be influenced as well,

but probably in a negative way. Kaul (2007) temporarily observed spontaneous interruptions in spiking activity of pond snail neurons cultured on poly-L-lysine and considered the chemical being responsible. Beside chemical properties of the growth substrates, further surface properties as topography and wettability can influence adhesion and growth behavior. Thus, electrode topography has already been modified for an improved cell adhesion (Hai et al. 2009) and electrode metals complemented with carbon nanotubes with enlarged surface profiles could show improved signal transfer properties (Lovat et al. 2005). Göbbels et al. (2010b) presented the possibility to prepare iridium oxide surface profiles of different roughness. Although, different roughness conditions did not affect cell adhesion in the case of locust neurons (Göbbels et al. 2010b), a positive effect on other cell types, like *Lymnaea*, cannot be excluded. Furthermore, electrical properties of neurons cultured on different roughness´s of IrO have not been compared yet.

5.6 Conclusion

B27 is able to enlarge the vitality of neurons from the pond snail in culture but had no effect on the development of neurites. As no negative effect could be found, the supplement could be recommended for standard use, as increased cell survival is beneficial for possible long-term experiments. As we could not observe any effect on cell survival or neurite formation with RA, like it was shown previously (Dmetrichuk et al. 2008), further experiments are recommended to decipher the reasons. Eventually, undefined neurotrophic factors, contained in the medium, already lead to maximum effects. In this case, the additional supplement of RA would not make sense. Further supplements to improve neuritic branching should be investigated. The biocompatibility study with IrO culture substrate lead to satisfying results. Pond snail neurons were able to adhere without any chemical coating to the electrode material and maintained viability, thus gave evidence that IrO does not have any cytotoxic effects on the neurons of the pond snail. Consequently, the use of IrO as electrode material for a future integrated system of neuron culture and MEA chip seems to be possible.

6 General Discussion

The main part of this thesis presents two innovative approaches to converge the positioning problem of invertebrate neurons on the electrode surfaces of MEAs, a necessity on the way towards an integrated biohybrid system for long-term observations of small and geometrically defined neuronal networks *in vitro*.

The first approach addresses the positioning problem with the opportunities of microfluidic technology. Here, the transport of particles and cells occurs hydrodynamically within a laminar flow in a closed channel system of micro scale produced by lithographic techniques (Xia & Whitesides 1998). Through defined geometrical properties of the channel system, leading to different fluidic resistances in different channel pathways, cells become deflected to defined locations, the cell traps. Thereby, we first adapted similar geometries, already presented in other studies (Tan & Takeuchi 2007; Kobel et al. 2010; Frimat et al. 2011; Krumpholz et al. 2014). While the application with artificial test particles, the polystyrene beads, achieved promising results, similar results could not be achieved with living test systems, neurons from the locust and from the pond snail. Deflection rate of cells into the traps turned out to be too low and flow velocities, necessary to overcome the fluidic resistance of the channel system and thus to introduce the cells reliably into the systems, too high. Either cell traps did not become occupied at all, or the cells became negatively influenced by the shear stress and the fluidic pressure they were exposed. Modifications of these first generation microfluidic devices of the “serpentine type”, which mainly was lengthening of the serpentine loops (Kobel et al. 2010), a modified cell loading

technique and declined flow velocities, should eradicate the mentioned problems. However, contrary to expectations, they did not lead to the desired success. Previous studies registered success with these kinds of microfluidic devices (Kobel et al. 2010; Frimat et al. 2011), but actually with other cell types. We concluded that our biological test systems are more sensitive to the forces within microfluidic devices. The neurons from locusts and pond snails have large diameters, which was actually one of the properties why we chose to work with these species. However, it emerged that with size an increase of their sensitivity to the pressure and shear stress in such a fluidic system seems to occur. Furthermore, the extreme heterogeneous cell suspensions, concerning cell type, cell size, and non-neuronal debris, have to be considered an issue. These kind of cells are relatively unique compared with other reported approaches, where a technique for cell trapping is aimed for (Kobel et al. 2010; Bell et al. 2014). These circumstances possessed an extraordinary challenge to us, concerning the construction of the right channel dimensions.

From that point on, our focus shifted away from the channel design of the first generation, and we developed a completely new geometry, the second generation of the “triangle type”. The simple main channel geometry with mainly straight paths and widening of the channel entrance declines the general fluidic resistance, therefore facilitated cell loading at lowest velocities and declined channel blocks. Furthermore, several pathways, each containing a single cell trap turned out to be very valuable concerning the risk of channel blocks and fluidic fluctuations. With this new approach, it is possible to achieve a reliable and gentle cell positioning success with pond snail neurons in a microfluidic device for the first time. Thereby we tested 10 prototypes with only slightly varying parameters, like trap number, width of the trap gap, and trap interconnecting channels. With the exception of the trap gap, no significant differences in flow behavior of particles and trapping success between the different prototypes could be estimated. Concerning trap gap width, it turned out that the gaps should be as narrow as possible to enhance maintained trapping.

Indeed, the present devices are still prototypes, and modifications of the actual design are still outstanding to increase trapping efficiency, maintenance of cell viability and network formation. However, so far, the system we developed presents a step forward towards an automated, gentle, and

reliable cell trapping method for sensitive, large invertebrate neurons, but also for other cell types. The integration of the electrodes of semiconductor chips in such a channel system is scheduled. If this becomes realized, the devices have the potential to comply with the ambitions to create an isolated automated biohybrid system with highest control of the cell´s microenvironment.

In the second project to direct neuronal growth *in vitro*, we adapt the idea of the common used substrate patterning technique (for review see: Théry 2010). This is most commonly implemented by microcontact printing (Wheeler et al. 1999) or laser ablation techniques (Corey et al. 1991). To improve cell growth guiding, chemical substrate patterning is supplemented by a physical guiding of the cells with topographically raised structures (Merz & Fromherz 2002; Suzuki et al. 2004; Zhang et al. 2006). As already reported, various different techniques exist to create such topographical modifications. Approaches that are more modern work with expensive laser technologies (Suzuki et al. 2004). In contrast, the micromolding technique is more simple and the more cost effective variant, but often shows different deficits in comparison to the possibilities of laser technology. Our aim in this approach was the development of a new, simple, cost effective technique to produce a combination of chemical and topographical substrate modification to guide locust and pond snail neurons on different substrates, MEA chips included. The challenge was to achieve the advantageous properties of expensive laser technology but at the same time invest only minor technical effort. As one of the features of our favored biological test systems is the unpretentiousness concerning their growth substrate, it was decided to manage the chemical guiding of the invertebrate neurons by an aversive cue, instead of by an adhesive one. Agarose turned out to be the material of choice. Thus, the chemical guiding as well as the physical guiding of the cells could be assumed both by the agarose material. Silicon microtemplates of defined geometry were produced by photolithographic techniques. Liquid agarose molded the pattern consisting of wells and closed channels precisely, comparable with results achieved by laser application. With the help of a vibratome, very thin slices could be cut from the hardened agarose replica. These slices were positioned successfully to

any tested culture substrate without any adhesive substances. Slice adherence could be maintained over long time periods under different experimental conditions, but at the same time could be removed easily, which is an advantageous pre-requisite in terms of the application with reusable MEA chips. Further, we managed the application of agarose slices with neurons from the pond snail and the locust. The cell only adhered to the agarose free wells. The closed channels prevented somata from occupying them and guided their neuritic growth successfully. Thus, with the new method, we present a promising alternative to other substrate patterning techniques, especially usable for invertebrate neuron cultures. However, as the techniques allows for high flexibility, geometrical design of micromolds as well as slice thickness can be modified and adjusted on demand, it seems to serve the potential for the application of various different cell types, including vertebrate systems.

The two different techniques represent two very different possibilities leading to the relatively similar goal. Thereby, both approaches possess their individual advantages and drawbacks that can be weighed up against each other. We already discussed different advantages of closed microfluidic culture systems in terms of growth control, medium perfusion and the similarity to *in vivo* conditions. On the other hand, the automated process of cells applied to a streaming fluid seems to have limits as well, which may probably limit the application to all cell types, or the translation of any desired architecture for example. Thus, the general strain on the test objects should not be underestimated and geometry of channels, cell loading procedure, and flux ratios should be balanced to serve as gentle conditions for the test objects as possible. Thus, channel architecture and application technique seem to have to be adjusted individually depending of the used biological test system to achieve the requirements that are necessary to develop vital and active *in vitro* networks.
The second agarose slice approach lacks the opportunity to create an isolated and fully automated system for noninvasive long-term *in vitro* investigations, but for different reasons it has its own eligibility and has the potential to find application in various fields of interest as well. Beside noninvasive extracellular recordings with integrated MEAs, the open wells can be additionally used for intracellular recordings, as the cells are freely assessable

from the top. Furthermore, the probably most crucial positive property of the agarose slice, beside the simple production and application, is the possibility to reuse the culture substrates unrestrictedly.
Further improvements of the accomplished results in cell positioning have to be processed. Here, further geometrical and technical modifications concerning the two cell growth guiding techniques are planned for the future.

One of the major issues that has to be processed additionally is the reliable network building between positioned cell somata and a long lasting cell survival. Therefore, a good cell adherence to the substrate and perfect medium compositions inhering the potential to induce neurite growth and to enhance the viability, are essential requirements. Especially concerning the microfluidic approach, there still seems to be room for improvements. Extensiveness of neurite outgrowth at trapped cells has to be increased for a reliable development of connections between supposed network participants on MEA electrodes. This issue was trying to be investigated in the third part of this thesis. The biocompatibility test of pond snail neurons with IrO, our preferred electrode material for future devices, provided a positive outcome. We compared neurite growth and cell survival of neurons cultured on IrO with neurons cultured on standard culture substrates. As no differences could be observed, biocompatibility could be confirmed, thus the successful use of IrO in combination with pond snail neurons seems to be realizable. Further, basic electrophysiological experiments, should be taken into account to test electrical activities of cultured pond snail neurons on IrO in comparison to other standard electrode materials like gold or platinum. Preliminary attempts to improve culture conditions with NGF, B27, and RA, to date, were only slightly successful. Indeed, we could confirm an Influence of B27 on long-term cell survival, which is beneficial for future long-term experiments, but the more ambitious goal to increase neurite growth could not be attained, yet. Prospective, even more detailed analyzes have to be performed to find the reasons for the failure, at least concerning NGF and RA, as the positive effect of these substances could be shown previously (Ridgway et al. 1991; Dmetrichuk et al. 2006). In this context, the possibility that the effect of such substances probably strongly depends on the cell type, should be kept in mind. Not least, further candidates proposed to effect neurite growth, should be tested.

In summary, the presented studies represent several steps forward toward the development of a biohybrid system of invertebrate neurons and MEA chips. Together with the thesis of Göbbels (2010) it could be confirmed, that locust neurons as well as pond snail neurons are suitable test objects for this approach. Pivotal prework could confirm the neurocompatibility with favored electrode materials and yielded to possibilities to converge the problem of a directed cell growth *in vitro* (Göbbels et al. 2010a; Göbbels 2010). Picking up these hints, it was now possible to develop concrete solutions in this context that are cost effective and applicable at the same time, without impairing the effectiveness. For the future, the presented achievements can be followed up directly to work further towards the far objective to be achieved.

Summary

This project strived to develop technical solutions to guide neuronal growth *in vitro*. The long-term objective in this context is the development of an integrated biohybrid system consisting of cultured low-density neuronal networks and multi electrode arrays (MEAs). Here, the non-invasive coupling of planar electrodes and neuron somata is envisaged to enable the long-term observation of basic physiological cell-cell interactions. Thereby, a one-to-one coupling of electrode and neuron allows for the highest spatial resolution as the allocation of individual signals to single neurons can be achieved. In this context, we are faced with the main challenges to achieve a defined positioning and growth guiding of such neurons *in vitro* to enable a one-to-one coupling of electrode and cell in combination with a controlled network development between them. As biological test systems, pond snail (*Lymnaea stagnalis*) and locust neurons (*Locusta migratoria*) were used for this study.

The first part of this thesis describes the developmental process of a combined cell positioning, culturing and growth guiding technique by using laminar fluid flow through micro-scale channels. Defined geometrical conditions direct the introduced cells to pre-defined locations hydrodynamically. Within the mentioned developmental process, we designed different channel geometries and tested their functionality in neuron trapping and the possibility to culture trapped neurons for longer periods in these microenvironments. Advantages and drawbacks of individual parameters of these different channel geometries and experimental procedures were analyzed and modified until a new system has been designed that enables a reliable and gentle guiding of the applied invertebrate neurons for the first time. The final design comprises a triangle shaped channel system with two rectangular main flanks and several transverse channels interconnecting the two flanks with less fluidic resistance. Each transverse channel is equipped with a cell trap in form of a narrow gap, which in turn is interconnected to neighboring cell traps via small channels intended for neurite growth. To fill the system, first, particles or neurons in a suspension were introduced to the channel by gravity and afterwards successfully directed to the traps by

taking the path of less resistance. Several trapped cells maintained their viability for up to two weeks and developed neuritic branching within the traps. The presented microchannel provide the potential to be a valuable alternative to common microfluidic cell traps as they offer multiple advantages especially for the application with invertebrate neurons. As a next step towards a biohybrid system allowing long-term investigations, the integration of a MEA within the cell traps would constitute a pre-requisite.

In the second part of this thesis a new technique for substrate modification is presented, which provides patterned cell culture. The technique for processing patterned slices, based on a non-adhesive agarose hydrogel, combines low cost and high reproducibility. The hydrogel structures are molded from lithographically processed silicon micro-templates. They consist of cylindrical pins that are arranged equidistantly in squares and connected by bars forming corresponding wells and channels into the hydrogel. Subsequent agarose slice production with a standard vibratome, comprising the described template pattern, completes substrate production. They are 50 µm thick and can be placed on glass, polystyrene or MEAs. This substrate modification allows the selective positioning of cells and a chemically and mechanically directed guiding of their extensions at the same time. Applied neurons can only adhere in the agarose-free wells. The slice height immobilizes the somata and the channels guide their neurite outgrowth towards neighboring wells. In addition to the application with invertebrate neurons, the technique may also provide the potential for the application on a wide range of cell types.

The third part of this thesis describes the approach to improve conditions for pond snail neuron culture. Further, the compatibility of the neurons with the preferred electrode material, iridium oxide (IrO), was tested. An improved neurite outgrowth and an improved long-term cell survival appear to be beneficial for the reliable development of *in vitro* networks between distant neurons on MEA devices. For this reason, the conditions for pond snail neuron culture were studied by the addition of supplements to the culture medium. B27, a commercially available serum-free supplement for neuronal cell cultures, and retinoic acid (RA), the metabolite of retinol and long known to play important roles in various developmental processes, were tested for their individual influence on cell survival rate and neurite

outgrowth. The choice to study B27 and RA was made as different previous studies showed the effectiveness of these supplements on different cell types across the species and therefore promised the expansion of their use beyond the original applications. Biocompatibility of IrO was proven by checking cell survival rate and neurite outgrowth comparing to the standard culture substrate polystyrene. Biocompatibility of locust neurons and IrO had already been successfully tested in a previous study. The results indicate that B27 is able to improve cell survival rates significantly and therefore is recommended to use as medium supplement in future applications. An assumed improvement of neurite formation under the influence of B27 could not be confirmed so far. For RA, a positive effect could be verified neither on cell survival nor on neurite formation. The biocompatibility study of IrO and pond snail neurons led to the conclusion that IrO seems to have no cytotoxic effects on the neurons and offers a suitable surface condition for a sufficient cell adherence. No differences in terms of cell survival rate or neurite formation could be observed in comparison to the standard substrate polystyrene.

Zusammenfassung

Im Zuge dieses Projekts wurden technische Lösungen für das Erreichen eines gerichteten neuronalen Wachstums *in vitro* entwickelt. Das Fernziel in diesem Zusammenhang ist die Entwicklung eines integrierten Biohybridsystems, bestehend aus kultivierten kleinen neuronalen Netzwerken und Multielektroden Arrays (MEAs). Hierbei wird die nicht invasive Kopplung zwischen planaren Elektroden und Neuronen angestrebt, was u.a. Langzeituntersuchungen von grundlegenden physiologischen Zell-Zell-Interaktionen ermöglicht. Eine 1:1 Kopplung von Neuron und Elektrode bietet dabei die höchste räumliche Auflösung, sodass gemessene individuelle Signale direkt den entsprechenden Zellen zugeordnet werden können. Die Umsetzung dieses Konzepts, nämlich die gezielte Positionierung und das Lenken des Neuritenwachstums hin zu einem kontrollierten kleinen Netzwerk *in vitro* zu erreichen, stellt dabei die Herausforderung dar. Für diese Studie wurden Neurone der Spitzschlammschnecke *Lymnaea stagnalis* und der Wanderheuschrecke *Locusta migratoria* als biologische Testsysteme eingesetzt.

Der erste Teil dieser Arbeit beschreibt den Entwicklungsprozess eines technischen Bauteils für das kombinierte Positionieren, der Kultivierung und Wachstumslenkung von Invertebratenneuronen mithilfe einer laminaren Strömung in Kanalsystemen im Mikrometermaßstab. Die definierte Geometrie des Systems lenkt Zellen dabei hydrodynamisch an vordefinierte Positionen. Im Zuge des Entwicklungsprozesses wurden verschiedene Geometrien entwickelt und auf ihre Funktionalität Neurone zu positionieren getestet, sowie auf die Möglichkeit diese über einen längeren Zeitraum in der Mikroumgebung zu kultivieren. Vor-und Nachteile individueller Parameter und der experimentellen Durchführung wurden dabei analysiert und modifiziert bis ein neues System vorgestellt werden konnte, dass zum ersten Mal die zuverlässige und sensitive Lenkung von Invertebratenneuronen ermöglicht. Das finale Design besteht dabei aus einem dreiecksförmigen Kanalsystem mit zwei rechtwinklig zueinander stehenden Hauptflanken und mehreren Querkanälen mit im Vergleich geringerem Flüssigkeitswiderstand, die die Hauptflanken miteinander verbinden. Jeder Querkanal ist mit einer Zellfalle in Form eine Kanalenge ausgestattet, die wiederum untereinander mit

feinen Kanälen für das Neuritenwachstum verbunden sind. Für die Anwendung werden Partikel oder Neurone in einer Suspension per Schwerkraft eingeleitet und dann über den Weg des geringeren Widerstandes zu den Fallen geführt. Viele der gefangenen Zellen blieben für einen Zeitraum von bis zu zwei Wochen optisch vital und entwickelten neuritische Verzweigungen in den Zellfallen. Das präsentierte mikrofluidische System hat das Potential zu einer wertigen Alternative zu anderen geläufigen mikrofluidischen Zellfallsystemen, da es entscheidende Vorteile bietet, besonders für die Anwendung mit Invertebratenneuronen. In einem nächsten Schritt auf dem Weg zu einem Biohybridsystem, das eine Langzeituntersuchung erlaubt, soll die Integration eines MEAs in das Zellfallsystem folgen.

Im zweiten Teil dieser Arbeit wird eine neue Technik zur Substratmodifikation für eine gerichtete Neuronenposition präsentiert. Die Technik, mit der gemusterte Scheiben aus einem aversiven Agarosehydrogel hergestellt werden, kombiniert einen geringen Arbeits- und Kostenaufwand mit hoher Reproduzierbarkeit. Die Strukturen in den Scheiben werden mit wiederverwendbaren lithographisch prozessierten Mikrostrukturen auf einem Siliziumwafer geformt. Die Mikrostrukturen bestehen aus im Quadrat angeordneten Zylindern, die mit feinen Stegen verbunden sind. Sie formen entsprechende Löcher und Kanäle in das für die Zellen aversive Gel. Mithilfe eines herkömmlichen Vibratoms werden die Scheiben, die das entsprechende Muster beinhalten, geschnitten. Sie haben eine Dicke von 50 µm und können auf verschiedenen Oberflächen wie Glas, Polystyrol oder MEAs positioniert werden. Die Substratmodifikation bietet die selektive Zellpositionierung und ein gleichzeitig chemisches und mechanisches Leitsystem für das definierte Auswachsen der Neuriten. Applizierte Neurone können nur in den agarosefreien Vertiefungen adherieren. Die Höhe der Scheibe immobilisiert die Neurone und die Kanäle lenken die Neuriten in Richtung der benachbarten Vertiefungen und damit der benachbarten Zellen. Neben der Anwendung mit Invertebratenneuronen, bietet die Technik die Möglichkeit, Zelltypen anderer Spezies anzuwenden.

Der dritte Teil der Arbeit stellt Experimente zur Verbesserung der Zellkulturbedingungen für Neuronenkulturen der Spitzschlammschnecke vor. Des Weiteren werden die Ergebnisse eines Kompatibilitätstest dieser Neurone mit Iridiumoxid (IrO), dem bevorzugten Elektrodenmaterial, präsentiert. Ein

verbessertes Neuritenwachstum sowie Langzeitüberleben wird in Hinsicht auf eine verlässliche Netzwerkbildung zwischen einzelnen Neuronen in Kultur als vorteilhaft bewertet. Aus diesem Grund wurden die Bedingungen für die kultivierten Neurone unter dem Einfluss verschiedener Supplemente untersucht. B27, ein kommerziell erhältlicher serumfreier Zusatz für neuronale Zellkulturen und Retinsäure (RS), ein Metabolit des Vitamin A und seit langem bekannt wichtige Einflüsse auf entwicklungsbiologische Prozesse zu haben, wurden auf ihren individuellen Einfluss auf das Zellüberleben und das Neuritenwachstum getestet. Die Entscheidung für das Testen von B27 und RS fiel, da vorangegangene Studien bereits die Effektivität dieser Supplemente auf verschiedene Zelltypen, über Speziesgrenzen hinweg, zeigen konnten, und daher ein erweitertes Spektrum, über die ursprüngliche Anwendungsspezifikation hinaus, angenommen werden kann. Die Biokompatibilität mit IrO wurde anhand der Überprüfung der Zellüberlebensrate und des Neuritenwachstums auf dem Elektrodenmaterial im Vergleich zu dem Standartkultursubstrat Polystyrol getestet. Die Biokompatibilität von Heuschreckenneuronen und IrO wurde bereits in einer früheren Studie bestätigt. Die Resultate zeigen, dass B27 in der Lage ist das Zellüberleben signifikant zu verlängern, weshalb es als Zusatz zum Medium für zukünftige Anwendungen empfohlen werden kann. Eine Verbesserung der Neuritenbildung unter dem Einfluss von B27 konnte nicht bestätigt werden. Für RS konnte bisher weder ein positver Effekt auf das Zellüberleben noch auf das Neuritenwachstum verzeichnet werden. Der Biokompatibilitätstest von IrO und Neuronen der Spitzschlammschnecke führte zu dem Ergebnis, dass IrO keine zytotoxischen Effekte auf die Neurone zu haben und geeignete Oberflächenbedingungen für ausreichend Zellhaftung zu bieten scheint. Es wurden keine Unterschiede bzgl. der Zellüberlebensrate oder der Neuritenbildung im Vergleich zu gebrauchsüblichem Polystyrol festgestellt.

References

Andersson, H. & Berg, A. Van Den, 2004. Microfabrication and microfluidics for tissue engineering: state of the art and future opportunities. *Lab on a Chip*, 4, 98–103.

Angevin, V. et al., 2000. Quantitative morphological analysis of embryonic cockroach (Periplaneta americana) brain neurons developing in vitro. *Cell and Tissue Research*, 299, 129–143.

Ballini, M. et al., 2014. A 1024-Channel CMOS Microelectrode Array With 26,400 Electrodes for Recording and Stimulation of Electrogenic Cells In Vitro. *IEEE Journal of Solid-State Circuits*, 49, 2705–2719.

Beebe, D.J., Mensing, G.A. & Walker, G.M., 2002. Physics and applications of microfluidics in biology. *Annual Review of Biomedical Engineering*, 4, 261–286.

Bell, L. et al., 2014. A microfluidic device for the hydrodynamic immobilisation of living fission yeast cells for super-resolution imaging. *Sensors and Actuators B: Chemical*, 192, 36–41.

Blau, A., 2013. Cell adhesion promotion strategies for signal transduction enhancement in microelectrode array in vitro electrophysiology: An introductory overview and critical discussion. *Current Opinion in Colloid & Interface Science*, 18, 481–492.

Branch, D.W. et al., 2000. Long-Term Maintenance of Patterns of Hippocampal Pyramidal Cells on Substrates of Polyethylene Glycol and Microstamped Polylysine. *IEEE Transactions on Biomedical Engineering*, 47, 290–300.

Braschler, T. et al., 2005. Gentle cell trapping and release on a microfluidic chip by in situ alginate hydrogel formation. *Lab on a Chip*, 5, 553–559.

Brewer, G.J. et al., 1993. Optimized Survival of Hippocampal Neurons in B27-Supplemented Neurobasalm , a New Serum-free Medium Combination. *Journal of Neuroscience Methods*, 35, 567–576.

Brewer, G.J., 1995. Serum-Free B27lNeurobasal Medium Supports Differentiated Growth of Neurons From the Striatum , Substantia Nigra , Septum , Cerebral Cortex , Cerebellum , and Dentate Gyrus. *Journal of Neuroscience Research*, 42, 674–683.

Bui-Göbbels et. al., 2015. Is retinoic acid a signal for nerve regeneration in insects? *Neural Regeneration Research*, 10, 901–903.

Buitenweg, J.R. et al., 1998. Measurement of sealing resistance of cell-electrode interfaces in neuronal cultures using impedance spectroscopy. *Medical & Biological Engineering & Computing*, 36, 630–637.

Bulloch, A.G.M. & Syed, N.I., 1992. Reconstruction of neuronal networks in culture. *Trends in Neurosciences*, 15, 422–427.

Bulloch, A.G.M., Syed, N.I. & Ridgway, R.L., 1994. Neurite outgrowth and synapse formation by *Lymnaea* neurons: Towards a characterization of molluscan neurotrophic factors. *Netherlands Journal of Zoology*, 44, 317–326.

Burrows, M., 1996. *The Neurobiology of an Insect brain*, Oxford University Press, Oxford.

Di Carlo, D., Wu, L.Y. & Lee, L.P., 2006. Dynamic single cell culture array. *Lab on a Chip*, 6, 1445–1449.

Claverol-Tinturé, E. et al., 2005. Multielectrode arrays with elastomeric microstructured overlays for extracellular recordings from patterned neurons. *Journal of neural engineering*, 2, 1–7.

Claverol-Tinturé, E., Rosell, X. & Cabestany, J., 2005. Interfacing with Patterned in Vitro Neural Networks by Means of Hybrid Glass-

Elastomer Neurovectors: Progress on Neuron Placement, Neurite Outgrowth and Biopotential Measurements. In *Computational Intelligence and Bioinspired Systems*. Springer-Verlag Berlin Heidelberg, 433–437.

Claverol-Tinturé, E., Rosell, X. & Cabestany, J., 2007. Technical steps towards one-to-one electrode–neuron interfacing with neural circuits reconstructed in vitro. *Neurocomputing*, 70, 2716–2722.

Corey, J.M., Wheeler, B.C. & Brewer, G.J., 1991. Compliance of Hippocampal Neurons to Patterned Substrate Networks. *Journal of Neuroscience Research*, 30, 300–307.

Delacour, C. et al., 2014. Combined magnetic and chemical patterning for neural architectures. *Journal of Physics D: Applied Physics*, 47, 1–6.

Dinh, N.-D. et al., 2013. Microfluidic construction of minimalistic neuronal co-cultures. *Lab on a Chip*, 13, 1402–1412.

Dmetrichuk, J.M. et al., 2008. Detection of endogenous retinoids in the molluscan CNS and characterization of the trophic and tropic actions of 9-cis retinoic acid on isolated neurons. *The Journal of Neuroscience*, 28, 13014 – 13024.

Dmetrichuk, J.M., Carlone, R.L. & Spencer, G.E., 2006. Retinoic acid induces neurite outgrowth and growth cone turning in invertebrate neurons. *Developmental Biology*, 294, 39–49.

Dworak, B.J. & Wheeler, B.C., 2009. Novel MEA platform with PDMS microtunnels enables the detection of action potential propagation from isolated axons in culture. *Lab on a Chip*, 9, 404–410.

Edwards, D. et al., 2013. Two Cell Circuits of Oriented Adult Hippocampal Neurons on Self- Assembled Monolayers for Use in the Study of Neuronal Communication in a Defined System. *ACS Chemical Neuroscience*, 4, 1174–1182.

Eick, S. et al., 2009. Iridium oxide microelectrode arrays for in vitro stimulation of individual rat neurons from dissociated cultures. *Frontiers in Neuroengineering*, 2, 1-12.

El-Ali, J., Sorger, P.K. & Jensen, K.F., 2006. Cells on chips. *Nature*, 442, 403–411.

Erickson, J. et al., 2008. Caged neuron MEA: a system for long-term investigation of cultured neural network connectivity. *Journal of Neuroscience Methods*, 175, 1–16.

Eversmann, B. et al., 2003. A 128 × 128 CMOS Biosensor Array for Extracellular Recording of Neural Activity. *IEEE Journal of Solid-State Circuits*, 38, 2306–2317.

Faley, S. et al., 2008. Microfluidic platform for real-time signaling analysis of multiple single T cells in parallel. *Lab on a Chip*, 8, 1700–1712.

Frimat, J.-P. et al., 2011. A microfluidic array with cellular valving for single cell co-culture. *Lab on a Chip*, 11, 231–237.

Fromherz, P., Schaden, H. & Vetter, T., 1991. Guided outgrowth of leech neurons in culture. *Neuroscience Letters*, 129, 77–80.

Gawad, S. et al., 2009. Substrate arrays of iridium oxide microelectrodes for in vitro neuronal interfacing. *Frontiers in Neuroengineering*, 2, 1-7

Göbbels, K., 2010. *Development and characterisation of neuronal biohybrid systems*. Doctoral thesis, RWTH Aachen University.

Göbbels, K. et al., 2010a. Low density cell culture of locust neurons in closed-channel microfluidic devices. *Journal of Insect Physiology*, 56, 1003–1009.

Göbbels, K. et al., 2010b. Neuronal cell growth on iridium oxide. *Biomaterials*, 31, 1055–1067.

Gomez-Sjöberg, R. et al., 2007. Versatile, Fully Automated, Microfluidic Cell Culture System. *Analytical Chemistry*, 79, 8557–8563.

Greenbaum, A. et al., 2009. One-to-one neuron-electrode interfacing. *Journal of Neuroscience Methods*, 182, 219–224.

Gross, G.W. et al., 1993. Stimulation of monolayer networks in culture through thin-film indium-tin oxide recording electrodes. *Journal of Neuroscience Methods*, 50, 131–143.

Gross, G.W. et al., 1995. The use of neuronal networks on multielectrode arrays as biosensors. *Biosensors & Bioelectronics*, 10, 553–567.

Gross, P.G. et al., 2007. Applications of microfluidics for neuronal studies. *Journal of the Neurological Sciences*, 252, 135–143.

Hai, A. et al., 2009. Spine-shaped gold protrusions improve the adherence and electrical coupling of neurons with the surface of micro-electronic devices. *The Journal of the Royal Society, Interface*, 6, 1153–1165.

Hamakawa, T. et al., 1999. Excitatory Synaptogenesis between Identified *Lymnaea* Neurons Requires Extrinsic Trophic Factors and Is Mediated by Receptor Tyrosine Kinases. *The Journal of Neuroscience*, 19, 9306–9312.

El Hasni, A. et al., 2011. Focusing and sorting of particles in spiral microfluidic channels. *Procedia Engineering*, 25, 1197–1200.

Herculano-Houzel, S., 2005. Isotropic Fractionator: A Simple, Rapid Method for the Quantification of Total Cell and Neuron Numbers in the Brain. *Journal of Neuroscience*, 25, 2518–2521.

Heuschkel, M.O. et al., 2002. A three-dimensional multi-electrode array for multi-site stimulation and recording in acute brain slices. *Journal of Neuroscience Methods*, 114, 135–148.

Hosokawa, C. et al., 2010. Micro-channel fabrication by femtosecond laser to arrange neuronal cells on multi-electrode arrays. *Applied Physics A*, 101, 423–428.

Ingensiep, C., 2015. *Größenauftrennung von Neuronen der Spitzschlammschnecke (Lymnaea stagnalis) mit Hilfe von mikrofluidischen Spiralfiltern*. Bachelor thesis, RWTH Aachen University, Aachen.

Jaber, F.T., Labeed, F.H. & Hughes, M.P., 2013. A dielectrophoresis and Image processing based system for loading micro-well in planar microelectrode arrays. In *IEEE International Workshop on Systems, Signal Processing and their Applications*. 180–184.

Jäckel, D. et al., 2012. Applicability of independent component analysis on high-density microelectrode array recordings. *Journal of Neurophysiology*, 108, 334–348.

Jan, L.Y. & Jan, Y.N., 1982. Antibodies to horseradish peroxidase as specific neuronal markers in *Drosophila* and in grasshopper embryos. *Proceedings of the National Academy of Sciences*, 79, 2700–2704.

Jenkner, M., Müller, B. & Fromherz, P., 2001. Interfacing a silicon chip to pairs of snail neurons connected by electrical synapses. *Biological Cybernetics*, 84, 239–249.

Jun, S.B. et al., 2007. Low-Density Neuronal Networks Cultured using Patterned Poly-l-Lysine on Microelectrode Arrays. *Journal of Neuroscience Methods*, 160, 317–326.

Jungblut, M. et al., 2009. Triangular neuronal networks on microelectrode arrays: an approach to improve the properties of low-density networks for extracellular recording. *Biomedical Microdevices*, 11, 1269–1278.

Kang, G. et al., 2009. Agarose microwell based neuronal micro-circuit arrays on microelectrode arrays for high throughput drug testing. *Lab on a Chip*, 9, 3236–3242.

Kaul, R., Syed, N. & Fromherz, P., 2004. Neuron-Semiconductor Chip with Chemical Synapse between Identified Neurons. *Physical Review Letters*, 92, 1–4.

Kaul, R.K., 2007. *Chemical Synapses on Semiconductor Chips*. Doctoral thesis, Technische Universität München, München.

Khademhosseini, A. et al., 2004. A Soft Lithographic Approach To Fabricate Patterned Microfluidic Channels. *Analytical Chemistry*, 76, 5783–5789.

Kirchhof, B. & Bicker, G., 1992. Growth properties of larval and adult locust neurons in primary cell culture. *The Journal of Comparative Neurology*, 323, 411–422.

Kleinfeld, D., Kahler, K.H. & Hockberger, P.E., 1988. Controlled Outgrowth of Dissociated Neurons on Patterned Substrates. *The Journal of Neuroscience*, 8, 4098–4120.

Kobel, S. et al., 2010. Optimization of microfluidic single cell trapping for long-term on-chip culture. *Lab on a Chip*, 10, 857–863.

Kobel, S. a et al., 2012. Automated analysis of single stem cells in microfluidic traps. *Lab on a Chip*, 12, 2843–2849.

Krsko, P. et al., 2009. Length-scale mediated adhesion and directed growth of neural cells by surface-patterned poly(ethylene glycol) hydrogels. *Biomaterials*, 30, 721–729.

Krumpholz, K. et al., 2014. A Microfluidic Device for Selective Positioning of Invertebrate Neurons. In *MEA Meeting, 9th International Meeting on Substrate-Integrated Microelectrode Arrays*. 318–319.

Kwiat, M. et al., 2012. Highly Ordered Large-Scale Neuronal Networks of Individual Cells – Toward Single Cell to 3D Nanowire Intracellular Interfaces. *ACS Applied Materials Interfaces*, 4, 3542–3549.

Lang, K.J.D. et al., 2004. Differentiation of Embryonic Stem Cells to a Neural Fate : A Route to Re-Building the Nervous System ? *Journal of Neuroscience Research*, 192, 184–192.

Lawrenz, A., Nason, F. & Cooper-white, J.J., 2012. Geometrical effects in microfluidic-based microarrays for rapid , efficient single-cell capture of mammalian stem cells and plant cells. *Biomicrofluidics*, 6, 1–17.

Lee, I. et al., 2005. Iridium Oxide as A Stimulating Neural Electrode Formed By Reactive Magnetron Sputtering. *Key Engineering Materials, Trans Tech Publications Inc.*, 289, 307–310.

Lee, W.C. et al., 2011. High-throughput cell cycle synchronization using inertial forces in spiral microchannels. *Lab on a Chip*, 11, 1359–1367.

Li, W. et al., 2014. NeuroArray: A Universal Interface for Patterning and Interrogating Neural Circuitry with Single Cell Resolution. *Scientific Reports*, 4, 1–7.

Lin, L. et al., 2013. Microfluidic cell trap array for controlled positioning of single cells on adhesive micropatterns. *Lab on a Chip*, 13, 714–721.

Lovat, V. et al., 2005. Carbon nanotube substrates boost neuronal electrical signaling. *Nano Letters*, 5, 1107–1110.

Lovell, P. & Moroz, L.L., 2006. The largest growth cones in the animal kingdom: an illustrated guide to the dynamics of *Aplysia* neuronal growth in cell culture. *Integrative and Comparative Biology*, 46, 847–870.

Maher, M.P. et al., 1999. The neurochip: a new multielectrode device for stimulating and recording from cultured neurons. *Journal of Neuroscience Methods*, 87, 45–56.

Marconi, E. et al., 2012. Emergent Functional Properties of Neuronal Networks with Controlled Topology. *PloS ONE*, 7, 1–12.

Massobrio, P. et al., 2009. Helix neuronal ensembles with controlled cell type composition and placement develop functional polysynaptic circuits on Micro-Electrode Arrays. *Neuroscience Letters*, 467, 121–126.

Massobrio, P. et al., 2015. In Vitro Studies of Neuronal Networks and Synaptic Plasticity in Invertebrates and in Mammals Using Multielectrode Arrays. *Neural Plasticity*, 2015, 1–18.

Massobrio, P. et al., 2013. Selective modulation of chemical and electrical synapses of Helix neuronal networks during in vitro development. *BMC Neuroscience*, 14, 1-18.

Mazzoni, A. et al., 2007. On the Dynamics of the Spontaneous Activity in Neuronal Networks. *PLoS ONE*, 2, 1–12.

McDonald, J.C. & Whitesides, G.M., 2002. Poly(dimethylsiloxane) as a Material for Fabricating Microfluidic Devices. *Accounts of Chemical Research*, 35, 491–499.

Mercey, E. et al., 2010. The application of 3D micropatterning of agarose substrate for cell Culture and in situ comet assays. *Biomaterials*, 31, 3156–3165.

Merz, M. & Fromherz, P., 2002. Polyester Microstructures for Topographical Control of Outgrowth and Synapse Formation of Snail Neurons. *Advanced Materials*, 14, 141–144.

Merz, M. & Fromherz, P., 2005. Silicon Chip Interfaced with a Geometrically Defined Net of Snail Neurons. *Advanced Functional Materials*, 15, 739–744.

Millet, L.J. et al., 2007. Microfluidic devices for culturing primary mammalian neurons at low densities. *Lab on a Chip*, 7, 987–994.

Minerbi, A. et al., 2009. Long-term relationships between synaptic tenacity, synaptic remodeling, and network activity. *PLoS Biology*, 7, 1–20.

Moriguchi, H. et al., 2002. An agar-microchamber cell-cultivation system: flexible change of microchamber shapes during cultivation by photothermal etching. *Lab on a Chip*, 2, 125–132.

Moriguchi, H., Tamai, N. & Takayama, Y., 2007. Site-selective Electrical Recording from Small Neuronal Circuits using Spray Patterning Method and Mobile Microelectrodes. In *3rd International IEEE EMBS Conference on Neural Engineering*. 494–497.

Nelson, C.M. et al., 2003. Degradation of Micropatterned Surfaces by Cell-Dependent and -Independent Processes †. *Langmuir*, 19, 1493–1499.

Neuhof, A., 2014. *Auftrennung von Neuronen mit Hilfe mikrofluidischer Bauteile*. Master thesis, RWTH Aachen University, Aachen.

Nilsson, J. et al., 2009. Review of cell and particle trapping in microfluidic systems. *Analytica chimica acta*, 649, 141–157.

Novak, J.L. & Wheeler, B.C., 1988. Multisite hippocampal slice recording and stimulation using a 32 element microelectrode array. *Journal of Neuroscience Methods*, 23, 149–159.

Odawara, A., Gotoh, M. & Suzuki, I., 2013. Control of neural network patterning using collagen gel photothermal etching. *Lab on a Chip*, 13, 2040–2046.

Park, J. et al., 2007. Radial Flow Hepatocyte Bioreactor Using Stacked Microfabricated Grooved Substrates. *Biotechnology and Bioengineering*, 96, 1199–1210.

Pine, J., 1980. Recording action potentials from cultured neuones with extracellular microcircuit electrodes. *Journal of Neuroscience Methods*, 2, 19–31.

Pirlo, R.K. et al., 2011. Laser-guided cell micropatterning system. *AIP Review of Scientific Instruments*, 82, 1–7.

Prinz, A.A. & Fromherz, P., 2000. Electrical synapses by guided growth of cultured neurons from the snail *Lymnaea stagnalis*. *Biological Cybernetics*, 82, 1–5.

Rajnicek, A.M., Britland, S. & Mccaig, C.D., 1997. Contact guidance of CNS neurites on grooved quartz : influence of groove dimensions , neuronal age and cell type. *Journal of Cell Science*, 110, 2905–2913.

Reska, A. et al., 2008. Ultrathin Coatings with Change in Reactivity over Time Enable Functional In Vitro Networks Of Insect Neurons. *Advanced Materials*, 20, 2751–2755.

Richards, R.G., 1996. The effect of surface roughness on fibroblast adhesion in vitro. *Injury*, 27, 38–43.

Richardson-Burns, S.M. et al., 2007. Polymerization of the conducting polymer poly(3,4-ethylenedioxythiophene) (PEDOT) around living neural cells. *Biomaterials*, 28, 1539–1552.

Ridgway, R.L. et al., 1991. Nerve Growth Factor (NGF) Induces Sprouting of Specific Neurons of the Snail , *Lymnaea stagnalis*. *Journal of Neurobiology*, 22, 377–390.

Ristanović, D., Milosević, N.T. & Stulić, V., 2006. Application of modified Sholl analysis to neuronal dendritic arborization of the cat spinal cord. *Journal of Neuroscience Methods*, 158, 212–218.

Ruardij, T.G., van den Boogaart, M.A.F. & Rutten, W.L.C., 2002. Adhesion and Growth of Electrically Active Cortical Neurons on Polyethylenimine Patterns Microprinted Onto PEO-PPO-PEO Triblockcopolymer-Coated Hydrophobic Surfaces. *IEEE Transaction on Nanobioscience*, 1, 4–11.

Sasaki, D. et al., 2009. Mass preparation of size-controlled mouse embryonic stem cell aggregates and induction of cardiac differentiation by cell patterning method. *Biomaterials*, 30, 4384–4389.

Schmold, N. & Syed, N.I., 2012. Molluscan neurons in culture: shedding light on synapse formation and plasticity. *Journal of Molecular Histology*, 43, 383–399.

Schoen, I. & Fromherz, P., 2007. The mechanism of extracellular stimulation of nerve cells on an electrolyte-oxide-semiconductor capacitor. *Biophysical Journal*, 92, 1096–1111.

Shin, S. et al., 2006. Long-Term Proliferation of Human Embryonic Stem Cell-Derived Neuroepithelial Cells Using Defined Adherent Culture Conditions. *Stem Cells*, 24, 125–138.

Skelley, A.M. et al., 2009. Microfluidic control of cell pairing and fusion. *Nature Methods*, 6, 147–152.

Smagghe, G., Goodman, C.L. & Stanley, D., 2009. Insect cell culture and applications to research and pest management. *In vitro Cellular & Developmental Biology -Animal*, 45, 93–105.

Sorribas, H. et al., 2001. Adhesion proteins for a tight neuron-electrode contact. *Journal of Neuroscience Methods*, 104, 133–141.

Sugio, Y. et al., 2004. An agar-based on-chip neural-cell-cultivation system for stepwise control of network pattern generation during cultivation. *Sensors and Actuators B: Chemical*, 99, 156–162.

Sukiban, J. et al., 2014. Retinoic acid as a survival factor in neuronal development of the grasshopper , *Locusta migratoria*. *Cell and Tissue Research*, 358, 303–312.

Suzuki, I. et al., 2004. Modification of a neuronal network direction using Stepwise photo-thermal etching of an agarose architecture. *Journal of Nanobiotechnology*, 2, pp.1–8.

Suzuki, I. et al., 2004a. Individual-Cell-Based Electrophysiological Measurement of a Topographically Controlled Neuronal Network Pattern Using Agarose Architecture with a Multi-Electrode Array. *Japanese Journal of Applied Physics*, 43, 403–406.

Suzuki, I. et al., 2004b. Stepwise pattern modification of neuronal network in photo-thermally-etched agarose architecture on multi-electrode array chip for individual-cell-based electrophysiological measurement. *Lab on a Chip*, 5, 241–247.

Suzuki, I., Hattori, A. & Yasuda, K., 2007. On-Chip Multichannel Action Potential Recording System for Electrical Measurement of Single Neurites of Neuronal Network. *Japanese Journal of Applied Physics*, 46, 1028–1031.

Suzuki, I. & Yasuda, K., 2007. Detection of tetanus-induced effects in linearly lined-up micropatterned neuronal networks: application of a multi-electrode array chip combined with agarose microstructures. *Biochemical and Biophysical Research Communications*, 356, 470–475.

Suzuki, M. et al., 2013. Neuronal cell patterning on a multi-electrode array for a network analysis platform. *Biomaterials*, 34, 5210–5217.

Syed, N., Richardson, P. & Bulloch, A., 1996. Ciliary neurotrophic factor, unlike nerve growth factor, supports neurite outgrowth but not synapse formation by adult *Lymnaea* neurons. *Journal of Neurobiology*, 29, 293–303.

Syed, N.I., Bulloch, A.G.M. & Lukowiak, K., 1990. *In Vitro* Reconstruction of the Respiratory Central Pattern Generator of the Mollusk *Lymnaea*. *Science*, 250, 282–285.

Tan, W.-H. & Takeuchi, S., 2007. A trap-and-release integrated microfluidic system for dynamic microarray applications. *Proceedings of the National Academy of Sciences of the United States of America*, 104, 1146–1151.

Tanghe, S.J., Najafi, K. & Wise, K.D., 1990. A Planar IrO Multichannel Stimulating Electrode for Use in Neural Prostheses. *Sensors and Actuators B1*, 464–467.

Taylor, A.M. & Jeon, N.L., 2010. Micro-scale and microfluidic devices for neurobiology. *Current Opinion in Neurobiology*, 20, 640–647.

Tehranirokh, M. et al., 2013. Microfluidic devices for cell cultivation and proliferation. *Biomicrofluidics*, 7, 1–33.

Théry, M., 2010. Micropatterning as a tool to decipher cell morphogenesis and functions. *Journal of Cell Science*, 123, 4201–4213.

Thomas, C.A. et al., 1972. A miniature microelectrode array to monitor the bioelectric activity of cultured cells. *Experimental Cell Research*, 74, 61–66.

Tourniaire, G. et al., 2006. Polymer microarrays for cellular adhesion. *RSC, Chemical Communications*, 2118–2120.

Tsai, I.Y., Crosby, A.J. & Russell, T.P., 2007. Surface patterning. In *Methods in Cell Biology*. Elsevier Inc., 67–87.

Wagenaar, D. a et al., 2005. Controlling bursting in cortical cultures with closed-loop multi-electrode stimulation. *The Journal of Neuroscience*, 25, 680–688.

Wagenaar, D. a & Potter, S.M., 2004. A versatile all-channel stimulator for electrode arrays, with real-time control. *Journal of Neural Engineering*, 1, 39–45.

Walker, G.M., Ozers, M.S. & Beebe, D.J., 2002. Insect Cell Culture in Microfluidic Channels. *Biomedical Microdevices*, 4, 161–166.

Weigel, S. et al., 2012. Locust primary neuronal culture for the study of synaptic transmission. *Journal of Molecular Histology*, 43, 405–419.

Wessling, B. et al., 2007. Reactively Sputtered Iridium Oxide. *Journal of the Electrochemical Society*, 154, 83–89.

Wessling, B., Mokwa, W. & Schnakenberg, U., 2006. RF-sputtering of iridium oxide to be used as stimulation material in functional medical implants. *Journal of Micromechanics and Microengineering*, 16, 142–148.

Wheeler, B.B.C., Ieee, F. & Brewer, G.J., 2010. Designing Neural Networks in Culture. *Proceedings of the IEEE*, 98, 398–406.

Wheeler, B.C. et al., 1999. Microcontact printing for precise control of nerve cell growth in culture. *Journal of Biomechanical Engineering*, 121, 73–78.

Whitesides, G.M., 2006. The origins and the future of microfluidics. *Nature*, 442, 368–373.

Wong, R.G. et al., 1981. Neurite Outgrowth in Molluscan Organ and Cell Cultures: The Role of Conditioning Factor(s). *The Journal of Neuroscience*, 9, 1008–1021.

Wong, R.G., Martel, E.C. & Kater, S.B., 1983. Conditioning Factor(s) Produced by Several Molluscan Species Promote Neurite Outgrowth in Cell Culture. *Journal of Experimental Biology*, 105, 389–393.

Woodin, M.A. et al., 1999. Trophic Factor-Induced Plasticity of Synaptic Connections Between Identified *Lymnaea* Neurons. *Learning & Memory*, 6, 307–316.

Xia, Y. & Whitesides, G.M., 1998. Soft Lithography. *Angewandte Chemie International Edition*, 37, 550–575.

Zeck, G. & Fromherz, P., 2001. Noninvasive neuroelectronic interfacing with synaptically connected snail neurons immobilized on a semiconductor chip. *Proceedings of the National Academy of Sciences*, 98, 10457–10462.

Zervantonakis, I.K. et al., 2011. Microfluidic devices for studying heterotypic cell-cell interactions and tissue specimen cultures under controlled microenvironments. *Biomicrofluidics*, 5, 1–15.

Zhang, J. et al., 2006. Combined topographical and chemical micropatterns for templating neuronal networks. *Biomaterials*, 27, 5734–5739.

Supplementary Information on CD-ROM

Figures:

- Fig. 1: Cell trapping in modified first generation device of sub type 3 a
- Fig. 2: Cell adherence in loops of first generation device
- Fig. 3: Cells in inlet of first generation device
- Fig. 4: Soma diameter exceeds dimension of first generation device

Videos:

- Vid. 1: Bead trapping, random, multitrapping
- Vid. 2: Neuron trapping, random, multitrapping

Danksagung

Ohne die Unterstützung diverser Menschen aus meiner beruflichen und familiären Umgebung wäre der erfolgreiche Abschluss dieser Arbeit nicht zustande gekommen. Daher möchte ich abschließend Danke sagen:

Peter, danke, dass du mir dein Vertrauen in meine Arbeit geschenkt hast. Bereits meine Diplomarbeit durfte ich bei dir durchführen. Nachdem unser erstes gemeinsames Projekt nach meinem Diplom unter keinem guten Stern stand, hast du trotzdem an meinen Fähigkeiten festgehalten und mir den Wechsel in das jetzige Projekt und somit die Promotion ermöglicht. Dafür und für deine immer währende Präsenz, dein Interesse, deine Kritik und deine Unterstützung bin ich dir sehr dankbar.

Katrin, du bist die beste Betreuerin, die ich mir je hätte vorstellen können. Deine neuen Ideen und deine bewundernswert positive Art mit schwierigen Situationen oder scheinbar schlechten Ergebnissen umzugehen, haben mich immer wieder motiviert. Du hast mir das Gefühl geben können, dass ich gute Arbeit leiste und standst mir immer kompetent mit Rat und Tat zur Seite. Gleichzeitig warst du eine tolle Bürokollegin; wir hatten viel Gesprächsstoff. Es war eine schöne Zeit mit dir. Ich danke dir von Herzen für Alles.

Uwe und Akram, ich danke euch für die nette Zusammenarbeit, sowie die technische Umsetzung unserer Ideen für die Mikrostrukturen. Es ist toll, dass wir eure Labore nutzen durften. So konnten wir unsere Arbeitsabläufe entscheidend optimieren. Vielen Dank für eure Unterstützung.

Rudolf, auch über deine Bachelorarbeit hinaus warst du im Rahmen deiner wissenschaftlichen Assistenz eine unschätzbare Hilfe, und hattest durch deinen motivierten und kompetenten Einsatz entscheidenden Anteil an der erfolgreichen Entwicklung der mikrofluidischen Systeme. Toll, dass du auch später, nach deinem Weggang, immer Interesse am Entwicklungsstand des Projekts hattest.

Julia, dein Einsatz und deine gute Arbeit bei der Entwicklung der Agarosescheiben kann man nur loben. Ohne deinen Beitrag wären wir heute vielleicht noch nicht da, wo wir jetzt sind.

Phong, ich danke dir für deine tollen neuen Ideen, Impulse und Hilfe mit Ansys.

Lennart, **Claudia** und **Fabio**, ich danke euch, dass ihr bei mir eure Bachelorarbeit durchgeführt habt. Ihr habt motiviert und eigenständig für mich Daten gesammelt und so zum Gesamterfolg des Projekts beigetragen. Ich habe durch meine Funktion als Betreuerin auch einiges gelernt und danke euch für die positive Erfahrung.

Rita, vielen Dank für das Korrekturlesen mit Lichtgeschwindigkeit. Das hat mir sehr geholfen!

Meine Eltern, ich danke euch, dass ihr mich immer unterstützt habt und ohne nachlassendes Interesse nachgefragt habt, wie „es läuft". Ihr habt mir stets ein gutes Gefühl gegeben. Danke, dass ich immer willkommen bin und mich immer noch bei euch zuhause fühle.

Andreas, danke, dass du an meiner Seite stehst. Du bist mein Ausgleich, mein Fels, mein Zuhause.

Lebenslauf

Persönliche Daten:

Name	Katharina Walczuch, geb. Krumpholz
Geburtstag	16.01.1985
Geburtsort	Lingen (Ems)
Staatsangehörigkeit	deutsch
Familienstand	verheiratet

Schulische und wissenschaftliche Ausbildung:

1991 – 1995	Grundschule Baccum, Lingen (Ems)
1995 – 2001	Franziskusgymnasium, Lingen (Ems)
2001 – 2004	Gymnasium Johanneum, Lingen (Ems)
05/2004	Abitur
10/2004 – 09/2011	Studium der Biologie an der RWTH Aachen University
12/2010 – 09/2011	Diplomarbeit am Institut für Biologie II, Abteilung Entwicklungsbiologie und Morphologie der Tiere (EMT), RWTH Aachen University
09/2011	Abschluss zur Diplom-Biologin
Seit 11/2011	Wissenschaftliche Angestellte und Promotion am Institut für Biologie II, Abteilung Entwicklungsbiologie und Morphologie der Tiere (EMT), RWTH Aachen University